ACTIVE BODYSUIT FOR

ADULT DEGENERATIVE SCOLIOSIS (ADS)

CHUNG WING YAN, CLAIRE

MPhil

The Hong Kong Polytechnic University

2022

The Hong Kong Polytechnic University

Institute of Textiles and Clothing

Active Bodysuit for Adult Degenerative Scoliosis (ADS)

Chung Wing Yan, Claire

A thesis submitted in partial fulfillment of the requirements for

the degree of Master of Philosophy

December 2021

CERTIFICATE OF ORIGINALITY

I hereby declare that this thesis is my own work and that, to the best of my knowledge and belief, it reproduces no material previously published or written, nor material that has been accepted for the award of any other degree or diploma, except where due acknowledgement had been made in the text.

___________________________________(Signed)

Chung Wing Yan Claire (Name of Student)

Abstract

Adult degenerative scoliosis (ADS), which is also known as de novo scoliosis, is a condition of the ageing population caused by degenerative changes of spine in individuals who do not have any pre-existing spinal deformities, with a Cobb angle that exceeds 10° in the coronal plane. Globally, there is an approximate overall incidence rate of ADS of 6% for people aged 50 or older, and the average progression of the spinal curvature is 3.3° each year. Patients with ADS usually suffer from progressive lower back pain with radiculopathy and neurogenic claudication, spinal stenosis, and progression of the spinal curve which negatively affect the health-related quality of life. Patients are required to wear a rigid brace to relieve pain, correct their posture and reduce the progression of the spinal curvature, which could lead to the problems of discomfort and pressure sores, and cause psychological barriers to compliance with treatment. In response, this project aims to develop a novel flexible brace that provides adequate corrective forces, as well as improves the wear comfort and aesthetics perspective towards bracing treatment.

To achieve the project goal, this study will carry out four tasks, including: (a) a study on the posture, balance and muscle activity of ADS patients, b) a clinical study that involves radiographic examination and questionnaires to investigate the corrective effect, thermal comfort and psychological impact of an existing active bodysuit, (c) the construction of a finite element model to predict the initial in-brace spinal correction of an existing active bodysuit, and (d) the optimisation of a proposed active bodysuit through material testing and D-optimal design.

The posture, balance and muscle utilisation of ADS patients are still unclear. To enhance current understanding of how ADS contributes to the posture, balance and muscle activity, a total of 10 ADS subjects and 10 asymptomatic subjects are recruited to perform habitual standing and sitting.

A three-dimensional (3D) motion capturing system, force platform and surface electromyography are used in this study. The ADS subjects demonstrated higher knee flexion in the standing posture and increased hip and knee flexion in the sitting posture at the convex side of their spinal curvature. Moreover, the paraspinal muscles and lower extremities at the convex side of the spine generally showed increase in muscle activity compared to the concave side. The findings demonstrated that ADS patients change their balance pattern to compensate for the shift of the gravity line caused by spinal deformity and have asymmetrical muscles that are elongated and stretched at the convex side of the curvature.

A clinical study is conducted to investigate the efficacy of the existing active bodysuit in terms of the in-brace correction, health-related quality of life and feedback from the recruited subjects. Most of the subjects experience a reduction of Cobb angle greater than 5 degrees while the pain score is reduced after 3-months of brace wear. However, the initial in-brace correction effect of the 2-hour clinical study is not adequate due to possible influential variables, such as a low compliance rate and the material used for the bodysuit. Therefore, the correction effect of the active bodysuit should be enhanced in order to prevent the progression of spinal curvature as well as maintain the ability of ADS patients to perform daily activities.

Based on the results of the clinical study, the thermal comfort and corrective effect of the proposed active bodysuit are the areas that require more attention. First, different fabrics are sourced, and material tests are conducted for the inner vest. A biomechanical model is then developed and validated by comparing the results with those of an actual radiographic examination. The model also eliminates the problems of repeated radiation exposure, subject involvement, long manufacturing time, and brace wear time when conducting a wear trial. The biomechanical model shows a trend of spinal correction with good accuracy. To optimise the spinal corrective effect of the proposed active bodysuit, the different material properties of the shoulder straps, waistband, and side and middle struts are modified by using a D-optimal design. It is found that the design combination of woven shoulder straps with Young's Modulus of 243 MPa, elastics Young's Modulus of 0.45 MPa, 6061 aluminum alloy and polyoxymethylene provides the highest in-brace spinal correction which reduces the predicted in-brace Cobb angle from 29.2° to 27°. The stiffness of the waistband is regarded as the most important factor in reducing the Cobb angle, followed by stiffness of the side struts, shoulder straps and lastly the middle strut.

The research results in this study enhance current knowledge on the balance, posture and muscle activity of ADS patients, as well as provide useful information for the design, thermal comfort and mechanics of flexible braces to control spinal deformities and maintain daily activities of ADS patients. The use of FEM and D-optimal design provides an objective, efficient and reliable methodology to evaluate the performance of different brace materials in correcting spinal deformities and optimising the effectiveness of the proposed active bodysuit. The output of this project can be extended to the development of similar orthotic devices and textile medical products.

Publications arising from the thesis

Journal papers

Chung, W. Y. C., Yip, J., Yick, K. L., & Ng, S. P. (2021). Affective association with and preference for flexible brace colors in older adults with spinal deformities. *Color Research & Application*, 47(1), 194-203. https://doi.org/https://doi.org/10.1002/col.22706

Wan, K. W. F., **Chung, W. Y. C.**, Mak, T. H., & Yip, J. (2022). Development of an active video game for postural training for older adults with spinal deformities. *IEEE Transactions on Neural Systems and Rehabilitation Engineering*. (In preparation)

Conference publication

Chung, W. Y. C., Yip, J., Yick, K. L., & Ng, S. P. (2021). Active Training Bodysuits for Adult Degenerative Scoliosis. *Postgraduate Conference on Interdisciplinary Learning,* Lingnan University, Hong Kong, 27-28 March.

Acknowledgements

I would like to express my sincerest gratitude to my Chief Supervisor, Dr. Joanne YIP, Associate Professor of the Institute of Textiles and Clothing at The Hong Kong Polytechnic University for her continuous support, patience, guidance and trust throughout the study and related research. My appreciation also extends to my co-supervisors, Dr. Kit-lun YICK, Associate Professor of the Institute of Textiles and Clothing at The Hong Kong Polytechnic University, and Dr. Sun-Pui Zereance NG, Associate Division Head at the Hong Kong Community College, for their encouragement, insightful comments, and professional knowledge.

I would also forward my appreciation to the Institute of Active Ageing of The Hong Kong Polytechnic University for their assistance with project promotion and subject recruitment, Ngai Hing Hong Company Limited for their technical advice and recommendation for the 3D printing. Further appreciations are also given to all the patients for their dedication and trust in my work.

My special thanks are also extended to my research colleagues and teammates, especially Dr. Annie YU, Dr. Jim LUK, Dr. Jess CHAN, Dr. Frances WAN, Dr. Queenie FOK, Mr. Garcia KWOK, Ms. Nico LIU, Ms. Olivia FUNG, Ms. Charlotte WONG, Ms. Linda SIT, Ms. Eunice TAM, Ms. Lily KWAN, Ms. Maple LEE, Ms. Lisa WONG, Mr. Alex MAK, Ms. Hallie CHEUNG, Mr. Lung CHOW, Mr. Matthew LEUNG, Ms. Charcoal WONG, Ms. Karolyn NING, Mr. Canford WONG, Ms. Joey NG, Mr. Ken HUI and Mr. Ivan OR for their immeasurable help, continuous encouragement and support.

Last but not least, I am greatly indebted to my dearest family members, adorable friends and cat for their unconditional love and support while I was working on my goals throughout the study.

Table of Contents

List of Figures

List of Tables

CHAPTER 1: Introduction

1.1 Research background

The alignment and natural curvature of the human spine are essential for protecting the spinal cord, maintaining an upright posture, and allowing for sufficient mobility and flexibility (Widmer et al., 2019). By maintaining the sagittal and coronal balances of the spine, less stress is exerted onto the spine with less likelihood of pain and fatigue (Muscolino, 2015). However, with ageing, the functional spinal unit of older adults may deteriorate when shifting and rotating of the spine occur. This is called adult degenerative scoliosis (ADS), which is found in the ageing population and caused by degenerative changes in the spine without pre-existing spinal deformities, and results in a Cobb angle that exceeds 10° in the coronal plane according to Silva and Lenke (2010), who developed a classification for degenerative scoliosis. The prevalence of adult scoliosis diagnoses is increasing with medical science advancements. Globally, an approximate overall incidence rate of 6% is found for people who are 50 or older, and 266 million people worldwide are afflicted with ADS (Boos & Aebi, 2008; Ravindra et al., 2018) with an average progression of the spinal curvature of 3.3° per year (Houten & Nasser, 2013); see Figure 1.1. Moreover, the majority or 90% of ADS patients suffer from various levels of lower back pain. In the 2017 Global Burden of Disease report (Figure 1.2), lower back pain was ranked as the primary cause of disability. These demonstrate that ADS is an important spinal condition that needs to be addressed in a timely manner.

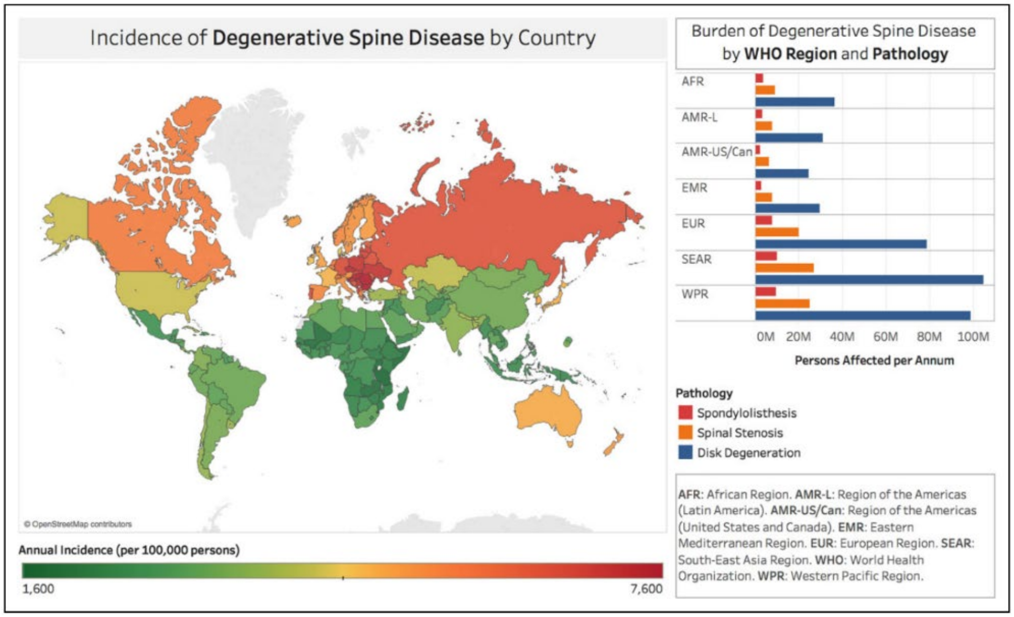

Figure 1.1 Incidence rates of ADS in World Bank and World Health Organization recognised countries (Ravindra et al., 2018)

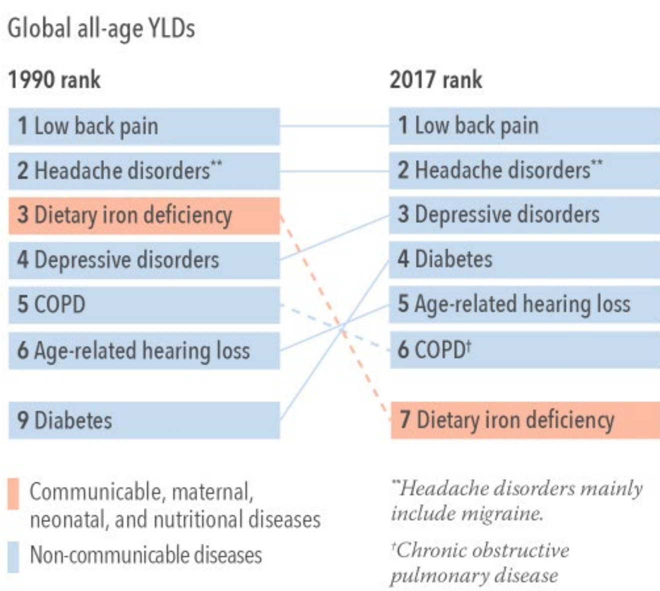

Figure 1.2 Leading causes of disabilities in 1990 and 2017 (Global Burden of Disease Collaborative Network, 2018)

The pathophysiology of ADS has not been completely elucidated. Asymmetric disc and facet joint degenerations are assumed to be the main aetiologies that contribute to the development of ADS (Harrop, Vaccaro, & Awad, 2015). There are some other known risk factors that affect the spinal structure and eventually result in ADS, like osteoporosis and vertebral body compression fractures (Everett & Patel, 2007). ADS is a long-term condition in which the spinal curvature will increase in severity over time. The corresponding spinal deformity causes axial back pain, abnormal posture, spinal claudication, neurological compromise, cosmesis, cardiopulmonary disease and disability (Heary & Albert, 2014) which negatively affect the health-related quality of life (HRQoL) of patients (Birknes et al., 2008). Thus, monitoring and controlling the progression of the spinal curvature are essential once ADS has been diagnosed.

Based on the measured Cobb angle of patients, different treatments are prescribed, including non-operative and operative treatments. Doctors are generally conservative in the surgical treatment of adult scoliosis because the patients have deteriorated bone quality and the complications can be high with surgery (Modi et al., 2010). Surgery would only be recommended if the spinal curvature of the patient is 45° or more, the spinal condition endangers the life of the patient, or conservative treatments have no effect on the patient. Smith et al. (2011) concluded that surgical techniques can be categorised into posterior, anterior and combined procedures for spine decompression and stabilisation. Non-operative treatments like weight loss, pain and anti-inflammatory medications, injections, exercises, manual manipulation and muscular relaxation aim to manage the cardinal symptoms of ADS and used in the early stages of the condition, including to: relieve pain, reverse neurological deficit, eliminate spinal claudication and prevent progression of the spinal curvature (Cox, 2011).

Bracing is regarded as the most traditional conservative treatment to relieve pain, correct posture and reduce the progression of the spinal curvature (Weiss & Werkmann, 2009). There are usually two types of braces available in the market - rigid and flexible braces, which aim to increase the sagittal alignment of the spine and reduce lower back pain by exerting corrective forces onto the back. Nevertheless, the heavy and non-breathable materials used to construct rigid braces can cause discomfort, pressure sores, mental health issues and low treatment compliance. Therefore, research has been conducted to focus on the development and design of brace wear that enhance the wear comfort, user friendliness and aesthetics of semi-rigid and soft braces.

Sit, Yip and Kwan (2020) developed an active bodysuit for older adults between the ages of 50-65 who have diagnosed with ADS. Instead of correcting the spinal deformity, the brace aims to reduce lower back pain, maintain current level of spinal function of patients and prevent progression of the spinal curvature. The active bodysuit is a combination of rigid and semi-rigid materials and textiles to increase the receptivity and wear comfort of patients as opposed to the shortcomings of conventional hard braces. The inner layer is a tightly fitting and breathable material that uses specific design components to passively support the spine and provide corrective forces along with the incorporation of a real-time biofeedback system to alert the user of poor posture. Although the brace configuration optimises fit and exerts corrective forces onto the problematic areas, there are other problems such as insufficient understanding of the balance, posture and muscle activity of ADS patients, limited control of the posture and spinal alignment of ADS patients and lack of durability and user friendliness of the active bodysuit. Therefore, the primary purpose of this study is to investigate the posture and muscle utilisation of ADS patients, evaluate the effectiveness of the active bodysuit, develop a biomechanical model and conduct material testing to modify the active bodysuit that provides the optimum corrective forces, support, wear comfort and fit for older adults with degenerative scoliosis.

1.2 Problem statements

1. Lack of investigation on posture and muscle utilisation of ADS patients

A systematic understanding of how ADS affects the posture and muscle utilisation of the spinal area is still lacking. Most of the previous literature has focused on examining the gait or balance differences between young and elderly which conclude that older adults usually have an unsteady balance and poor posture caused by age and other neurological conditions. Examining the balance and muscle utilisation of ADS patients may generate new insights into correction of their posture and treatment of their spinal deformity. However, there is very little scientific understanding towards the posture and muscle activity of ADS patients and more in-depth analyses should be conducted.

2. Ambiguity of efficacy of active bodysuit

Sit et al. (2020) developed an active bodysuit and conducted a clinical study with a number of subjects to investigate its efficacy. However, the spinal deformity of the subjects does not show significant improvements and the clinical study also involves a biofeedback system which is used to control posture. Therefore, their study may not be able to reflect the actual efficacy of the bodysuit itself and has limitations as an active bodysuit.

3. Low compliance with active bodysuit

In Sit et al. (2020), each subject is required to wear active bodysuit for at least 2 hours each day. Due to the frequent wearing and laundering, the durability of the brace is relatively low. The brace stretched out of shape during the three-months wear trial and the fit of the brace was reduced. Moreover, the design of the bodysuit is quite complicated, and the fabric used has low breathability which reduced the wear compliance of the patients due to the discomfort. Therefore, fabrics with high dimensional stability, wear comfort and durability should be chosen so as to increase the lifespan of the bodysuit while the brace design should be more user-friendly.

4. Limitations of FEMs developed for ADS patients

Recently, there have been a few research or journal papers that discuss the conservative treatment of degenerative scoliosis but most of them have shortcomings due to the absence of clinical trials, insufficient number of subjects involved or comparison with those who are not afflicted with degenerative scoliosis (Zheng et al., 2015). Moreover, the FEMs developed by other researchers are primarily used to address surgery as a treatment and only focuses on the spine or the lumbar part of the spine (Wang et al., 2016). The level of corrective forces imparted by the bodysuit is dependent on the location, magnitude and direction of the pressure exerted on the spine. To fabricate a brace that exerts optimum corrective forces, an FEM of the full-length of the spine, the trunk and skin needs to be formulated to evaluate the performance of the pressure garment without the involvement of real subjects.

1.3 Research Objectives

This project aims to investigate the physical, mechanical and thermal properties of different textiles and accessories that might be used in the development of the modified active bodysuit. By formulating a biomechanical model to simulate the forces exerted by the active bodysuit, the most suitable combination of textiles and accessories that provide optimum corrective forces and support for ADS patients can be identified.

1. To conduct background research on ADS and the different treatment methods and corrective mechanisms involved in order to determine textiles and materials suitable for the active bodysuit for ADS.

2. To investigate the posture, trunk and lower limb muscle utilisation of older adults with ADS in comparison with their asymptomatic counterparts.

3. To evaluate the performance of an existing active bodysuit developed by Sit et al. (2020) and study the materials, biomechanics and spinal corrective effect of the active bodysuit.

4. To formulate a biomechanical model to simulate the corrective forces exerted by the active bodysuit in relation to the mechanical and stress-strain properties of the materials, evaluation of the performance of different combinations of materials, and determine the optimum design.

1.4 Project Originality and Significance

ADS, also known as de novo scoliosis, is a condition of the ageing population caused by degenerative motion segments without pre-existing spinal deformities (Graham, Sugrue, & Koski, 2016). Asymmetric disc and facet joint degenerations are assumed to be the main aetiology that contributes to the development of ADS. The prevalence of adult scoliosis diagnoses is increasing with medical science advancements. Patients with ADS usually suffered from progressive lower back pain with radiculopathy and neurogenic claudication, spinal stenosis, and progression of curvature which negatively affected the HRQoL of patients. Treatments would be performed for ADS patients with Cobb's angle larger than 20˚. Surgery would only be recommended if the spinal curvature of the patient is 45° or more, the spinal condition endangers the life of the patient, or conservative treatments have no effect on the patient. Instead, bracing is a preferred type of conservative treatment for maintaining posture, preventing the progression of the spinal curvature, and relieving the symptoms. However, traditional braces usually lack breathability, and are heavy, and difficult to wear which cause skin problems, dyspnea, and discomfort.

The purpose of the active bodysuit in Sit et al. (2020) is to maintain a certain degree of physical function while minimising the progression and symptoms of ADS as well as enhancing the wear comfort of the brace. Nevertheless, the active bodysuit developed in Sit et al. (2020) was only evaluated based on the results of posture training sessions so that its effectiveness has not yet been verified. Furthermore, the design and materials of the active bodysuit reduce the acceptance and treatment compliance of the patients.

Therefore, an experiment is conducted in this study to compare the posture and muscle activity of ADS patients and asymptomatic individuals so as to identify the spinal abnormalities of ADS patients. A preliminary wear trial will also be conducted to understand the effects and mechanism of the existing active bodysuit. Furthermore, a biomechanical model will be formulated to evaluate the corrective forces exerted by the bodysuit with the aim to find the most effective textile materials with optimum corrective forces and identify the most crucial components for the posture correction of ADS patients. Lastly, an active bodysuit is developed which provides better wear comfort and easier access and optimises spinal correction with modifications made by using different materials for the modified active bodysuit.

This project can enhance the performance of the active bodysuit developed by Sit et al. (2020) and contribute with new knowledge towards posture, muscle activity and medical textiles for ADS, in which a higher level of wearing comfort and corrective effect of the bracing treatment can be achieved. Besides, the effectiveness of braces in treating degenerative spinal deformities can be predicted and evaluated by using the constructed FEM without conducting real life wear trials which translates into a higher degree of reproducibility and efficiency.

1.5 Outline of the thesis

There are a total of seven chapters in this thesis. Chapter 1 provides the background information, problem statement, objectives, project originality and significance and study outline.

Chapter 2 is a literature review which discusses the definition, aetiology and evaluation methods of adult spinal deformities, classifications for adult scoliosis, both conservative and invasive treatments available for ADS with reviews of the design, mechanism and performance of existing braces in the market, and lastly, the posture and muscle activity of ADS patients.

Chapter 3 provides a summary of the research plan and methodology of the study. The objectives of each experiment and procedures are reported with the corresponding testing methods, standards, equipment, and software listed in detail.

Chapter 4 examines the posture, static standing balance and muscle activity of ADS patients and their asymptomatic counterparts in order to identify the spinal abnormalities of ADS patients and determine the functional requirements for the proposed active bodysuit.

Chapter 5 outlines the evaluation results for the active bodysuit developed in Sit et al. (2020). The result is based on 2-hour and 3-month clinical trials which examine the effect of bracing on the spinal deformities, fit of the active bodysuit and the HRQoL of the subjects.

Chapter 6 elaborates on the design criteria of the proposed active bodysuit; the sourcing of different textile materials; and conducted laboratory tests to select the most appropriate types of materials for the proposed active bodysuit in accordance with the established design criteria.

Chapter 7 presents the formulation of the torso, skeleton and bodysuit models of the FEM. The model is validated by comparing in-brace radiographic images. The validated biomechanical model is used to optimise the corrective effect of the proposed active bodysuit by modifying the brace materials.

Chapter 8 is the last chapter which concludes all of the completed work, discusses the limitations of the study and provides recommendation for future works.

CHAPTER 2: Literature Review

2.1 Introduction

The purpose of the thesis is to investigate the posture and muscle activity of ADS patients as well as develop an FEM and improve on the mechanical performances and design of an active bodysuit developed by Sit et al. (2020) through the use of different textile compositions, accessories and soft and rigid materials. In this chapter, a brief description about the definition, assessment methods, classifications and treatments of adult spinal deformity will be discussed. Then, the features, functions, and mechanisms of different ADS treatments available in the market will be reviewed. Thirdly, the design, problems of the active bodysuit and critical elements for effective bracing treatment are examined in the following section. Lastly, the biomechanical model developed for measuring the pressure and corrective forces exerted by the brace and methods of conducting posture and muscle activity evaluation are revealed.

2.2 Overview of adult spinal deformity

2.2.1 Definition, aetiology, and evaluation methods of adult scoliosis

According to the Scoliosis Research Society Terminology Committee (1976), scoliosis is a three-dimensional (3D) deformity of the spine in the coronal and sagittal planes where the spine has an abnormal curvature with a Cobb angle greater than 10˚ or the spine is bending forward. The pathogenesis of adult scoliosis is assumed to be the degeneration of the intervertebral discs and facet joints which cause asymmetric loading and deformity of the spine segment (Bess et al., 2016). ADS is diagnosed at around the age of 40 and the prevalence of ADS is approximately 60% of the aging population (Kebaish et al., 2011). ADS patients suffer from progression of the spinal curvature, nerve pain like radiculopathy, and neurogenic claudication which leads to pinching, cramping or achy feeling in the spine and lower extremities, lower back pain which causes disability or feelings of fatigue when walking. Moreover, there is spinal stenosis due to the formation of osteophytes at the endplates of the vertebral bodies and facet joints which reduces the appearance of patients to a physical profile that is asymmetric, squished and deformed (Ma et al., 2017). These symptoms of ADS deteriorate the quality of life and mental health of ADS patients since they may have lower self-esteem due to reduced mobility and physical aesthetics. The Adam's forward bending test is a commonly used examination method to screen patients with scoliosis (Figure 2.1). Patients are instructed to stand upright, extend their arms forward with palms and feet together, then lower their head and bend forward at a 90-degree angle. The examiner would stand behind the patient to determine if a rib arch is present. The angle of trunk rotation (ATR) is measured during the test by using a scoliometer as the patient is bending forward (Ma et al., 2017). Patients with an ATR larger than 5 degrees may have scoliosis and a radiographic evaluation is recommended for a diagnosis of scoliosis.

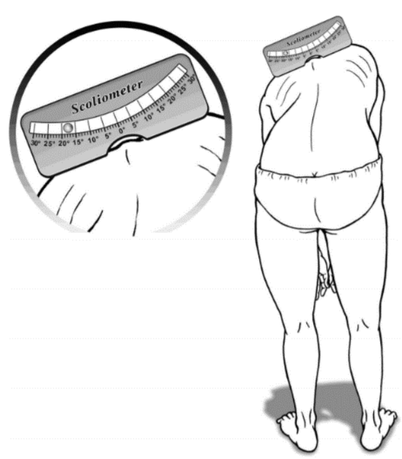

Figure 2.1 Adam's Forward Bending Test (Ma et al., 2017)

A diagnosis of scoliosis can be made through radiographic evaluation (Zhu et al., 2017) such as X-ray imaging, magnetic resonance imaging or computerised tomography (CT). The X-ray images should be taken in the upright standing position which includes the clavicle, full-length spine, pelvis and femoral heads in both the posterior-anterior (PA) and lateral views. Magnetic resonance imaging and CT are only used for radiographic evaluation when patients have symptoms in the lower extremities and cannot maintain the standing position (Lemmers, Lankveld, Westert, Wees & Staal, 2019). Using the radiographic images, the Cobb angle, coronal balance, shoulder symmetry, thoracic kyphosis (TK), lumbar lordosis (LL), subluxation, sagittal vertical axis (SVA), pelvic tilt (PT), pelvic incidence (PI) and sacral slope (SS) can all be measured. Scoliosis is determined by measuring the Cobb angle of the spine which is the angle between the intersecting lines drawn perpendicular to the upper endplate of the proximal vertebra and lower endplate of the distal vertebra (Sardjono et al., 2013) as shown in Figure 2.2.

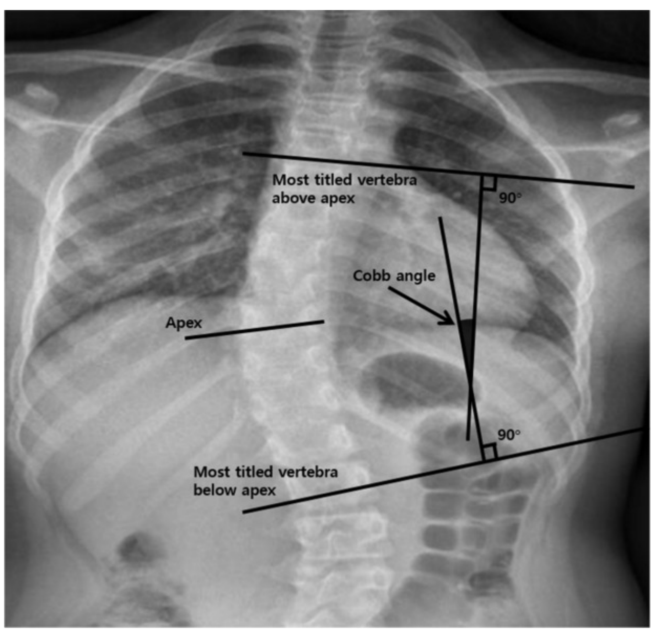

Figure 2.2 Measurement of Cobb angle (Lee et al., 2018)

Coronal balance (Figure 2.3) is associated with the alignment of the C7 plumb line (C7PL) and central sacral vertical line (CSVL). The C7PL can be found by drawing a vertical line downwards from the centre of the C7 vertebral body to the centre of the sacrum, while the CSVL can be found by drawing a vertical line upwards through the midpoint of S1. A neutral coronal balance is maintained if the C7PL and CSVL coincides, with a tolerance of ± 2 cm between these two lines (Cho et al., 2016). If the C7PL has a displacement greater than 2 cm on the right side of the CSVL, it is considered as positive coronal balance. If the displacement of C7PL is located on the left side of the CSVL, this is referred to as negative coronal balance. In the coronal plane, the clavicle angle (CA) and T1 tilt angle are used to assess the shoulder symmetry of patients (Sarwahi, Wendolowski, Gecelter, Amaral, & Thornhill, 2016). The CA is the angle between a line that passes through the highest point of the left and right clavicles and a horizontal reference line is drawn perpendicular to the lateral plane (Figure 2.4). The Tl tilt angle is measured by drawing a line at the cephalad end plate of T1 and a horizontal line perpendicular to the C7PL (Figure 2.5). If the right clavicle or right edge of T1 is higher than the left side, the CA and Tl tilt angle are regarded as negative, and vice versa. Coronal subluxation is the dislocation of the vertebral body, which is determined by measuring the distance between the superior corner of the caudal vertebrae to the inferior corner of the upper endplate of the next vertebral body (Menezes, Lima, Falcon, & De Souza, 2019).

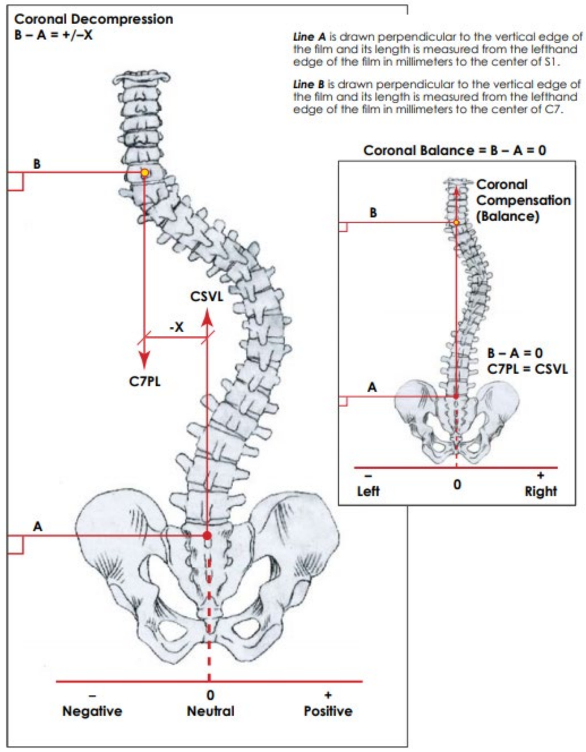

Figure 2.3 Coronal balance measurement (Kuklo, 2007)

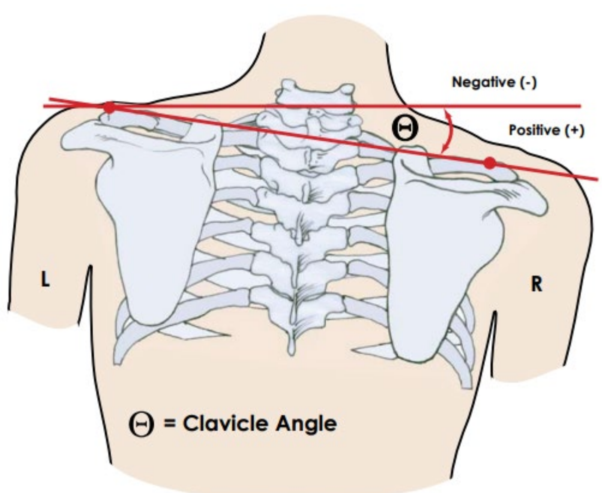

Figure 2.4 Clavicle angle (Luhmann et al., 2016)

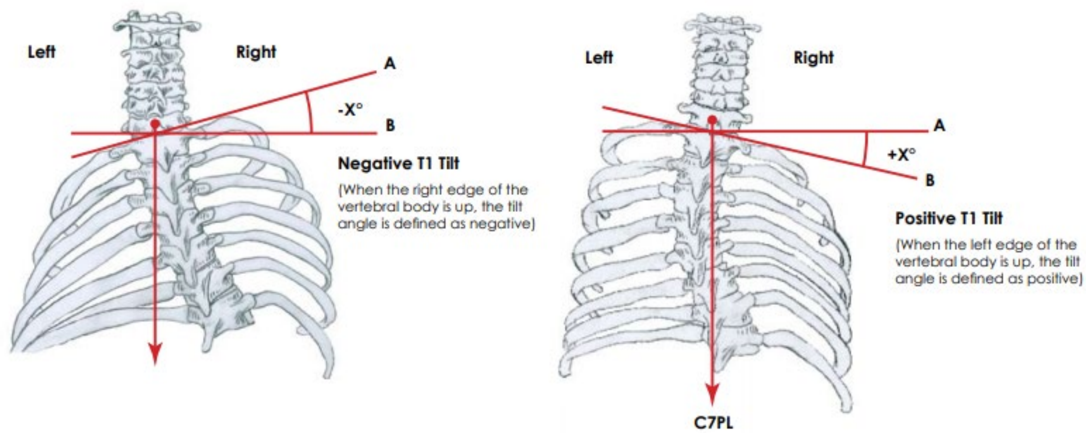

Figure 2.5 T1 tilt angle (Luhmann et al., 2016)

In the sagittal plane, measurements are taken to describe the spinopelvic relationship of the patients. Zhou et al. (2019) indicated that the TK is measured from the inferior endplate of T2 or T5 to the inferior endplate of T12 while LL is measured from the cephalad endplate of T12 to the caudal endplate of S1 by applying the Cobb method (Figure 2.6). Sagittal balance can be identified by the distance between the C7PL and the posterior edge of the sacral promontory (Figure 2.7), which is known as the SVA. Spines with normal sagittal alignment have a 0 to 4 cm SVA (Wu et al., 2014). When the C7PL falls more than 2-4 cm anterior to the dorsal rostral aspect of the S1 vertebrae, the sagittal balance is positive, and vice versa. Sagittal subluxation (Figure 2.8) is similar to coronal subluxation but measures the distance between the posterior-inferior corner of the caudal vertebrae to the posterior-superior corner of the upper endplate of the next vertebral body. Retrolisthesis is identified if the distance is less than zero while spondylolisthesis is classified if the distance is greater than zero (Freedman et al., 2009). PI is the angle between the line perpendicular to the midpoint of the sacral plate and a line that connects this point to the centre of the femoral heads. The PI can also be found by adding PT and SS (Figure 2.9). PT is the angle between a line that connects the midpoint of the sacral endplate and the centre of the femoral heads and the vertical axis while SS is the angle between the sacral plate and a horizontal line (Jeon et al., 2013). Detailed measurements and evaluation of the posture, shoulders, spine and pelvis are used to determine the treatments suitable for each patient.

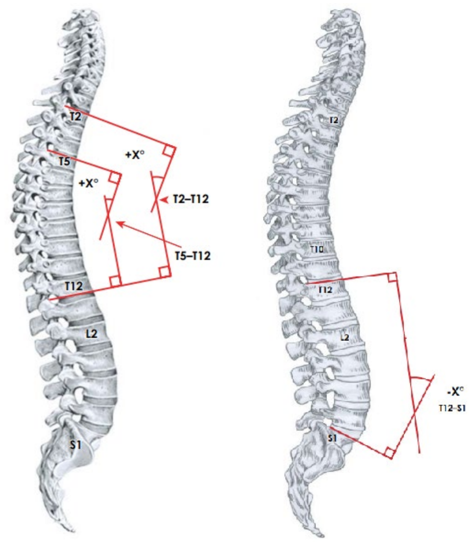

(a) (b)

Figure 2.6 (a) Angle of thoracic kyphosis and (b) lumbar lordosis (Palou, 2014)

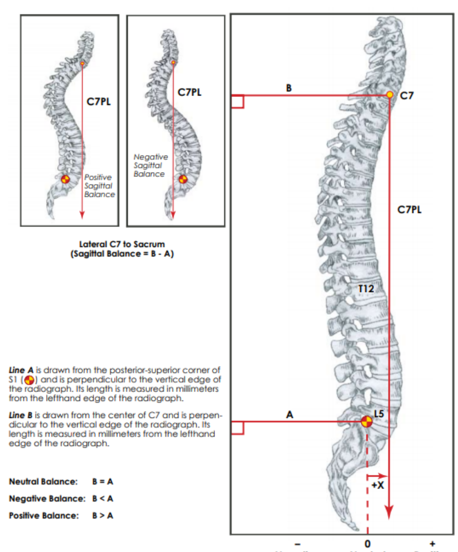

Figure 2.7 Sagittal balance measurement (Sullivan, Jain, Aziz, & Khanna, 2017)

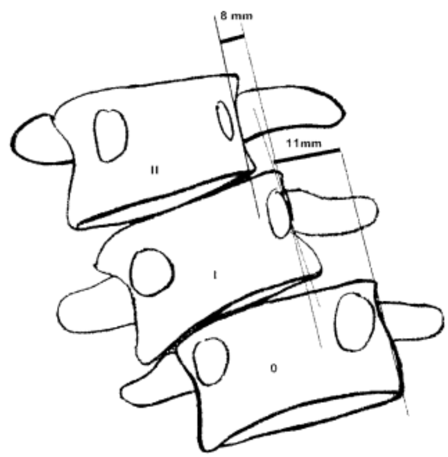

Figure 2.8 Coronal, sagittal and rotatory subluxations (Ploumis et al., 2006)

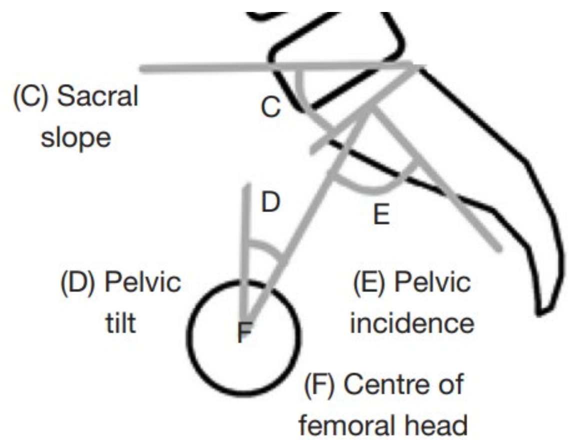

Figure 2.9 Measurement of pelvic incidence, pelvic tilt and sacral slope (Cheung, 2020)

2.2.2 Different classification systems of ADS

2.2.2.1 Aebi classification system

Aebi (2005) proposed a classification system based on the aetiology of patients which categorises adult scoliosis into three types: de novo scoliosis, adult idiopathic scoliosis (AdIS) and secondary scoliosis caused by extraverbal abnormalities (Figure 2.10). De novo scoliosis, also known as Type

1, is primary degenerative scoliosis, which is caused by asymmetric disc and facet joint degenerations developed during adulthood. The deformity is usually found in the lumbar or thoracolumbar region where the apex is between L2 to L4, with considerable apical vertebral rotation and sagittal malalignment. The asymmetric disc and facet joint degenerations may lead to spondylosis, facet joint arthritis and osteophytes which finally contribute to the formation of spinal stenosis. AdIS or Type 2 scoliosis is considered idiopathic scoliosis without a clear aetiology. The patients already have a pre-existing spinal deformity during childhood and might have received surgical or conservative treatments before. However, the progression of the curvature takes place in adulthood. The curvature mostly appears in the lumbar or thoracolumbar spine or as a double curve in those two areas. Patients may have poor sagittal balance with a flat back or kyphosis and spinal stenosis. Secondary scoliosis caused by extraverbal abnormalities or Type 3 scoliosis is an adult secondary degenerative scoliosis in which deformity has developed in the thoracolumbar, lumbar and lumbosacral parts of the spine. Secondary scoliosis caused by extraverbal abnormalities can be further divided into two subgroups, where the cause for Type 3a scoliosis can be idiopathic, neuromuscular or a congenital curve or related to the pelvic obliquity because of leg-length discrepancy or hip pathology or a lumbosacral transitional anomaly. For Type 3b scoliosis, deformities result from weak bones such as osteoporosis, along with asymmetric segmental degeneration. This classification is simple and able to predict the natural history of the deformity based on the aetiology (Tambe & Michael, 2011). Yet, the classification system cannot be used to direct surgical treatment as the system has not interpreted the individual features of scoliosis or taken into account spinopelvic alignment.

Type	Description	Etiology
I	Primary degenerative scoliosis ("*de novo*" scoliosis)	Asymmetric disc and facet joint degeneration
II	Progressive idiopathic scoliosis of the lumbar and/or thoracolumbar spine	Idiopathic scoliosis present since adolescence, progression due to mechanical reasons or bony and/or degenerative changes
III (a)	Secondary adult scoliosis mostly thoracolumbar or lumbosacral	Secondary to an adjacent thoracic or thoracolumbar curve of idiopathic, neuromuscular or congenital origin
		Obliquity of pelvis due to leg length discrepancy orhip pathology with secondary spinal curve
		Lumbosacral transitional anomaly
III (b)	Deformity progressing mostly due to bone weakness, for example, osteoporotic fracture with secondary deformity	Metabolic bone disease, osteoporosis

Figure 2.10 Aebi classification (Dagdia, Ito & Kokabu, 2019)

2.2.2.2 Schwab classification

Apart from the Aebi classification system, Schwab et al. (2006) presented a classification system based on a clinical trial of 947 adults with ADS where the patients are classified according to radiographic parameters, including the apex of the scoliosis curve, LL and subluxation (Figure 2.11). First, the system divided patients into five groups at the apical level. Type 1 is the thoracic curve where deformity only occurs in the thoracic region. Types 2 and 3 are the upper and lower thoracic major curves where the apex of the curve is located at T4-T8 and T9 – T10 respectively. Type 4 is the thoracolumbar major curve with the apex at T11 –L1 while Type 5 is the lumbar major curve with apex at the vertebrae of L2 – L4. The major curves are the largest Cobb angle measured by using the frontal radiograph images and minor curves in Types 2 to 4 are the other curvatures with less significant value. When patients have more than two major curvatures, the lower curve would be chosen as the major curve for grouping purposes. Patients are categorised into three groups by using lordosis and subluxation modifiers separately. For lordosis modifiers, a Cobb angle between the T12-S1 vertebral body is considered. Patients with lordosis modifier A have a marked lordosis in which the LL angle is larger than 40˚. Patients with lordosis modifier B have a moderate lordosis in which the LL angle is between 0˚ to 40˚ and patients with lordosis modifier C has no lordosis present where the Cobb angle is larger than 0˚. For the subluxation modifier, the maximum intervertebral subluxation found in the coronal or sagittal plane is classified, where zero subluxation indicates that the patient has no subluxation; a '+' sign implies a moderate subluxation of 1 – 6 mm and '++' is severe subluxation more than 7 mm. This comprehensive system is highly reliable and significantly and statistically correlated with the radiographic parameters and the clinical outcomes and treatment analyses. However, the distribution of the curve types is uneven, and the classification has little impact for surgical planning (Dagdia et al., 2019), so more parameters or descriptions should be used to refine the system.

Classification	Radiographic Criteria
TYPE	
I	Thoracic-only curve (no other curves)
II	Upper thoracic major, apex T4-8
III	Lower thoracic major, apex T9-10
IV	Thoracolumbar major curve, apex T11-L1
V	Lumbar major curve, apex L2-4
LUMBAR LORDOSIS MODIFIER	
A	Marked lordosis (> 40 degrees)
B	Moderate lordosis (0–40 degrees)
C	No lordosis present (Cobb > 0 degrees)
SUBLUXATION MODIFIER	
0	No intervertebral subluxation, any level
+	Maximal measured subluxation, 1–6 mm
++	Maximal subluxation > 7 mm

Figure 2.11 Schwab classification system (Schwab et al., 2006)

2.2.2.3 SRS Scoliosis Research Society classification system

The Scoliosis Research Society (SRS) also established a classification system in 2006 which categorises patients into seven groups based on their standing full-length X-rays. The SRS classification system considers both the coronal and sagittal planes along with the global spinal alignment through three modifiers (Lowe, Berven, Schwab, & Bridwell, 2006). In the beginning, surgeons would identify the type of curve based on the apex in the coronal plane, including single thoracic, double thoracic, double major, triple major, thoracolumbar, lumbar "de novo" and primary sagittal plane (SP) deformity (Figure 2.12). The major curves are defined as curvatures at the thoracic regions that are equal to or larger than 40˚, the proximal vertebrae are towards the side of the C7PL and have a CA or T1 tilted angle of 10˚ or larger while the thoracolumbar and lumbar curves are greater than 30˚ and apical vertebral body is away from the CSVL. In order to be classified as SP deformity, the regional sagittal modifier has to show the presence of kyphosis without a major spinal curvature in the coronal plane. The regional sagittal modifier describes the kyphosis or flat back in four different regions and only included when more than one sagittal measurement exceeds the designated normal range, the angle of the proximal thoracic at T2 to T5 and thoracolumbar of T10 to L2 should be less than 20˚, the main thoracic angle at T5 to T12 should be smaller than 50˚while the lumbar curve from T12 to S1 should be larger than -40˚. The lumbar degenerative modifier is applied when patients have loss of disc height and facet arthropathy (degenerative disc disease (DDD)) is found between L1 and S1, degenerative lumbar spondylolisthesis (LIS) is equal to or more than 3 mm in the lumbar region, and the vertebral subluxation angle (junctional L5-S1 curve (JCT)) is larger than 10 degrees in the coronal or sagittal plane. The last modifier is the global balance modifier which takes coronal and sagittal balances into account, and a sagittal imbalance that exceeds 5 cm or a coronal imbalance of 3 cm or higher are regarded as significant. Benzel (2012) showed that the detailed SRS classification system contributes to developing an evidence-based guide for patient management, but the system is too complicated and fails to consider clinical parameters like the symptoms and age of patients which surgeons feel are difficult to adapt in choosing the most suitable surgical intervention.

Primary curve types
- Single thoracic (ST)
- Double thoracic (DT)
- Double major (DM)
- Triple major (TM)
- Thoracolumbar (TL)
- Lumbar “de novo”/idiopathic (L)
- Primary sagittal plane deformity (SP)

Adult spinal deformity modifiers

Regional sagittal modifier (include only if outside normal range as listed)
- (PT) Proximal thoracic (T2–T5): ≥+20°
- (MT) Main thoracic (T5–T12): ≥+50°
- (TL) Thoracolumbar (T10–L2): ≥+20°
- (L) Lumbar (T12–S1): ≥−40°

Lumbar degenerative modifier (include only if present)
- (DDD) ↓ disc height and facet arthropathy based on x-ray include lowest involved level between L1 and S1
- (LIS) listhesis (rotational, lateral antero, retro) ≥3 mm include lowest level between L1 and L5
- (JCT) junctional L5–S1 curve ≥10° (intersection angle superior endplates L5 and S1)

Global balance modifier (include only if imbalance present)
- (SB) sagittal C7 plumb ≥5 cm anterior or posterior to sacral promontory
- (CB) coronal C7 plumb ≥3 cm right or left of CSVL

SRS definition of regions
- Thoracic: apex T2–T11–T12 disc
- Thoracolumbar: apex T12–L1
- Lumbar: apex L1–L2 disc–L4

Criteria for specific major curve types

1. Thoracic curves
   - Curve ≥40°
   - Apical vertebral body lateral to C7 plumbline
   - T1 rib or clavicle angle ≥10° upper thoracic curves
2. Thoracolumbar and lumbar curves
   - Curve ≥30°
   - Apical vertebral body lateral to CSVL
3. Primary sagittal plane deformity
   - No major coronal curve
   - One or more regional sagittal measurements (PT, MT, TL, L) outside normal range

Figure 2.12 SRS classification (Lowe, Berven, Schwab, & Bridwell, 2006)

2.2.2.4 SRS-Schwab classification

In 2012, a comprehensive classification system emerged which combined the SRS and Schwab classifications to emphasise the importance of the pelvis in controlling the movement of the spine and lower limbs. The system included spinopelvic parameters and global sagittal balance (Slattery & Verma, 2018). All of the radiographic parameters are relevant to treatment planning and clinical entities such as the HRQoL outcome score and the pain and disability scores in the Oswestry Disability Index (ODI). The system determines the curvature type of patients according to the maximal Cobb angle measured in the coronal plane (Schwab et al., 2012), Type D are the double major curves, while Type L is the thoracolumbar or lumbar major curve at T10 or below. Type T refers to thoracic-only curve with a lumbar curve less than 30˚ where the apex should be located at T9 or above and Type N denotes no major coronal deformity. The major curves for Types D, L and T should be larger than 30˚ while all of the angles measured in patients with Type N should be smaller than 30˚. Then, the sagittal deformities are characterised through three sagittal modifiers: PI-LL, SVA and PT which are important for operative planning, pelvic retroversion assessment, global body alignment and reducing the risk of pain and disability (Smith et al., 2013). The three modifiers are divided into three groups: non-pathologic for Group '0', moderate deformity for Group '+' and serious deformity for Group '++', as shown in Figure 2.13. The system describes the nature and severity of the curves and has a high degree of intra-rater and inter-rater reliabilities. The system is also easy to use and produces consistent results (Liu et al., 2013).

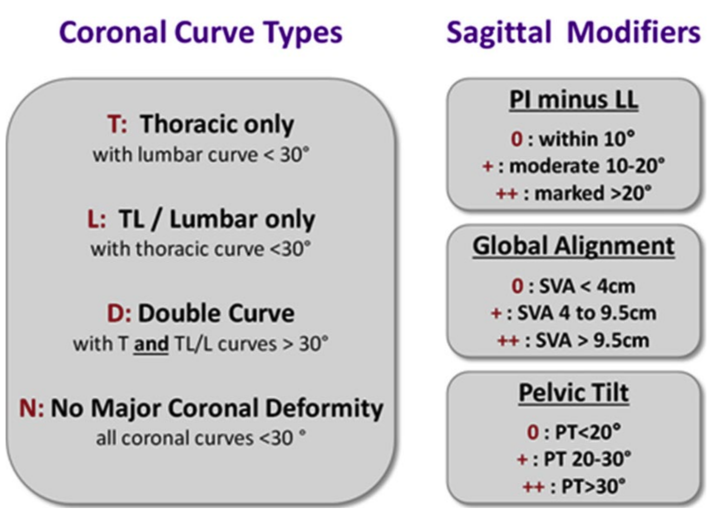

Figure 2.13 SRS-Schwab classification (Hallager et al., 2016)

2.2.3 Treatment for ADS

2.2.3.1 Invasive treatment - surgery

The goals of surgery for patients include nerve decompression, deformity correction, and reduction axial back pain. Surgical treatment is considered when pain has not been reduced through the use of conservative treatments, or is preventing daily activities from being carried out, worsening deformity, or causing radicular or neurogenic symptoms. Surgeons need to take into consideration the general conditions of the patients, osteoporosis, stiffness of the spinal curve and the coronal and sagittal imbalances. Prior to conducting the surgery, doctors need to examine various conditions such as age, body mass index (BMI), medical issues, surgical history, cardiac and pulmonary functions, bone density and whether the patient smoked cigarettes and if so, the rate of smoking (Weinreb, Bianco, Lafage, & Schwab, 2014). The importance of risk assessment and surgical planning in ADS is to predict the possibility of perioperative complications, readmissions, and mortality when patients undergo a lengthy surgery and require postoperative management. Osteoporosis is the second factor for consideration because spinal surgery for scoliosis is spinal fusion so if the patient has poor bone quality, the fixation strength would be reduced, corrective effect would be lower and pseudarthrosis (failed spinal fusion) may result. Segmental support or bone cement are used to strength the vertebral body before inserting other instrumentations (Scheufler et al., 2010). As ADS patients have reduced curve flexibility with spinal degeneration, it is difficult to correct the scoliosis. Lastly, the recovery of sagittal imbalance is more crucial than correcting the scoliosis itself (Faldini et al., 2015). Some scoliosis cases have increased the sagittal imbalance of the patient; therefore, the real aetiology and cause of clinical presentations should be investigated when considering an appropriate surgical option. Although different surgical approaches and classifications have been suggested, doctors have yet to reach consensus on the optimal solution due to the high complexity of ADS and numerous combinations of confounding comorbidities (Berven et al., 2018). Nevertheless, the preference of patients, risk aversion and perceive preoperative health status complicate the decision for the most suitable operative treatment (Fu et al., 2011). Therefore, different surgical techniques are elaborated in the following paragraphs instead of explaining about the different surgery classifications.

2.2.3.2 Decompression

Decompression is used in cases with mild lumbar scoliosis and patients with spinal stenosis. The surgery can be performed from the cervical to lumbar spine which reduces neurological compression and alleviates radiculopathy, neurogenic claudication or the corresponding symptoms (Cho et al., 2014). During the operation, patients are required to lie face down and an incision is made in the back muscles which are then lifted. The lamina and thickened ligaments are removed, allowing more space for the lateral spinal canal so that the bone spurs can be removed (Figure 2.14). Decompression surgery can be classified into 5 types according to Boos and Aebi (2008). One is laminectomy which removes the entire lamina while laminotomy is removing part of the lamina in order to create more space for the spinal canal. After that, the facet joint may be trimmed to provide more space for the nerve root. Two is discectomy, which is done to partially or completely remove the degenerated, displaced disc that exerts pressure onto the nerves. Third, laminaplasty aims to increase the space for the spinal canal by taking out the one side of the laminae at the cervical region (Wang et al., 2011). Finally, foraminotomy involves the removal of bones around the edge of the neural foramen. Compared to spinal fusion, decompression is less invasive and hence patients can recover more quickly.

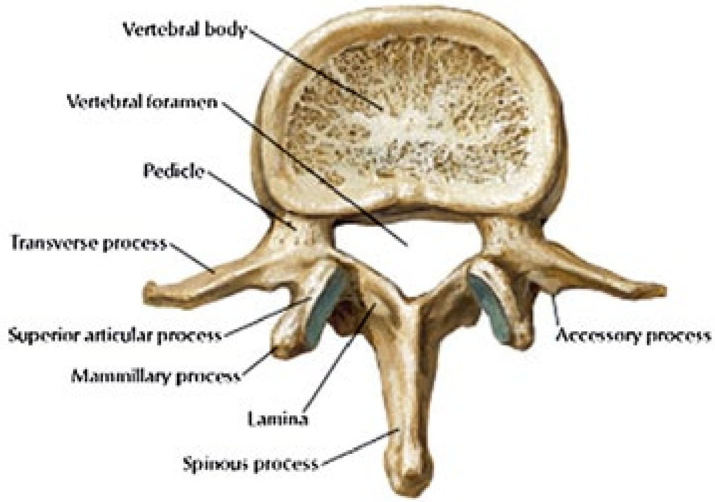

Figure 2.14 Anatomy of human lumbar vertebra (Kraft & Wozniak, 2011)

2.2.3.3 Fusion

Fusion surgery is performed to improve the spinal stability, correct deformity, reduce pain and muscle fatigue and prevent recurrence of nerve compression. When patients have a large Cobb angle with spinal instability, fusion and decompression surgeries can be executed together to fuse two or more vertebral segments (Faldini et al., 2013). Depending on the location of the spinal deformation, different fusion approaches can be used (Figure 2.15). Anterior lumbar interbody fusion (ALIF) requires an incision made from the abdominal or front leg which can significantly correct the deformity, is very well received by patients, involves minimal vessel injury and preserves supplementary motion segments (York & Kim, 2017). Nevertheless, ALIF may lead to several comorbidities such as vascular damage, subsidence, abdominal hernia and graft displacement. Posterior lumbar interbody fusion (PLIF) and transforaminal lumbar interbody fusion (TLIF) both require an incision to made on the back. Kurra et al. (2018) reported reduced Cobb angle and LL. Patients reported outcomes and high satisfaction rate of the two posterior approaches, but they both have a high complication rate and limited degree of correction at each level. Another approach that combines the above approaches is called anterior-posterior fusion in which surgery is performed in the front and back of patients who have a large curvature at the coronal and sagittal planes. This approach has a higher fusion rate, deformity correction and neural decompression and better overall treatment outcome (Mataliotakis et al., 2017). However, the combined procedures require a longer duration of the surgery, which result in increase in the stress of patients and larger amount of blood loss which mean more complications and higher mortality (Youssef et al., 2013). Finally, direct lateral interbody fusion (DLIF) and extreme lateral interbody fusion (XLIF) are performed from the side of the patients. These lateral approaches are minimally invasive for treating ADS patients (Wang et al., 2014) which reduces the perioperative complications and blood loss compared with the anterior and posterior approaches. Yet, Epstein (2019) concluded that the transpsoas approaches have higher risk of neural injury, malposition of the XLIF instrumentation, pseudarthrosis and subsidence. After making the incision, surgeons connect the adjacent vertebral body together through bone grafting (Burger, 2014). The bone grafts are taken from the pelvis bone of the patients (Minas, Ogura, Headrick, & Bryant, 2018), cadavers or synthetic substances like tricalcium phosphate which promote the growth of bone and speed up the healing process. Subsequently, doctors may apply different instrumentations like metal plates, screws or rods to hold the vertebrae in place while the bone grafts are healing.

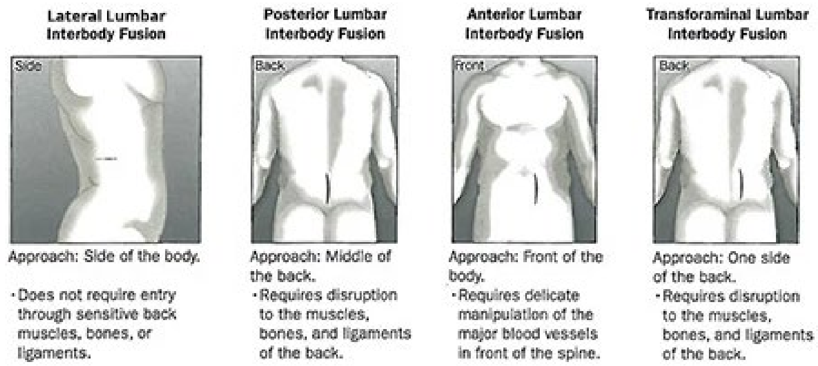

Figure 2.15 Different fusion approaches (The Spine Center, 2021)

2.2.3.4 Non-invasive treatment for ADS patients

The purpose of non-operative treatments is to improve the HRQoL by reducing the cardinal symptoms listed in Table 2.1, like pain relief, spinal claudication, spinal curvature progression and neurological deficit, and inhibit the functional disability of ADS patients (Slobodyanyuk et al., 2014). A variety of different treatment options have been recommended but there is limited evidence of their efficacy and few studies have provided conclusive findings on the efficacy of non-invasive treatments. Conservative treatments can be classified into five main categories, including: physical therapy, alternative therapy, injections, medication and bracing. Physical therapies aim to strengthen and stabilise the core muscles and address the muscle imbalance of patients by stretching the shortened muscles, so that the asymmetric muscles would relax and hence increase the flexibility and muscle support of ADS patients (Alanazi, Parent, & Dennett, 2018; Yang et al., 2015). Alternative therapies are nonconventional medical treatments that rely on pseudoscience; these have inadequate scientific evidence to support their efficacy, such as acupuncture, chiropractic, and rolfing. The theory behind these manual therapies is to alleviate the strain and stress of the body of the patient to create more spacing between the vertebral body (Liu et al., 2009; Morningstar, 2011), thus allowing the realignment and adjustment of the spine. Injections such as epidurals steroid injections or facet joint injections which fill the prone area (Yamada et al., 2016) and medications help to relieve the source of pain and reduce inflammation and pain temporarily. Bracing to treat ADS has distinctive corrective pressure principles compared to adolescent scoliosis which aims to decompress the disc and transfer the pressure on the iliac crest (de Mauroy et al., 2016b), and achieve coronal and sagittal balances by stabilising the lumbar spine, reduce pain and the progression of the spinal curvature (Everett & Patel, 2007). Some surgeons have been critical of brace wearing since this may weaken the trunk muscles. Instead, the daily duration of brace wear for effective treatment and the effects on the trunk muscles have yet to be confirmed. Discomfort is the most frequent reported side effect of wearing a brace, which leads to low wear compliance and results in uncertainties in the efficacy or poor result of the bracing treatment (Palazzo et al., 2017). Therefore, this project will investigate the wear comfort of an active bodysuit and the elements that lead to effective bracing treatment such as the materials used, duration of brace wear and the mechanisms of the brace.

Table 2.1 Treatment options for ADS patients (York & Kim, 2017)

Cardinal symptoms of ADS	Treatment options
Back Pain	Medication Bracing Facet Joints Injections Isometric Exercises Swimming
Radicular Pain & Neurological Deficit	Medication Exercise Immobilization Root Blocks Surgical Decompression
Spinal Claudication	Epidural Blocks Medication Exercise Surgical Compression
Curve Progression	Bracing Stabilizing Surgery

2.3 Features, functions and corrective mechanisms of existing braces

Bracing is a conventional non-invasive treatment to restore the balance and alignment of the spine in both in the frontal and sagittal planes, stabilise the spine, reduce spinal curvature progression, minimise the cardinal symptoms of scoliosis, and maintain the current functional ability of the patient while reducing the need for spinal surgeries. Usually, patients with mild scoliosis receive bracing treatment to reduce the curvature of the spine through the application of external mechanical forces towards the spine and trunk such as through the three-point pressure system or dynamic forces. Bracing is likely to minimise the possible risks, psychological barriers and care management found during or after the treatment compared to invasive treatments. In the following, both conventional and innovative braces available in the market including the active bodysuit will be deliberated and the important elements that result in effective bracing treatment will be examined accordingly.

2.3.1 Traditional braces

Lumbar spinal orthoses (LSO) and thoracic lumbar spinal orthoses (TLSO) are conventional rigid or semi rigid braces which have been widely accepted and adopted by doctors and physiotherapists (Figure 2.16). Each brace is custom made according to the body alignment of the patients in order the support, align and correct deformities, inhibit ADS symptoms while restricting and stabilising the affected parts of the body. Patients are to be maintained in the upright position when casting a mould for the brace, and then two pieces of heated thermoplastic, most likely polyethylene, are placed around the body (McAviney, Mee, Fazalbhoy, Du Plessis, & Brown 2020). The brace can either have an opening at the front or side with Velcro straps as the fastening. Professional physiotherapists may add pressure pads to the inner side of the brace and mark the appropriate tightness on the Velcro straps to create the best fit and exert optimal corrective forces. The difference between TLSOs and LSOs is that the former are an underarm brace that cover the rib cage, lower back and pelvis to treat more severe deformities and as surgery repair while the latter only control the movement of the lumbar part in the frontal, sagittal and transverse planes with less support and movement restriction. Both LSOs and TLSOs should be worn four to six hours each day, but the plaster cast may cause discomfort, pressure ulcers, pulmonary problems or even muscle atrophy (de Mauroy et al., 2016a).

(a) (b)

Figure 2.16 (a) Custom made LSO, and (b) TLSO brace (Kim et al., 2013)

2.3.2 sBrace

The sBrace is a customised TLSO brace that consists of 3 parts: the sBrace trunk module and two rBows with nylon straps on the left and right sides as shown in Figure 2.17. The biomechanics of the sBrace are based on the morphology of the patients based on body measurements, radiographic images and clinical pictures. The brace is then manufactured through the use of computer-aided design (CAD) software. During the fitting session, the trunk module can be trimmed according to the height of the patient when correcting the sagittal balance of the spine and the rbows can be adjusted which provide both active and passive corrective forces and stabilises the body without mobility restrictions. Gallo (2014) indicated that compared to traditional bracing, the sBrace is effective for pain reduction, improving the quality of life of ADS patients and preventing operative treatment with fewer side effects like pressure marks or discomfort, but there are challenges in donning the brace.

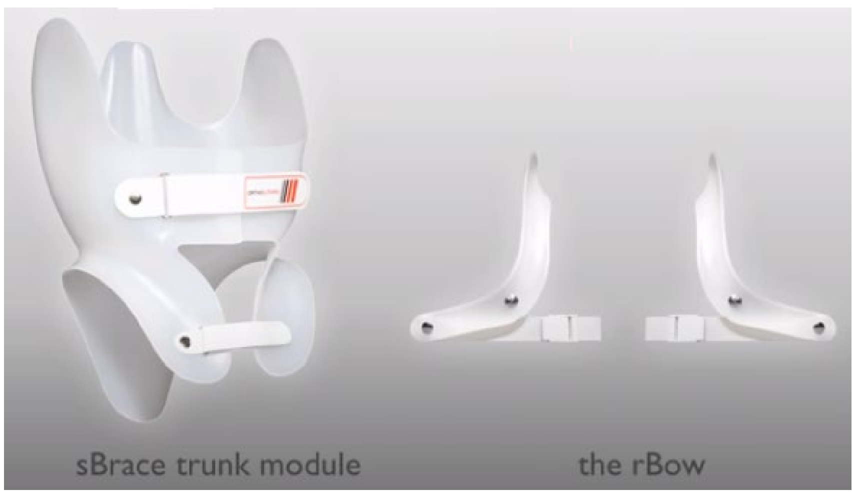

Figure 2.17 Design of sBrace (Gallo, 2014)

2.3.3 Physio-logic brace®

The physio-logic brace®, as known as the "sagittal realignment brace", is worn to address chronic lower back pain, loss of LL and changes in posture during daily activities by inhibiting the lateral movement of the lumbar. Patients are required to wear the physio-logic brace® for at least 20 hours daily in the first six months. After the user is measured, a foam model is developed from hard foam block via CAD techniques, and then a layer of heated polyethylene is vacuumed to the surface of the foam model. The brace is trimmed, further modified based on the body shape and a Velcro strapping system is adhered to both sides with the brace openings (Figure 2.18). The physio-logic brace® has a hollow at the centre front of the brace so that the hard brace exerts apical pressure at L2 and the hollow allows the trunk to shift for spine realignment and maintains the pulmonary functions of patients (Weiss & Werkmann, 2009). However, the spinal deformities and symptoms might be worsened such as the deconditioning of the paraspinal muscles, skin irritation and pressure marks (Graham, Sugrue, & Koski, 2016).

Figure 2.18 physio-logic brace® (Weiss & Werkmann, 2009)

2.3.4 SpineCor® Pain Relief Back Brace

In order to prevent muscle atrophy created by rigid braces, the SpineCor® Pain Relief Back Brace is a soft brace which aims to alleviate pain, provide dynamic support to unload the facet joints and correct or prevent progression of the spinal curvature. A physical therapy method can also be used together to correct the posture of the patient and balance the concave and convex side muscles (Del Campo, 2010). The brace consists of two shoulder straps and tightly fitted pelvic shorts for holding the shoulder and pelvis positions. Meanwhile, the elastic corrective bands and bolero provide corrective force to the core muscles and body movements can be limited by pulling and fixing the straps to the designated length and position (Figure 2.19). Marcotte (2010) revealed that this brace does not have a significant effect for reducing the Cobb angle, but the ADS subjects find that they are in less pain after wearing the brace. The design also caused inconvenience when toileting (Park et al., 2016).

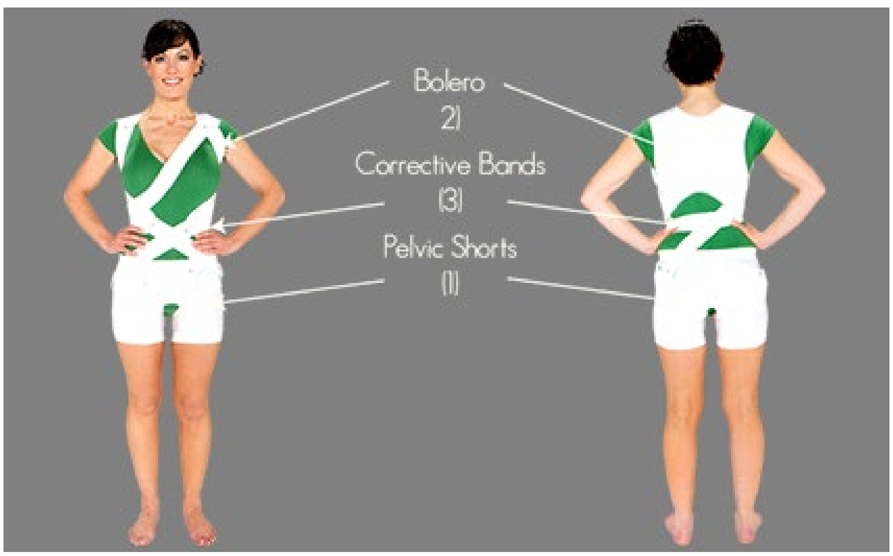

Figure 2.19 SpineCor® Pain Relief Back Brace (Houston Family Chiropractic, 2021)

2.3.5 ScolioSMART™

ScolioSMART™ is a neoprene exercise suit that comprises 4 components as shown in Figure 2.20: the anchor which is wrapped around the thigh, the lumbar and torso parts which rotate the lumbar ad thoracic muscles in different directions and realign the spine; and the tension straps which apply pressure and provide extra spinal support to realign the spine (Morningstar, Stitzel, Dovorany, & Siddiqui, 2017). The pressure exerted from the tension straps will then be transferred to the torso and lumbar components. All of the components are configured according to the pattern of the spinal curvature and the tension straps can be adjusted depending on the reaction and physical symptoms of the patient towards the brace. A lower score from the quadruple numeric pain rating scale and a higher score from the SRS-22 revised (SRS-22r) questionnaire show improved function and reduced pain of patients, respectively. The brace has the lowest effectiveness for patients with double major curves and difficult for patients with limited mobility to don on and off.

Figure 2.20 ScolioSMART™ (Morningstar et al., 2017)

2.3.6 Peak Scoliosis Bracing System™

The Peak Scoliosis Brace is a bracing system for improving both pain and posture of adult scoliosis. ADS patients have options in assembling the brace with a variety of configurations to optimise the brace performance. This flexibility allows patients to perform daily activities without any restrictions (Zaina, Poggio, Donzelli, & Negrini, 2018). The Peak Scoliosis Brace is a semi-rigid lumbar brace with a SlickTrack™ tightening system, Fit-lock® system and adjustable tension straps that exert pressure to correct body alignment and posture. The universal strut assembly and inserted struts can be modified with position and body size which add stability and support to the spine (Figure 2.21). Patients are required to wear the brace at the two to four hours each day, which reduces leg and back pain significantly, but the quality of life and Cobb angle of patients remain unchanged.

Figure 2.21 Peak Scoliosis Bracing System™ (Zaina et al., 2018)

Knowledge gap 1: There is uncertainty of the effect of braces available in the market. Recently, there are numerous developed braces available in the market which claim to reduce spinal deformities, posture, increase treatment compliance rate and reduce lower back pain of ADS patients. Moreover, limited scientific evidence and ambiguous methodology are found instead. Bracing treatment that is systematically assessed and scientifically evaluated should be conducted.

2.3.7 Design of the active bodysuit

The active bodysuit developed by Sit et al. (2020) is a flexible brace that takes into consideration the comfort, function, user friendliness, and effectiveness of spinal curvature reduction as well as pain management and the psychological needs of the elderly during the bracing treatment. The active bodysuit also facilitates body alignment and posture correction during the training sessions. The active bodysuit, as shown in Figure 2.22, consists of inner and outer layers which aim to correct the spinal curvature, eliminate lower back pain and improve posture via a training programme. The inner layer is a tightly fitted tank top with a fastening system that consists of a magnetic zipper and Velcro sewn on the gore (Figure 2.22). There are two bone casings, neckline cover and lumbar pads on the back of the tank top. The shape of the 3D printed bones is obtained by placing the flexicurve ruler at the spine of the patient and then drawn on Solidworks to create the best fit for the wearer. The 3D printed bones are inserted into the bone casing and covered with the neckline cover to prevent bone protrusion. Silicone lumbar padding for spinal correction at the inner side of the tank top allows position adjustment that creates better fit and corrective effects. As shown in Figure 2.23, the outer layer comprises of a corset-like waistband with elastic bones, neoprene shoulder straps and elastics straps wrapped around the shoulder, waist and hip which gives passive corrective force, de-rotation of shoulder and extra supports. The tightness of the Velcro on the corset-like waistband and elastic straps and the location of the laser-cut acrylic buckles can be adjusted according to morphology of the patient which eliminates the long manufacturing time of a custom-made brace. The silicone padding, neoprene shoulder straps and the open chest tank top have cushioning effects which may impart more comfort and reduce unnecessary pressure that causes pulmonary problems, irritation or pressure marks.

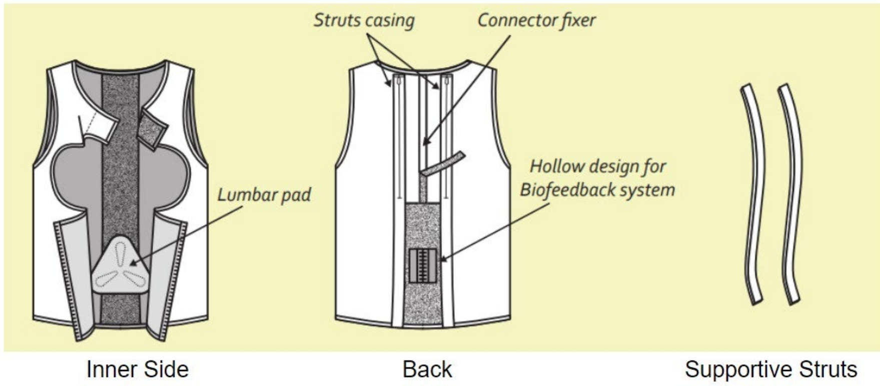

Figure 2.22 Inner layer of the active bodysuit

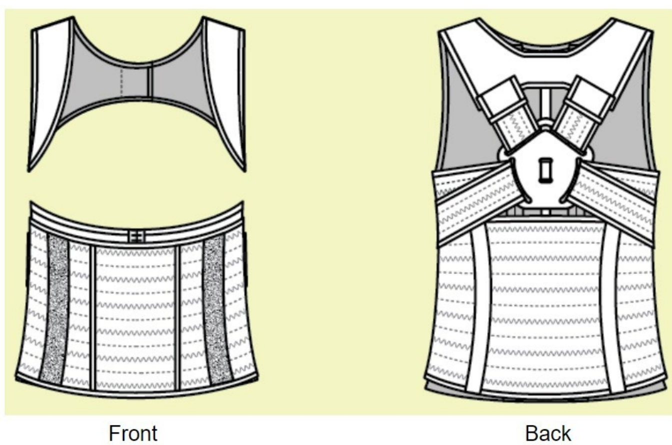

Figure 2.23 Outer layer of the active bodysuit

Corrective forces are exerted in the posture training session after all of the supporting accessories on the tank top and the outer layer are removed. The vibrotactile feedback (VTF) system which consists of connection wires and three sensors are placed along the spine at designated positions while the wire vibrator is placed at the shoulder as shown in Figure 2.24. The sensors would track the posture of the patients during the training sessions and transfer the data to the database via Bluetooth. If the posture exceeds the tolerance ranges, the vibrating board will vibrate to alert the patients until the posture is corrected.

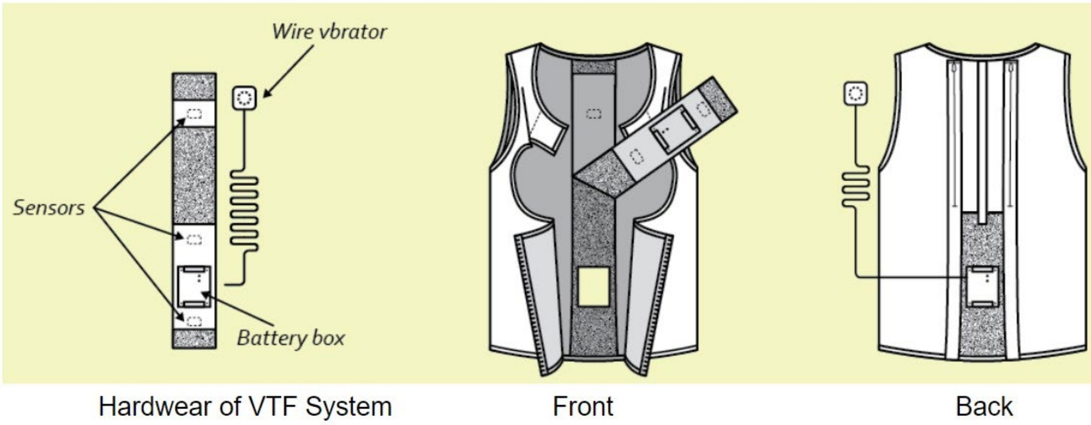

Figure 2.24 VTF system of the active bodysuit

2.3.8 Problems of existing braces

Conventional rigid braces are heavy and create many pressure sores, cause skin irritation and result in muscle atrophy with prolonged brace wear which discourages compliance with treatment. Non-breathable and bulky hard braces made of thermoplastic negatively affect the physical appearance of ADS patients during the bracing treatment which erodes their self-esteem, mobility, ability to function and quality of life, all of which further reduce compliance with treatment. Semi-rigid and soft braces have been developed to address these problems and alleviate the bulkiness and heaviness thus enhancing wear comfort and preventing the body from being fully restricted by the brace. However, the corrective forces given by these two types of braces are lower than those of rigid braces, so that they have only little or no effect in correcting the body alignment, balance and the abnormal curvature of the spine. The multiple layers and complicated designs of soft braces also reduce user friendliness, which increases difficulties to the brace wearer and creates more negative feelings such as feeling useless, lacking confidence, and having self-doubts. The braces currently available in the market can only relieve pain. Moreover, few studies have discussed the wear comfort and effectiveness of soft bracing treatment while demonstrating adequate evidence for spinal or posture correction.

2.3.9 Critical parameters for the effectiveness of bracing treatment

Sit et al. (2020) developed the active bodysuit for older adults with scoliosis as an alternative conservative method to increase the compliance with bracing, improve posture and body alignment and prevent progression of the spinal curvature by using breathable, durable and comfortable textile materials, thus enhancing the aesthetics and user friendliness of the brace. To evaluate the effectiveness of the active bodysuit, subjects who are 50 to 70 years old, suffer from long term chronic lower back pain and have limited mobility caused by degenerative scoliosis were recruited for a three-month wear trial. Questionnaires like the SRS-22R and ODI are utilised to understand the changes in pain status, physical functions, and physiological and psychological comfort after the wear trial.

During the three-month clinical trial of the active bodysuit, the subjects were also required to complete a home training session to improve their posture, which lends ambiguity on the effectiveness of the active bodysuit. Some of the subjects also reported that the durability of the brace is low for a three-month wear trial and the brace is difficult to don, which reduce the compliance with the bracing treatment and user acceptance. Therefore, there are several critical factors that affect the efficacy of bracing treatment, like the compliance rate, and materials applied for the bodysuit.

Knowledge gap 2: There are a lack of studies on the efficacy of the active bodysuit.

The active bodysuit which is made of flexible materials may not exert sufficient corrective forces to correct and maintain the correct posture, alleviate lower back pain and reduce the progression of spinal curvature. Few studies have been conducted that examine the effectiveness of this bodysuit.

2.3.9.1 Compliance

Treatment compliance refers to the act of obeying or complying with the treatments prescribed by doctors or medical professionals (Antoine et al., 2020). To achieve the best treatment outcomes and prevent progression of the spinal curvature, patients need to adhere to the proposed duration of brace use on a daily basis. Nevertheless, patients who receive bracing treatment usually have a low compliance rate between 27% to 47% (Konieczny et al., 2017), thus rendering the effectiveness of bracing uncertain. A low compliance rate can be caused by the external biomechanical forces exerted on the patient such as the size, location and hardness of paddings or supportive bones, tension of elastic straps, and stiffness and fit of the brace. Moreover, patients are required to wear the brace for a long period of time, which limits their body movement during daily life activities and increase perspiration, especially in the summer. The physical discomfort caused by bracing treatment may be due to pressure sores, skin irritation, difficulty in breathing and limited mobility. In addition, the unwillingness to undergo bracing treatment may trigger negative emotions such as low self-esteem, loneliness, and depression (Law et al., 2017), poor relationship with family members because of the poor aesthetics of the brace design.

2.3.9.2 Corrective forces

The three-point or four-point pressure system is commonly used to exert corrective forces onto the trunk of scoliosis patients during the bracing treatment. For rigid braces, one or two pads are placed below the apex of the spine, depending on the curve type, then two pads would be placed above and underneath the curve which act as the counterforce in the opposite direction (Lou et al., 2010). The pads are shaped by orthoptists based on their clinical experience so as to apply a suitable amount of pressure on the patients for spinal correction. For the soft braces, the corrective force exerted on the patients mainly rely on the supportive materials and tension of the straps. The supportive materials such as pads and supportive bones are found at the apex of the curve which push the apex back to its normal position (Chalmers et al., 2012); the elastic straps which provide dynamic corrective forces and counterforce while wrapped around the body and hold the shoulder and pelvis in position and restrict body movement. Rigid braces with stiffer materials can apply higher corrective forces compared to flexible braces composed of soft textile materials, and therefore soft braces may fail to produce sufficient corrective forces to the spinal deformity area and the efficacy of soft braces are relatively low. Hence, the location and the level of force required should be considered during the brace design and treatment process.

2.3.9.3 Treatment duration

The treatment time of bracing is not yet standardised, and the instructions given to the patients are based on clinical intuition of doctors or physiotherapists. The duration of bracing treatment varies from 2 to 23 hours each day while clinicians believe a six-month wear trial can have significant difference on the health and pain status, reported feedback or opinions on the bracing (Park et al., 2016). Different devices such as temperature loggers, pressure sensors and an inertial measurement unit are used to monitor the tightness of the brace, posture of patients and duration of brace wear (Donzelli, Zaina, & Negrini 2015). However, there is no consensus given to standard brace wear and the quality of brace wear are difficult to measure by monitoring devices. Thus, the effectiveness of correcting the spinal deformities, progression of spinal curvature and compliance cannot be determined accurately.

2.4 Finite Element Modelling

The finite element model is a common computer simulation adapted to evaluate the interfacial pressure between the skin and garment while predicting the corrective forces given by the brace and exerted onto patients. The biomechanical behaviors of the biological system or solutions for boundary conditions can be determined by inputting geometrical and physical properties of garments and human tissue and numeric models. The efficacy and design of scoliosis braces can be optimised via a finite element analysis without the need for clinical trials, subject involvement and repetitive exposure of subjects to x-rays for examining the in-brace correction of the patient (Haddas et al., 2016), which is a cost-effective and time efficient methodology. Finite element modelling has been adopted in different perspective problems such as solid mechanics and heat transfer problems, and fluid and multi-physics systems (Zhuming, 2017). For ADS, the FEM is commonly applied to model spinal characteristics (Xu et al., 2017; Zheng et al., 2015), brace action and stress simulation (Clin et al., 2011), brace design optimisation (Clin et al., 2010), and the surgery effects for correcting spinal deformities (Haddas et al., 2016). Different FEMs developed from previous studies would be displayed below in Figure 2.25.

(a)

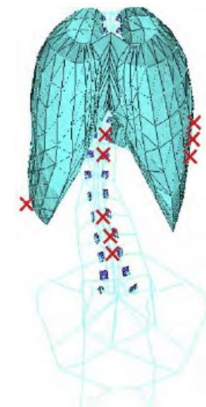

(b)

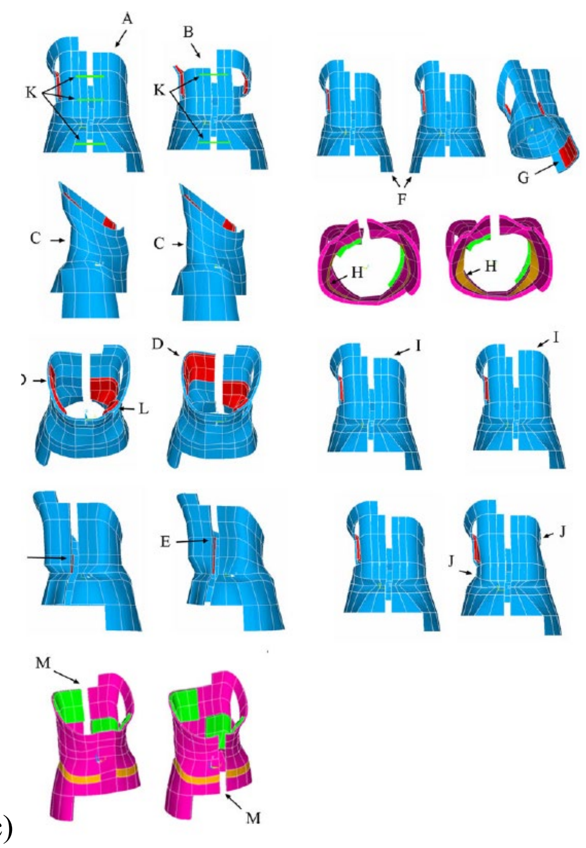

(c)

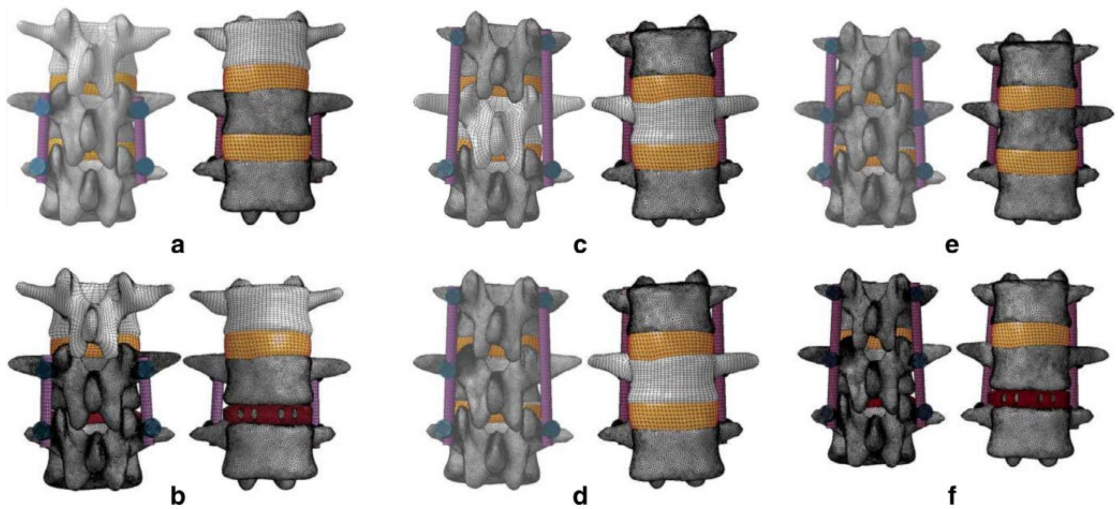

(d)

Figure 2.25 FEMs developed in the previous studies, including: (a) spinal characteristic of ADS (Zheng et al., 2015), (b) brace pressure distribution and action (Vergari et al., 2015), (c) brace design optimisation (Clin et al., 2010), (d) spinal changes of post-op (Haddas et al., 2016)

There are a variety of different finite element software such as ANSYS, Abaqus, COMSOL Multiphysics, TrueGrid and MARC which provide linear, nonlinear, static and dynamic analysis for numerous studies. Generally, there are total of three main steps for building a FEM: preprocessing, analyzing and post processing. As a finite element analysis requires the geometric characteristics of the brace and human body as the input (Chen et al., 2020), MRI, CT, 3D scanning and X-rays can be utilised for making the 3D model via CAD software such as Geomagic Studio, Solidworks and 3D Slicer.) After that, the smoothing process should be conducted to remove all the spikes and holes on the surface of 3D model and imported in the finite element software during the preprocessing phase (Haddas et al., 2019). The 3D model then defines the material properties and are divided into small elements via meshing while different boundary conditions and loading can be assigned to the 3D model. During analysis, finite element software compute and simulate the designated constraints, boundaries and loading conditions that predict the effect and performance of the FEM structure (Garfin et al., 2018). Finally, the data output can be displayed in the form of nodal outputs like displacement, stresses and strains and element outputs after the completion of the simulation. Most of the previous FEM studies have focused on the effectiveness of bracing treatments for adolescent idiopathic scoliosis, spinal displacement, FEM validation of the degenerative spine and the effects of invasive treatments for ADS patients, without investigating the pressure distribution of the brace and human body. Therefore, it is important to understand the pressure exertion and brace efficacy on the ADS patients objectively via finite element modelling.

Knowledge gap 3: There is a lack of FEMs for scoliosis bracing treatments.

There are a variety of FEM studies in the medical field that aim to understand or predict the biomechanics of the scoliotic spine and effects of different surgical treatments. However, no FEM has been established to determine the bracing effect on the body and spine of ADS patients.

2.5 Posture and balance

Balance is mandatory for posture maintenance, response to voluntary movement and external perturbation. The centre of mass must stay within the base of support (BOS) in order to maintain balance (Osoba et al., 2019). Sensorimotor and cognitive functions perform an important role in postural or balance control, which involve peripheral sensation, vision, the vestibular system, muscles, central nervous system processing and cognition (Figure 2.26). Principally, the vestibular system and cerebellum in the central nervous system have a critical role in controlling posture, changing body movement and balancing opposing muscles (Debenham et al., 2021). At the beginning, the position of the human body is perceived through the sensory system such as the proprioception, visual and vestibular systems. Then, sensory neurons carry the perceived somatosensory information to the central nervous system. Meanwhile, the motor neurons transmit signals to the muscles and glands such as the motor system where muscle contractions occur, and body posture is modified. However, balance or postural control can be disrupted by external factors such as sudden rotation or torque reversal, force applied to a specific body part, vibration, visual cues and galvanic stimulation.

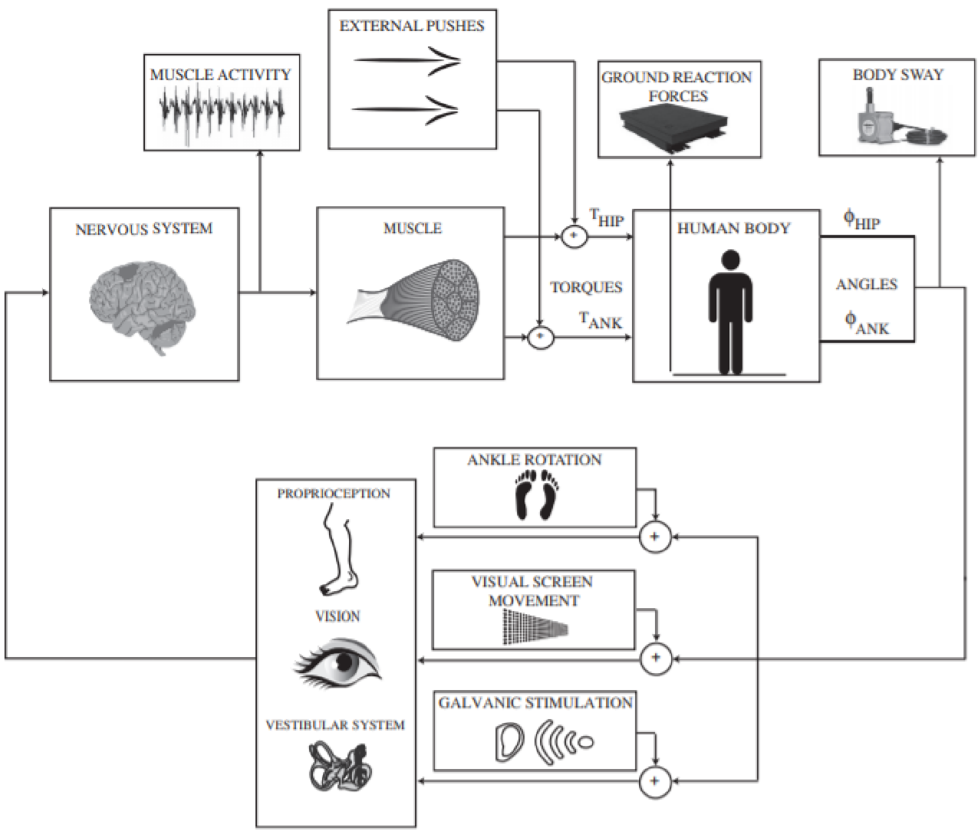

Figure 2.26 Closed loop of balance control (Pasma et al., 2014)

Unfortunately, the sensorimotor and cognitive systems deteriorate with age (Figure 2.27). In terms of the peripheral sensation, older adults have reduced proprioceptive acuity (Hatton et al., 2011), touch sensitivity, perception of the position and movement of the limbs, so that it becomes more difficult for the muscles, tendons, joints and skin to coordinate movement and balance control. Secondly, the visual inputs provide information to the central nervous system which facilitates the planning and undertaking of movement, detecting of hazards, adapting to environmental changes and making judgments (Zhang et al., 2019). Thicker and less flexible crystalline lens, smaller pupils and the disoriented and reduced number of photoreceptors in the central retina however led to reduced contrast sensitivity, depth perception, and glare recovery and limited visual field size. Thus, older adults have reduced ability to judge distance and perceive spatial relationships for postural control (Smith-Ray et al., 2015). Thirdly, almost all types of vestibular cells experience both anatomic and morphologic changes of which the degeneration of the brainstem, cerebellum and cerebral cortex are presumably responsible for the vestibular impairment of older people. The age-related changes in the vestibular function inhibit detection of the head position and motion, delay responses towards sensory information processing with more postural sway along with symptoms of nausea and dizziness (Reimann et al., 2020). Furthermore, reduced muscle mass, and muscle fibre number and size result in relatively low muscle strength and power. Older adults who become physically inactive with muscle weakness further reduce their ability to control their balance and postural sway. Lastly, the structural changes of the brain such as loss of neurons and axons and their signal quality due to aging negatively affects motor planning, attention control and decision making, while increasing reaction time and cognitive load for balance control (Callisaya et al., 2009). As such, the complexity and attentional requirements of maintaining balance or controlling posture increases due to degenerative age-related changes, and the balance and mobility of older adults' decline, which means that they are subsequently more prone to postural sway and risk of falls.

System/sense	Physiologic changes	Functional changes
Peripheral sensation	Muscle spindles show increased capsular thickness, decreased number of intrafusal fibers, reduced spindle diameter, change in shape of primary endings Unknown changes to Golgi tendon organs and joint mechanoreceptors Reduced number and morphologic changes to skin mechanoreceptors (Meissner and pacinian corpuscles) Additional effect of thinning of epidermis and reduced skin levels of collagen and elastin Age-related pathologies (e.g., diabetes)	Poorer proprioception: reduced sensitivity to static joint position and movement detection Loss of touch sensitivity, especially in lower limb Reduced vibration sense, especially in lower limb
Vision	Increased lens thickness Decreased pupil size Reduced flexibility of the lens Corneal changes Decreased depth of the anterior chamber of the eye Liquefaction and shrinkage of the vitreous humor Disorientation and reduction in number of photoreceptors in the macular zone	Reduction in: • static and dynamic visual acuity • contrast sensitivity • depth perception • visual field size Poor dark and glare adaptation Changes in refractive error Light scattering
Vestibular function	Deterioration of calcium carbonate crystals of otolith organs Changes and reduced number of hair cells, nerve fibers, ganglion cells, vestibular nucleus neurons	Poorer vestibulo-ocular reflex (loss of gaze stability) Altered vestibulospinal reflexes (head and body postural control) Dizziness Vertigo Nausea
Muscle function	Reduced number of muscle fibers Reduced fiber size Reduced reinnervation capacity	Reduced muscle strength Reduced muscle power (rapid force generation)
Central nervous system processing and cognition	Damaged myelin Loss of neurons Axonal loss Reduced number and quality of signals to and from the central nervous system	Poorer: • sensory integration • motor planning • attention control / task switching • inhibition • decision making Increased reaction time Increase in the cognitive load of balance control

Figure 2.27 Relationship between balance control and age-related changes of sensorimotor and cognitive systems (Lord, Delbaere & Sturnieks, 2018)

In the ideal standing posture, a straight line can be drawn between the mastoid processes, the shoulder joints, behind the centre of the hip joint, anterior to the knee joints centre and a 5 to 6 cm distance in front of the ankle joints, which is also known as the line of gravity (Case, 2016). The eyes are looking forward and the head positioned on top of relaxed, straight shoulders and upper back. Furthermore, the pelvis is in a posterior tilt to a neutral position, the iliac crests align vertically with the pubic bones, while the knees are unlocked (Zacharkow, 1988. For ideal posture during sitting, the line of gravity is located in the midline of the upper body, where it falls between the mastoid processes, shoulder joints, and hip joint centre (Novak, 2006). The head is right at the centre of relaxed shoulders with a lifted rib cage. The thighs are fully supported by the chair seat with a neutral pelvis position and the feet are flat on the ground. During the erect upright standing and sitting postures, the erector spinae and abdominal muscles such as the lower transversus abdominis, and internal and lateral obliques are activated continuously. A high and expanded chest with raised diaphragm allows the respiratory muscles to perform well to optimise breathing and heart rhythm while pressure on the discs is minimised (Kim & Choi, 2015). Both the ideal standing and sitting postures (Figure 2.28) should facilitate balance where the centre of mass (COM) of the human body stays within the BOS with minimum sway (Haddas & Lieberman, 2018). Nevertheless, the sustained contraction of the erector spinae muscles in an erect upright posture causes fatigue. Therefore, people tend to relax their posture and slump over on a daily basis. It is widely recognised that a slumped standing or sitting posture turns lumbar lordosis into kyphosis and inhibits internal oblique muscle activation and muscle stabilisation in the lumbopelvic region (O'Sullivan et al., 2002; O'Sullivan, Smith, Beales, & Straker 2011). Adopting a passive and slouched posture also increases the activity of the rectus abdominis and lower limb muscles and backward rotation of the pelvis and induces more pressure onto the lumbar discs, hence further leading to muscle fatigue (Gottipati, Stine, Ganju, & Fatone 2018), increased postural sway, reduced balance and lower back pain.

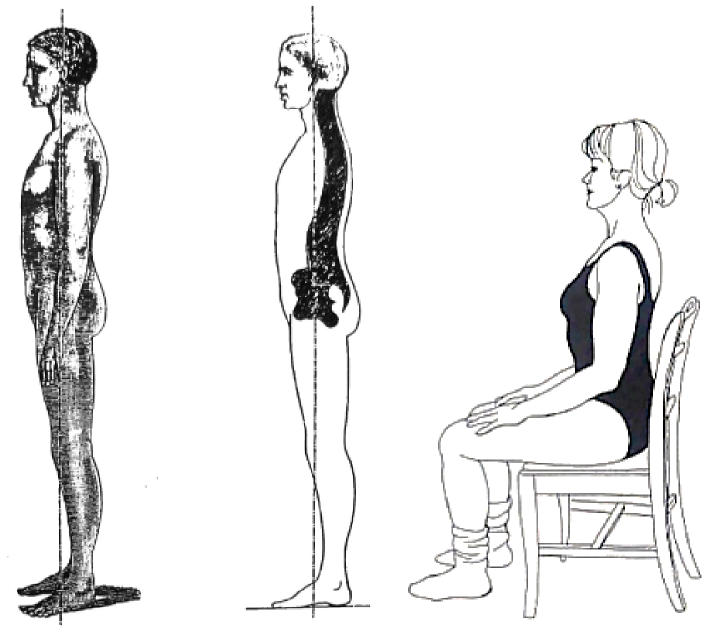

Figure 2.28 Idealised standing and sitting postures (Novak, 2006; Zacharkow, 1988)

2.5.1 Posture and balance of ADS patients

Maintaining an upright posture and balance is important for physical functions and sustaining quality of life which minimise energy expenditure and fatigue of the back muscles and the lower extremities. ADS patients demonstrate 3D spinal deformities like rotation of the bones in the axial plane, lordosis or a kyphotic spine in the sagittal plane and larger Cobb angle in the coronal plane, which shift the line of gravity to the front and the centre of pressure (COP) exceeds the BOS (Haddas et al., 2020). In order to bring the COP back within the BOS, compensatory mechanisms for spinal misalignment are then made by the ADS patients by reducing the thoracic kyphosis, hyperextending the spinal column, retroverting the pelvis, increasing hip and knee flexions along with ankle dorsiflexion to balance the upper body and pelvis (Barrey, Roussouly, Perrin, & Le Huec 2011; Gottipati et al., 2018; Yagi et al., 2017). Moreover, individuals who suffer from scoliosis are more prone to proprioception impairment in comparison to asymptomatic individuals which further deteriorates their ability to control their body movements (Godzik et al., 2020). Thus, ADS patients tend to have poorer posture control and standing balance with more head and COP sway, pelvic shifting, and neuromuscular activity with higher metabolic energy consumption which subsequently lead to lower back pain, disability and risk of falls.

2.5.1.1 Evaluation of posture and balance

Posture control can be evaluated by using both quantitative and qualitative methods. Qualitative analyses describe the mechanical and neurophysiological characteristics of postural control while quantitative analyses determine the changes in COM, COP, kinematics, and electromyographic activity of the muscles and the contribution of different types of sensory information.

Some simple non-instrumented postural tests can be conducted to identify the postural dysfunctions with pathologies, postural abilities and fall risks of older adults. Experienced physical therapists currently recommend the Berg balance scale (BBS) and Mini Balance Evaluation Systems test (Mini BesTest) (Godi et al., 2013; Schlenstedt et al., 2016). BBS is a 14-item objective measure that assesses the balance and fall risks of older adults under a series of predetermined tasks (Figure 2.29). Each task is ranked on a five-point scale that ranges from 0 (lowest functionality) to 4 (highest functionality). Individuals with a score of less than 45 out of 56 are considered to have a greater risk of falling. The Mini BesTest is also a 14-item test that is associated with anticipatory postural adjustments, reactive postural responses, sensory orientation and stability in gait (Marques et al., 2016). The highest score of the Mini BesTest is 28; 2 items are scored bilaterally, and the remaining 12 items are scored from 0 (severe impaired balance) to 2 (normal balance) (Benka Wallén, Sorjonen, Löfgren & Franzén, 2016). A higher score denotes better dynamic balance. However, non-instrumented postural tests can only identify those with very low postural ability and provide preliminary results in postural control efficiency. Detailed evaluation of posture can only be possible by using instrumented tests.

Tests	Sections	Items
BBS		- Sitting unsupported - Change of position: sitting to standing - Change of position" standing to sitting - Transfers - Standing unsupported - Standing with eyes closed - Standing with feet together - Tandem standing - Standing on one leg - Turning trunk (feet fixed) - Retrieving objects from floor - Turning 360 degrees - Stool stepping - Reaching forward while standing
Mini BesTest	Anticipatory	- Sit to stand - Rise to toes - Stand on one leg
	Reactive postural control	- Compensatory stepping correction: forward - Compensatory stepping correction: backward - Compensatory stepping correction: lateral
	Sensory orientation	- Stance; eyes open, firm surface - Stance; eyes closed, foam surface - Incline; eyes closed
	Dynamic gait speed	- Change in gait speed - Walk with head turns: horizontal - Walk with pivot turns - Step over obstacles - Timed up and go with dual task

Figure 2.29 BBS and Mini BESTest (Godi et al., 2013)

Force platforms (or force plates) are the most widely adopted device in assessing postural function which comprise dimensionally stable sensor board and positioned load sensors. There are two types of force plates: 1) uniaxial plates that only measure the vertical component (FZ) of the ground reaction force and 2) multiaxial plates that measure three components (FX, FY and FZ) of the ground reaction force and the moment of force acting on the force plates (MX, MY and MZ)

(Paillard & Noé, 2015). The COP coordinates in the anteroposterior and mediolateral directions are recorded during postural testing which are commonly used to determine the static postural steadiness and control performance. For example, time-domain distance measures describe either the velocity of the COP, or the displacement of COP to the central point of stabilogram (Soares & Rebelo, 2012). The time-domain area measures estimate the area of the stabliogram while the frequency domain measures characterise the frequency distribution of the COP displacement (Chao & Jiang, 2017). During the assessment of posture, a 3D motion capturing system is also used to record the body kinematics. Reflective markers are used to generate the biomechanical model with rigid articulated segments on 3D motion capture software so as to evaluate the skeletal alignment and body angle of the subjects in different postural conditions.

2.5.2 Muscle activity of ADS patients

Muscles are groups of soft tissues that maintain blood flow, posture and balance for daily life activities via co-contraction. The elderly tends to have physical and cognitive losses which lead to lower muscle mass and strength, thus increasing the risk of falls and fatty degeneration of the muscles. Sarcopenia is a common syndrome found in the elderly, where their muscles are deformed and no longer functional, especially for ADS patients. According to Eguchi et al. (2019), a higher prevalence rate of 59.8% of sarcopenia is found in ADS patients as opposed to 42.8% of the healthy control group. ADS patients have to exert 30% to 50% more muscular energy for daily activities compared to their healthy counterparts (Mahaudens et al., 2009), thus resulting in high energy expenditure, muscular inefficiency, and discouragement of physical activities. Sarcopenia is also correlated with ADS which further increases sagittal imbalance and spinopelvic mismatch (PI-LL) while reducing the LL. The spinopelvic parameters of PI, LL, SVA, TK and PT are evaluated based on Hiyama et al. (2018), Eguchi et al. (2017), and Ohyama et al. (2019), both they found that the skeletal and trunk muscle masses are associated with slump posture, increases the PT, TK and SVA and the occurrence of vertebral rotation to compensate for the spinopelvic mismatch. Hence, spinopelvic mismatch leads to spinal misalignment in the sagittal plane and a larger Cobb angle in the lumbar spine, which subsequently aggravates lower back pain and deteriorates the quality of life of ADS patients.

ADS patients frequently experience muscle imbalance caused by the scoliosis where muscle volume and energy consumption on the concave and convex sides of the spine are different. For example, the multifidus and longissimus muscles of the paravertebral muscles that provide stability to the spine and facilitate trunk movement are shorter in length on the convex side of the spine compared to the concave side (Mattei, 2013; Xie et al., 2019). The cross-sectional area of the quadratus lumborum muscle is shorter on the convex side of the spine (Kim et al., 2013). Moreover, the upper and lower trapezius, erector spinae, psoas and neck muscles show a significant difference between the concave and convex sides of the spine (Hyun, Bae, Lee, & Rhim, 2013; Tecco et al., 2011; Yagi et al., 2015). Thus, the tension load is higher on the convex side and there is more muscle activity which allow to trunk and paraspinal muscles to stretch and elongate. Meanwhile, more fat where there are inactive muscles on the concave side means that the muscles are shrunk and soft.

2.5.2.1 Evaluation of muscle activity

Due to the imbalance in strength, volume and length of the muscles, the posture of ADS patients during resting, sitting and standing might be abnormal so that it is difficult to achieve the ideal posture through muscle activity along. Hence, surface electromyography (sEMG) can be used to record muscle activity or the activity of muscle segments which can be used as a non-invasive method to analyse the motor control and muscle balance of an individual with profound precision and ease (Anders et al., 2017). Typically, two electrodes are placed onto the same muscle on the left and right sides of the body. During muscle co-contraction, the electrical signals are recorded and sum up the potential activity generated by the corresponding muscle fibres (Michell, 2013). The raw data is expressed in magnitude or frequency and then processed to reduce unwanted noise or other contamination via normalisation, or amplitude and various other filters (Staudenmann, Roeleveld, Stegeman, & van Dieën, 2010). For standing that involves the utilisation of the lower extremities (Figure 2.26), the activity of the rectus femoris, semitendinosus, gluteus maximus, soleus, medial gastrocnemius, lateral gastrocnemius and tibilis anterior muscles are recorded according to Haddas, Lieberman, & Block (2018), Iwamoto, Takahashi, & Shinkoda (2017), Cattagni, Scaglioni, Laroche, Gremeaux, & Martin (2016). The muscle co-contraction index (CI) of the elderly is lower while the contribution of the ankle muscles in maintaining an upright position is increased for older adult fallers. For sitting, the longissimus, iliocostalis, multifidus, transversus abdominis, obliquus internus, obliquus externus and rectus abdominis muscles are utilised (Figure 2.27). Those who suffer from lower back pain demonstrate large fluctuations in the muscle activity of the longissimus muscles but low muscle activity in the multifidus muscles (Claus, Hides, Moseley & Hodges, 2018), thus the lordosis of those with lower back pain is longer than those who do not have the ailment, so suffers more easily feel tired in attempts to maintain a similar posture for a longer period of time.

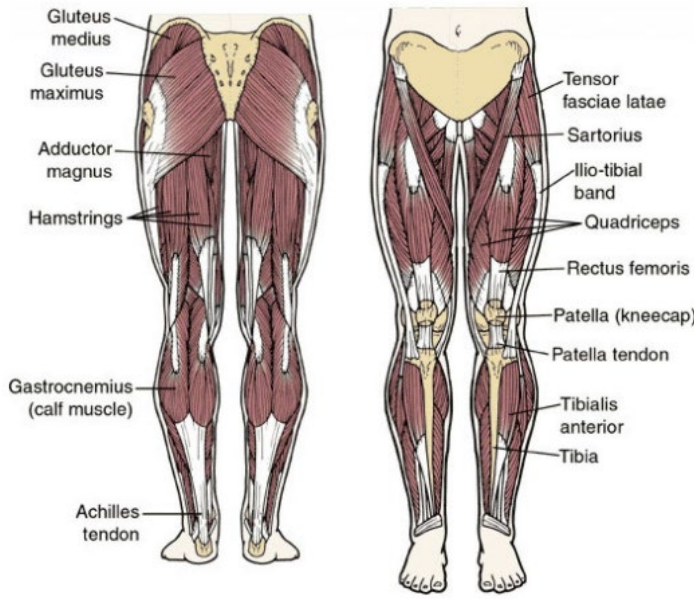

Figure 2.30 Leg muscles (Anatomy Note, 2019)

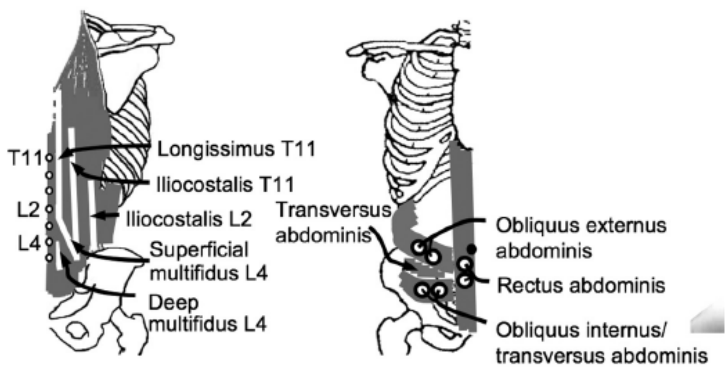

Figure 2.31 Muscles used during sitting (Claus et al., 2018)

Knowledge gap 4: There is insufficient understanding on the posture and muscle activity of ADS patients.

Studies related to the posture and muscle activity of ADS are lacking and there may be some potential parameters influenced by ADS. Moreover, only a few studies have investigated the relationship between ADS and posture and muscle activity.

2.6 Summary

ADS is a condition that involves spinal and trunk deformities in mature adults who are 40 or older with a Cobb angle larger than 10 degrees via radiographic evaluation. The aetiology of ADS is uncertain, but most doctors believe that facet joint and dis degenerations are factors that contribute to ADS. The patients are classified based on their curve type and the parameters of the spine in the sagittal plane. As ADS patients already have a mature skeleton, it is difficult to correct their Cobb angle. Usually, doctors recommend conservative treatment to prevent further deterioration of the spinal deformity. Bracing is the most commonly adopted non-invasive type of treatment. There are rigid, semi-rigid and soft braces available in the market. Rigid braces are usually non-breathable, uncomfortable and limit movement of the wearer. The bulky and awkward appearance of rigid braces may cause mental health issues and pressure exerted creates pressure sores, skin irritation and pain that reduce the compliance rate and subsequently the efficacy of bracing. Flexible braces have been developed in response to reduce the discomfort caused by rigid braces; however, their corrective forces based on textile materials may not be enough to treat scoliosis. As such, the posture, muscle activity of ADS patients and efficacy of the active bodysuit (in Sit et al., 2020) should be investigated. Following that, a biomechanical model should be formulated and validated to identify the appropriate amount of corrective force exertion and pressure distribution which would optimise the flexible brace design when modifying the materials used in the brace. The results contribute to the development of an active bodysuit which has a better fit, more wear comfort, higher compliance rate as well as higher efficacy.

CHAPTER 3: Methodology

3.1 Introduction

In this chapter, the procedures for optimising the active bodysuit, developing the FEM and conducting clinical trials for ADS patients are deliberated in detail. The methodology includes: a) analysing the posture and muscle activity of ADS subjects, b) conducting a clinical study of the existing active bodysuit, c) formulating and validating a biomechanical model to predict the mechanical performance of the active bodysuit, and d) material testing and design optimisation for the active bodysuit by using the FEM.

3.2 Experimental design

The implementation plan of this study is shown as a flowchart in Figure 3.1. The detailed literature review in Chapter 2 has provided a comprehensive and scientific understanding of the physiological and psychological behaviours of ADS patients with the aim to develop and validate an FEM that would simulate the effect of in-brace correction and identify the crucial brace components which can exert corrective forces. Moreover, the balancing pattern of ADS patients is studied to understand the abnormalities of their balance, posture and muscle activity. Furthermore, the findings and background information of the active bodysuit in Sit et al. (2020) are examined, which offers a comprehensive understanding towards the limitations and mechanisms of this bodysuit. During the design and development process of the active bodysuit, its comfort, fit and design are optimised through a comparison with the physical properties of textiles used in the previous bodysuit developed by Sit et al. (2020). Lastly, the corrective components of the proposed active bodysuit are optimised through the D-optimal design approach and FEM simulation.

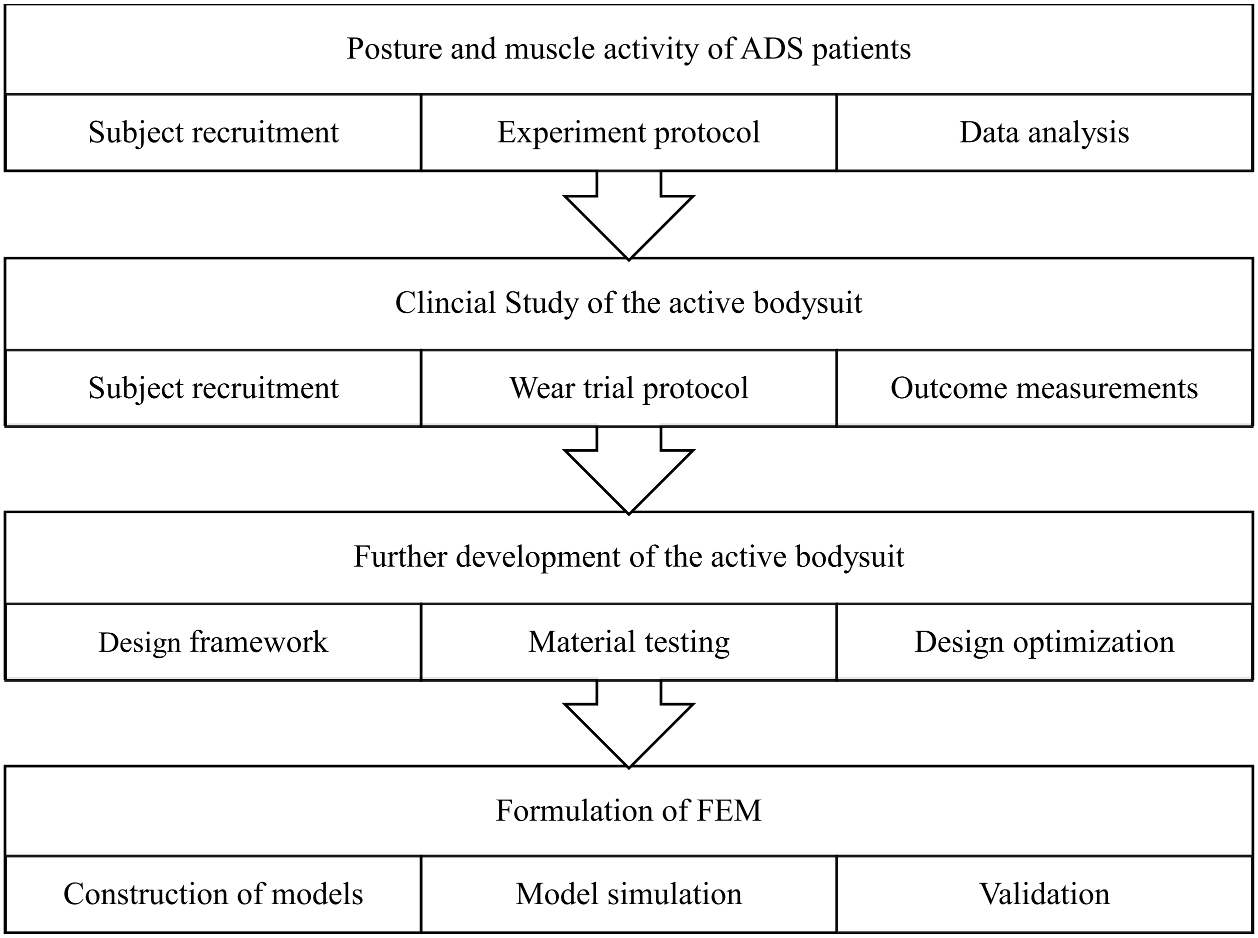

Figure 3.1 Study flowchart

3.3 Balance, posture and muscle activity of ADS patients

3.3.1 Inclusion criteria for subject recruitment

The subject recruitment process was done at the Hong Kong Polytechnic University by posting leaflets and collaborating with the Institute of Active Ageing. Ten subjects with ADS were recruited in accordance with the inclusion criteria. The inclusion criteria for participation are: 1) 50 to 70 years old; 2) a Cobb angle that is larger than 20 degrees; 3) chronic lower back pain for more than 24 months and limited mobility; 4) capable of reading and speaking in Chinese or

English for efficient communication purposes. Moreover, 10 healthy subjects in the same age range were also recruited to compare balance, posture and muscle activity. These subjects should not have history of cardiopulmonary disease, musculoskeletal disorders, cognitively impaired and are capable of reading and able to speak Chinese or English for efficient communication purposes. All of the participants were required to complete and sign a consent form before they took part in the study and agree to the usage of their personal information and research data for research purposes.

3.3.2 Study of balance, posture and muscle activity

The goals of this study are to gain a better understanding of the balance, posture, and muscle activity of ADS patients versus those without ADS and compare them. At the beginning of the experiment, the subjects wore a tightly fitting bathing suit, and their body measurements were taken, including body weight (kg), height (mm), the left and right leg lengths from the anterior superior iliac spine (ASIS) to medial malleolus (mm), knee width (mm), ankle width, and shoulder offsets (mm) which are required by the VICON system to capture the data. A total of 41 retro-reflective markers were positioned on the subjects as reference points, among which, 39 markers were attached to the subjects in accordance with the VICON full body plug-in-gait model and 2 additional markers were attached to T6 and L3 to record the angles and movements of the spine and body alignment in more detail (Figure 3.2). The balancing patterns of the participants were captured by using a Vicon Nexus 3D motion capture system (Vicon Motions Systems, Oxford, UK) which consisted of eight cameras, to capture retroreflective markers in three-dimensional space at a rate of 120 Hz.

Each subject was required to stand and sit in their habitual posture with feet placed 10 cm apart as measured between the medial malleoli of each ankle. For natural standing, the subjects were required to stand as motionless as possible in their bare feet, with their feet placed on a designated location (Figure 3.3) on two force plates for 3 trials, which were 30 seconds each in length. The eyes of the subject were opened, and the subject started at a point marked in the front at eye level while the arms were relaxed at the side of the body (MacRae et al., 2018). A break of 1 minute was given between each trial. The procedures of the habitual sitting task were similar to those of natural standing, but the subjects would sit on a height adjustable stool without using the force plates, with their knees and hips perpendicular to their feet, and arms relaxed at the side of the body. Under standardised instructions, the participants were positioned by the same investigator for all of the trials.

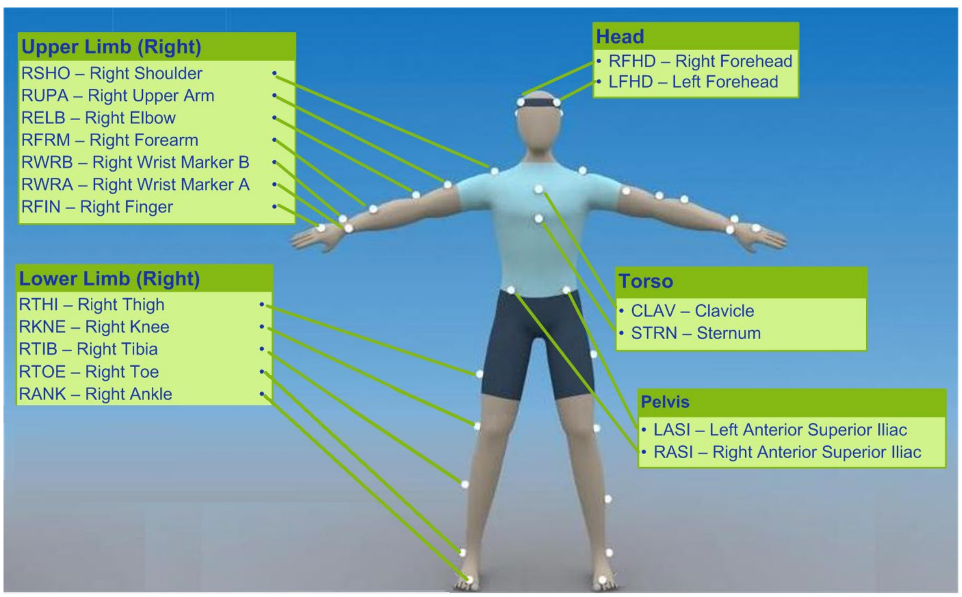

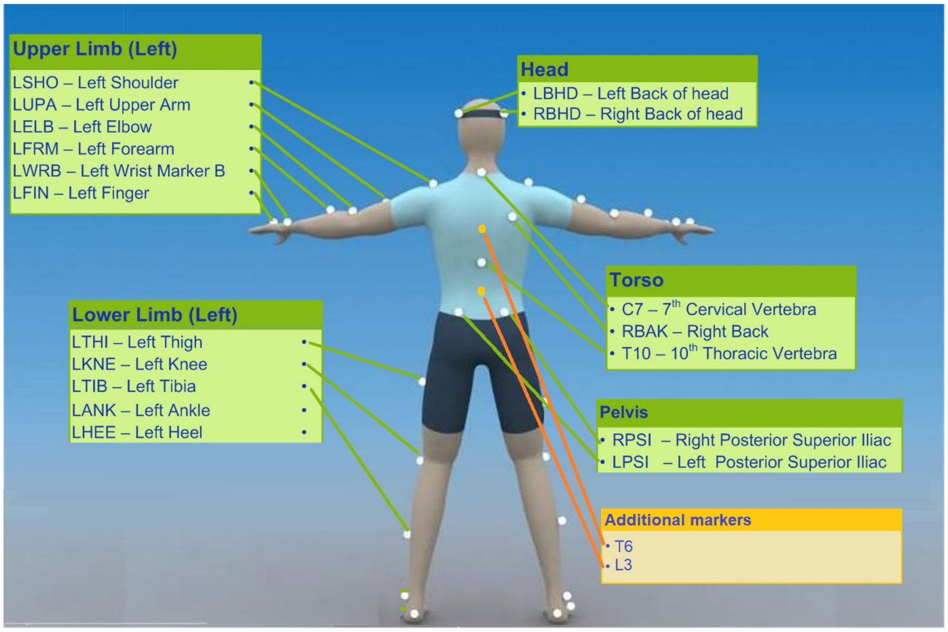

Figure 3.2 Placement of retro-reflective markers (front and back views)

(VICON Documentation, 2021)

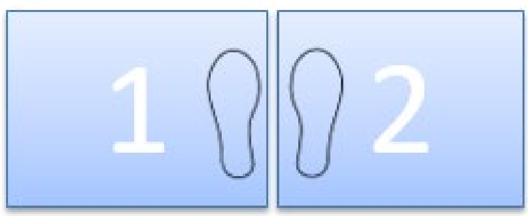

Figure 3.3 Designated location for standing on force plates

3.3.3 Muscle activity

The muscle activity of the ADS and normal subjects was recorded and examined via a Noraxon Ultrium EMG sensor system with 10 channels and synchronised with the Vicon system. Before the start of the experiment, the patients were prepared by shaving the tested area and sterilising their skin with alcohol to reduce the input impedance. The sEMG electrodes were attached to the erector spinae (ES) thoracic and ES lumbar regions, lumbar multifidus (LM), rectus femoris (RF) and tibialis anterior (TA) of the left and right sides of the body (Figure 3.4). Apart from the muscle activity during the experiment, the EMG at rest was captured for 30 seconds in a prone lying position during which the muscles were completely relaxed. Moreover, the maximum voluntary contractions (MVCs) of the lower back and leg muscles were recorded twice by extending the trunk and raising the legs with knees bent at 90° and toes lifted from the floor respectively (Kooistra et al., 2008; Souron et al., 2016; Vera-Garcia et al., 2010). Measurement of the muscle activity was also done during habitual standing and sitting postures and categorised as the convex and concave sides of the tested muscles.

Muscles	Electrode locations	
Erector Spinae (Thoracic region)	Vertically at 2 finger width lateral from the spinous process of T9	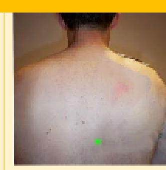
Erector Spinae (Lumbar region)	Vertically at 2 finger width lateral from the spinous process of L1	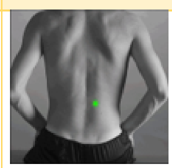
Lumber Multifidus (LM)	At the level of L5 spinous process	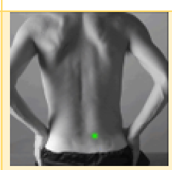
Rectus Femoris (RF)	At 50% on and along the line from the anterior spina iliaca superior to the superior part of the patella	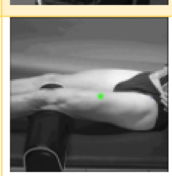
Tibialis Anterior (TA)	At 1/3 on and along the line between the tip of the fibula and the tip of the medial malleolus	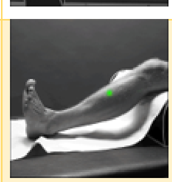

Figure 3.4 Location of sEMG electrodes (light green dots)

3.3.4 Data processing and analysis

To evaluate the postural steadiness in the standing posture, five COP-related variables, the root-mean-square distance (RDIST) and mean velocity (MVELO) in both the medio-lateral (ML) and anterior-posterior (AP) directions and also the 95% confidence circular area (AREA-CE) of the COP displacement were calculated for the static phase of each trial. Moreover, to evaluate the posture of the ADS patients and asymptomatic individuals, the mean value of the pelvis, hip, knee and ankle angles, as well as the spinal tilt angle proposed in Yagi et al. (2016) were calculated. The spinal tilt angle was estimated between the line drawn from C7 to the mid-point of the marker of the LPSI and RPSI and a line drawn perpendicular to the floor. For the measurement of the sEMG activity of the muscle pairs, the data were band pass filtered between 10 to 500 Hz with a fourth order no pass zero-phase-lag Butterworth filter and then fully rectified. The sEMG data were normalised to the MVC recorded during the experiment. The mean values and standard deviations of the above parameters obtained from trials of the same posture of each subject were calculated and statistically analysed with SPSS Statistic 21 (IBM Corp., Armonk, New York) software.

3.4 Clinical study of the existing active bodysuit

3.4.1 Inclusion criteria for subject recruitment

In the clinical study of the existing active bodysuit, subjects with ADS were recruited based on the inclusion criteria which are: 1) those who are 50 to 70 years old; 2) a Cobb angle that is larger than 20 degrees; 3) chronic lower back pain for more than 24 months and limited mobility; 4) capable of reading and speaking in Chinese or English for efficient communication purposes. All of the participants were required to complete and sign a consent form before they took part in the study and agree to the usage of their personal information and research data for research purposes.

3.4.2 Exclusion criteria for subject recruitment

Those who are not eligible for the study have a history of 1) receiving surgical treatment for spinal conditions; 2) cardiac, pulmonary, renal, metabolic diseases or other musculoskeletal disorders; 3) contraindicating to X-ray exposure; 4) mental disorder; or 5) skin allergies. Both the medical history and recent health conditions were verified before participation in the study.

3.4.3 Clinical study protocols

The potential participants took part in a screening session before officially joining the study as a subject for wearing the active bodysuit. The potential subjects were required to complete the Adam's bending test and those with an ATR that is greater than 5 degrees and potential subjects were referred by doctors to conduct a radiographic evaluation at a clinic during which the spinal parameters and deformity were assessed. The subjects who met all of the inclusion requirements would be recruited for the wear trial study (Figure 3.5). After that, the subjects were invited to attend a fitting session at the Hong Kong Polytechnic University. The orthopaedist would ensure that the subject was fitted with the correct size of the active bodysuit and the maximum possible force that can be tolerated by the subject was exerted. During the wear trial process, blood pressure and finger tapping tests were used to monitor the health of the subjects. The subjects were required to wear the active bodysuit and complete the SRS-22r and ODI questionnaires. Lastly, the subject would undergo a radiographic examination again to record the in-brace effect after two hours of donning the bodysuit and 3-months wear trial respectively.

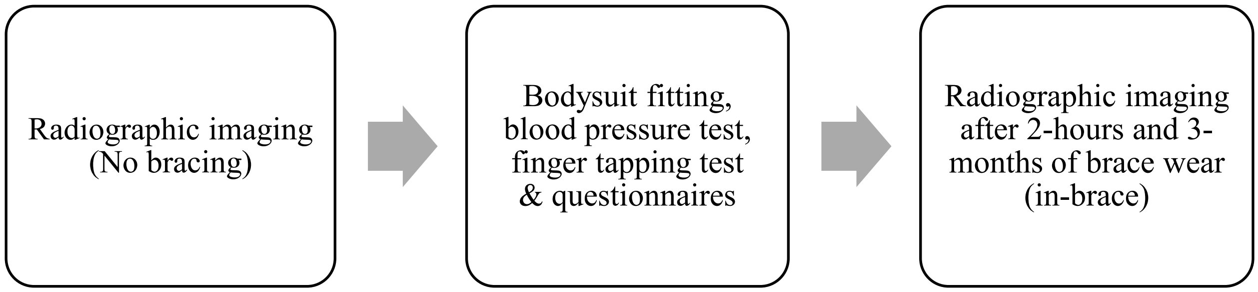

Figure 3.5 Flowchart of 2-hours and 3-months wear trial protocol for active bodysuit

3.4.4 Radiographic examination

X-rays are the primary outcome measure used to evaluate the effectiveness of the active bodysuit on spinal deformity. The potential participants underwent a standard full-length spine radiography at Hong Kong Advanced Imaging where the X-ray images of the coronal and sagittal planes were obtained and measured.

The subjects who met all of the inclusion criteria were required to undergo a radiographic examination again after wearing the active bodysuit for two hours and 3 months respectively. The measurement of the spinal deformity between pre and post intervention was compared. A positive value indicates an increase in spinal deformity while a negative value indicates a reduction of the spinal curvature.

3.4.5 Questionnaires

The clinical improvement after both non-invasive and invasive treatments can be obtained through statistically significant changes of the HRQoL scores with the use of questionnaires like the SRS-

22 and ODI. The SRS-22 questionnaire is a disease-specific instrument for scoliosis patients which consists of five domains, including: function (5 questions), pain (5 questions), self-image (5 questions), mental health (5 questions), and satisfaction/ dissatisfaction (2 questions); that is, a total of 22 questions with scores that range from 1 to 5. The scores for each question would be averaged so that the total score of each domain is also scored from 1 to 5. A higher score means a higher quality of life. The ODI is an index for patients with lower back pain which would measure the functional disability of daily activities and is highly correlated to the HRQoL of ADS patients. The questionnaire comprises 10 questions, and each question has a total of six statements that can be scored from 0 to 5. The index is then calculated by using Equation 3.1.

$$ODI = \frac{Total\ score\ of\ the\ patients}{50} \times 100 \qquad (3.1)$$

Table 3.1 Level of disability and interpretation of the ODI score

ODI score	Interpretation of the score
0% to 20% (Minimal disability)	The patient can cope with most daily life activities. Usually, no treatment is needed apart from advice for lifting, sitting and exercising.
21%-40% (Moderate disability)	The patient experiences more pain and difficulty with sitting, lifting and standing. Travelling and socialising are more difficult, and they may experience work disability. Personal care, sexual activity and sleep are not grossly affected, and the symptoms of the patient can usually be managed by conservative means.

41%-60% (Severe disability)	Pain remains the main problem in this group of severely disabled individuals, and daily life activities are affected. These patients require a detailed check-up.
61%-80% (Crippled)	Back pain impinges on all aspects of the patient's life. Positive intervention is required.
81%-100%	These patients are either bed-bound or have exaggerated symptoms.

3.5 Design and development of the active bodysuit

3.5.1 Design framework

The conceptual framework for apparel design that applies the functional, expressive and aesthetic consumer needs model proposed in Lamb and Kallal (2016) is adopted in this study; see Figure 3.6. This framework for apparel design comprises the following six stages: identifying the problem(s), coming up with the preliminary ideas, refining the design, developing the prototype, evaluating the prototype and finally, implementing the design which take the functional, expressive and aesthetic considerations of the garment into account and involve a problem-solving process to optimise the active bodysuit.

The design process first begins with identifying the problems of the active bodysuit through a preliminary wear trial. Using a validated FEM, the brace components that are related to efficacy and wear comfort can be identified which completes the second stage of generating preliminary ideas for design solutions. The third stage is design refinement which would be conducted by selecting the right materials, optimising the design via an FEM, and modifying the design and fit.

The efficacy of the active bodysuit can be optimised by adopting, modifying and eliminating the preliminary ideas that concern the functional, expressive and aesthetic criteria of the active bodysuit. The prototype of the active bodysuit is evaluated via a wear trial and questionnaires to obtain both subjective and objective measurements and determine whether the prototype has fulfilled the requirements. If not, the designer has the repeat the stages again and modify design of the prototype. Then when the final design and all of the modifications are completed, the garment can be commercialised in the market and mass production commenced, and finally, the garment is sold in the market.

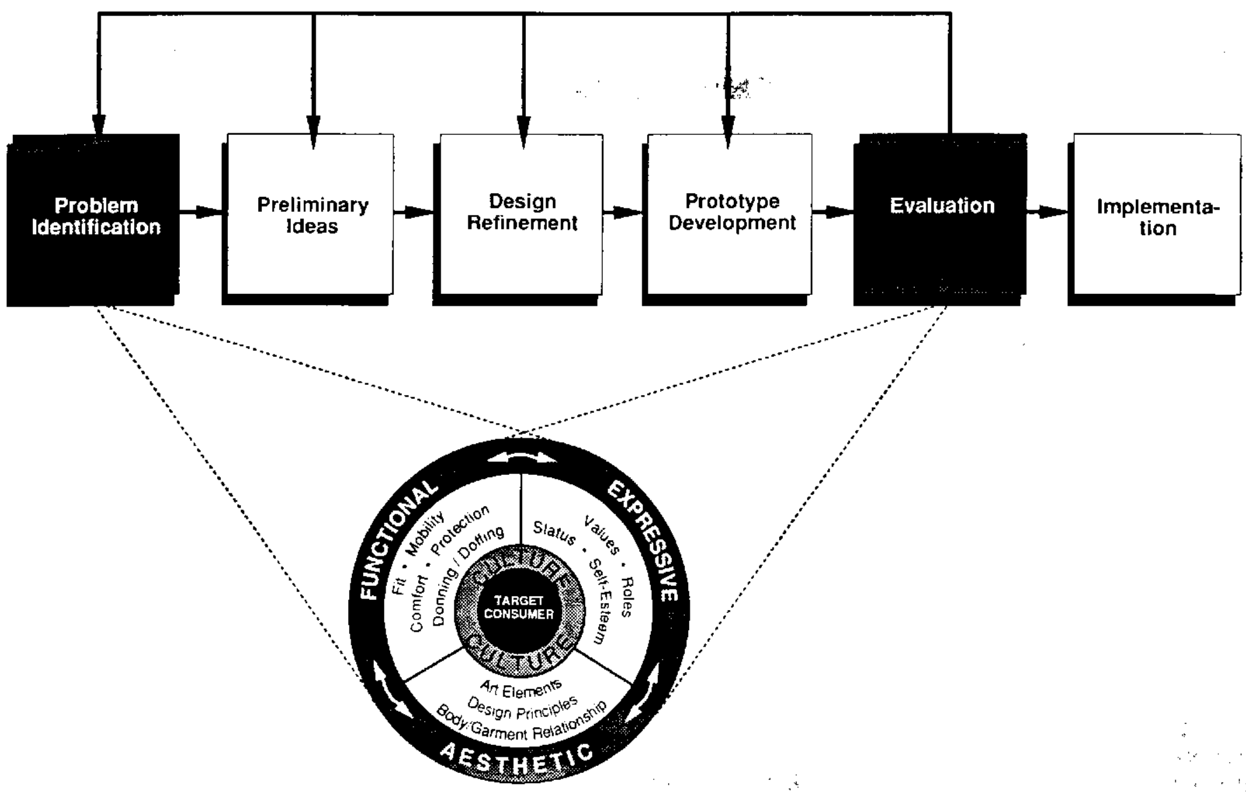

Figure 3.4 Apparel design framework (Lamb & Kallal, 2016)

3.5.2 Material selection

Material selection is important for the active bodysuit because the process impacts the physical properties of the textile materials and the performance of the bodysuit. The following section will involve the deliberation of various testing methods to select the appropriate fabrics for the inner vest of the proposed active bodysuit. The main fabrics used are related to the thermal comfort, durability and dimensional stability of the active bodysuit. Their function and description are listed in Table 3.2. The main fabric determines the basic frame and shape of the bodysuit which needs to be light in weight, breathable, elastic, and tightly fitting with high durability, dimensional stability and wear comfort for a long period of brace treatment.

Table 3.2 Purpose and requirements of the three major types of textiles for active bodysuit

Component	Function	Application	Requirement
Main fabric	Provide main frame of the garment which is conducive to ADS patients	Shell fabric for the vest-like top, and lining fabric for the corrective component	- High stretch and recovery - High thermal comfort - Low dimensional changes

3.5.2.1 Material conditioning and testing

All of the fabric specimens were prepared and testing in the laboratory was conducted in accordance with EN ISO 139:2005 Textiles — Standard atmospheres for conditioning and testing, at a temperature of 20 ± 1ºC and relative humidity of 65 ± 2% for at least 24 hours before commencing the material testing. The fibre content, thickness, density and weight of all the purchased materials were subsequently determined and then the different fabric components were examined.

3.5.2.2 Stretch and recovery test

The stretch and recovery test was conducted in accordance with ASTM D6614 which determines the elasticity of elastic fabrics in the strip form. The Instron 4411 tester was used in the experiment because this device provides a constant rate of extension (Figure 3.7). The dimensions of the specimens are 350 mm ± 0.5 mm in length and 50 mm ± 0.5 mm in width with reference marks of 250 mm drawn parallel on the short edge to identify the elongated length. A constant load of 4.0 ± 0.02 lbs was applied to the specimens, which were then stretched and subjected to loading for 5 ± 0.1 min and relaxed for 5 ± 0.1 min. The difference between the length of the strip specimens in the loaded and relaxed states was recorded by using the corresponding software and calculated by using Equations 3.2 and 3.3.

Figure 3.5 Instron 4411 tester

$$\textit{Fabric stretch } \% = [(B\text{-}A)/A] \times 100 \qquad (3.2)$$

$$\textit{Fabric growth } \% = [(C\text{-}A)/A] \times 100 \qquad (3.3)$$

where:

A = original distance between the jaw faces,

B = distance between the jaw faces measured while the specimens are under load, and

C = distance between the jaw faces measured after the removal of slack.

3.5.2.3 Water vapour permeability test

The testing method in ASTM E96 Standard Test Methods for Water Vapor Transmission of Materials was used to determine the rate of water vapour transmission from the textile materials to the external environment. The fabric specimens were cut according to the edges of the cup. The cup was then filled with distilled water until it was three-quarters full, and the back side of the fabric specimens was glued onto the mouth of the cup in order to simulate the vapour transmission from the fabric to the surrounding environment. The weight of each cup was recorded at the beginning at the experiment and after 24 hours had elapsed. Three samples of each specimen were tested, and the water vapour transmission rate was calculated as follows:

$$WVT = \frac{G}{tA} \qquad (3.4)$$

where:

WVT = rate of water vapour transmission (g/h·m^2),

G = weight change (from the straight line; g)

t = time (h) and

A = test area (area of the mouth of the cup; m^2).

3.5.2.4 Air permeability test

The breathability and permeability of the fabric samples were measured by using a KES-F8-AP1 air permeability tester (Figure 3.8). The resistance of the textile materials to the passage of air is closely correlated to the wear comfort. Five 50 mm × 50 mm specimens of each fabric sample were placed onto a 2π cm^2 vent pressing plate at the piston speed of 2 cm per second and air flow per unit area of 4π m/s. The ventilation resistance can be measured by the pressure detector and recorded as kPa·s/m. A lower average value of ventilation resistance denotes higher permeability and breathability of the fabric sample.

Figure 3.8 KES-F8 air permeability tester

3.5.2.5 Thermal conductivity test

The KES-F7 Thermo Labo II (Figure 3.9) was used to examine the microclimate between the active bodysuit and human skin. A 5x5 cm copper heat plate called the BT-Box was heated at a constant temperature of 30°C. Five specimens of each sample were placed on the water box at a temperature of 20°C. The back side of the specimens was placed so that it came into contact with the BT-Box so that the amount of stored heat of the BT-Box could be transferred to the textile material which was then recorded. The water box replicates the human skin and the entire experimental procedure simulates the immediate heat loss of the skin in watts (W) when the skin touches the textile. Equation 3.5 is used to calculate the thermal conductivity of the fabric and Equation 3.6 converts the thermal conductivity value to an SI unit.

$$\mathrm{k} = \frac{W \cdot D}{A \cdot \Delta T_0} \,(\mathrm{W/cm \cdot {}^{\circ}C}) \qquad (3.5)$$

$$k_{SI}(W/mk) = k \times 10^2 \qquad (3.6)$$

where:

k= thermal conductivity ($Wm^{-1}K^{-1}$);

W= rate of heat transferred (watts);

D= thickness of sample (m);

A= area of the heat plate of the BT-box (m^2); and

ΔT= temperature difference between the heat plate and water box (K).

Figure 3.6 Thermo Labo II Tester

3.5.2.6 Dimensional changes after laundering

The dimensional stability of the fabrics after laundering was determined based on the test method in AATCC 135. Three specimens of 38 cm × 38 cm were taken from each fabric sample with three sets of benchmarks of 25 cm made parallel to the warps and courses of the specimens. Each benchmark was at least 65 mm in distance away from the edge of the specimens. AATCC 1993 was referenced for the amount of detergent (66 g ± 1 g) and total weight of the fabric specimens and dummy load (1.8 kg) which were laundered under a normal wash cycle at 41°C along with a rinse cycle that was under 29°C and then tumble dried for 2 hours. After laundering, the length of each benchmark was measured, and the average dimensional changes of the specimens calculated by using:

$$\%\ dimensional\ changes = \frac{(B-A)}{A} \times 100\% \qquad (3.7)$$

where:

A = original dimensions of the benchmark, and

B = dimensional changes of benchmark after laundering.

3.6 FEM formulation

FE modelling is a scientific method that is used to predict the performance of the active bodysuit in this study and attain a better understanding of the amount of interface pressure between the garment and body by validating the performance of the active bodysuit. The simulation was carried out by using a commercial FEM software, ABAQUS/CAE 6.14-4 (Dassault Systèmes Simulia Corp., USA). The FEM had three main components, including: the torso of the body, skeleton of the subject and the bodysuit. The modelling simulated the stress and strain experienced by ADS patients. A total of 6 tasks were carried out for the simulation of the brace: 1) constructing the geometric topology of the body, spine and bodysuit, 2) defining the type of element and material parameters, 3) meshing the model, 4) defining the initial boundary conditions, 5) numerically processing the displacement and loading of the active bodysuit, and 6) validating the FEM.

3.6.1 Geometric modelling of the body, skeleton, and active bodysuit

3.6.1.1 Constructing torso and skeletal model

To predict the biotechnical behaviour and pressure distribution of the active bodysuit on ADS patients, a female subject recruited in the clinical trial also participated in the development of the FEM. The Vitus Smart XXL 3D body scanner (Human Solutions GmbH, Germany) was used, which is capable of measuring the body in 3D space with a 1 mm error for a measurement range of 2100 mm × 1000 mm × 1200 mm (height × width × depth). A laser sensor with optical triangulation was used (Human Solutions GmbH, 2015). Using a 3D scanner is an advanced, safe and non-invasive means of obtaining comprehensive measurements of the external geometry of the trunk (Roy et al., 2019) and thus effective in monitoring the body contours and spinal deformity changes during bracing treatment.

The subject donned a white colour tightly fitting tank top and shorts for the procedure. Her long hair was tied up and she was instructed to stand at a designated location which ensured the accuracy and precision of the 3D body imaging and prevented scanning interference or errors. The subject slightly opened her arms and was instructed to maintain her habitual standing posture without moving during the scanning session. After the 3D body scanning was done, the images captured were exported to Geomagic Studio 2012® and Solidworks software for data processing. As for the skeleton model, the spinal vertebras, pelvis, femoral head and intervertebral disc models were drawn with Solidworks 2012 x64 Edition (Dassault Systèmes SolidWorks Corp., USA) based on the frontal and lateral X-rays of the recruited subject. These x-rays were taken at Hong Kong Advanced Imaging.

3.6.1.2 Constructing active bodysuit

The model of the active bodysuit contains shoulder straps, a tank top, supportive bones, buckle, lumbar pad and elastic waistband. To ensure that the bodysuit can be fitted onto the torso model, it was extracted from the model of the torso by using Solidworks 2012 x64 edition, and the thickness of the model was 3 mm based on the thickness of the active bodysuit.

3.6.2 Defining material properties

The model is this study has five different material properties: the human torso, spinal vertebrae, intervertebral discs, textile materials of the active bodysuit and materials for the supportive bones. All of the models are assumed to be homogeneous, isotropic and linearly elastic. The material properties of the torso, vertebrae and intervertebral discs were based on those in Garfin et al. (2018), Wang et al. (2016) and Chen et al. (2020) while material testing was conducted to examine the tensile strength of the supportive bones and textile materials of the bodysuit respectively. BS EN 14704-1:2005 was referenced to measure the elasticity of the textile materials with the Instron 4411 tensile tester. The stress-strain was plotted by using Equation 3.2 so that the true tension stress (ε_t), strain (σ_t) and Young's modulus (E_t) could be calculated. The Poisson's ratio of the materials was determined by using the results in previous studies of Pawlaczyk et al. (2013), Xu et al. (2019), Wang et al. (2016) and Chan (2019). Meanwhile, the tensile properties of the supportive bones were tested by using the plastic tensile test in ASTM D638 which also identifies the true tension stress (ε_t), strain (σ_t) and Young's modulus (E_t) with:

$$\mathrm{E} = \frac{\sigma}{\varepsilon} = \frac{S(1+e)}{In(1+e)} = \frac{S(1+\left(\frac{D1-D0}{D0}\right))}{In(1+\left(\frac{D1-D0}{D0}\right))} \qquad (3.8)$$

where:

E = Young's modulus (MPa);

σ = true stress (N/mm^2);

$\boldsymbol{\varepsilon}$ = true strain;

S = engineering stress;

e = engineering strain;

D_0 = initial thickness or length of specimen (mm); and

D_1 = final compressed thickness or elongated length of specimen (mm).

3.6.3 Defining type of mesh element

An appropriate mesh element is important for developing an FEM as there is reciprocity among the mesh density, duration of FE processing or analysis and the fidelity of the FEM compared to real-life conditions (Shivanna, Tadepalli, & Grosland, 2010). More accurate results can be acquired with finer meshes and more meshing, but this would mean more computation time and cost to do the finite element analysis (FEA). A simplified model with less meshing would generate results with lower fidelity, but the duration and cost of the FEA can be reduced. Therefore, a compromise can be made among accurate FEA results, mesh element size and computation time and resources. Triangular and quadrilateral elements can be used to develop a two-dimensional FEM while tetrahedron or hexahedron elements are adopted in 3D FEMs (Lo, 2015).

3.6.4 Defining boundary conditions

The boundary conditions are divided into two major categories: essential and natural boundary conditions, which are essential in FEMs and related to the response and behaviour of the elements. Essential boundary conditions describe the condition of the primary variables such as temperature and displacement while natural boundary conditions describe the secondary variables like force and thermal conduction. In this study, the boundary conditions are used to describe the displacement during the wear process of the active bodysuit. During the wear process, surface-to-surface contact is used to simulate the inter-surface interaction between the bodysuit and torso.

3.6.5 Validation of FEM

The validation of the FEM is conducted by comparing the result of the FEM with the clinical trial results of the subject who underwent an in-brace radiographic examination. The spinal curvature of the vertebral model was examined by considering the vertebrae position, Cobb angle, SVA, PI-LL and PT of the X-ray images. The correlation coefficient between the X-ray measurements and simulation model is calculated as follows:

$$Correlation\ coefficient = \frac{\sum_{i=1}^{17}[(T_i-\bar{T})\times(E_i-\bar{E})]}{\sqrt{\sum_{i=1}^{17}(T_i-\bar{T})^2}\times\sqrt{\sum_{i=1}^{17}(E_i-\bar{E})^2}} \quad (3.9)$$

where:

T= vertebral displacement measured from the radiographic image;

E= vertebral displacement estimated from the FEM;

$\bar{T}$= average vertebral displacement measured from the radiographic image;

$\bar{E}$= average vertebral displacement estimated from the FEM; and

i= vertebral body in the scoliotic spine.

3.7 Optimisation with FEM

In the active bodysuit, the corrective forces are mainly applied through three components on the bodysuit: the elastic straps, supportive bones and buckle. The 3D printed supportive bones on the active bodysuit still allow wearers to move around or bend their torso after donning the bodysuit. However, the buckle at the back of the bodysuit can be damaged or easily broken. Moreover, the corrective forces exerted by the active bodysuit have little effect on posture control, body alignment restoration and pain relief. Therefore, more rigid materials with higher durability and strength are investigated in this study to enhance the corrective performance of the supportive bones and buckle in the active bodysuit.

3.7.1 Design optimisation through D-optimal design

In the design optimisation process of the active bodysuit, optimising the corrective effect for the body alignment of ADS patients is the objective function during the evaluation of the performance of the brace design. The FEM is a useful tool for predicting the corrective effect of the active bodysuit with different design components. Three design factors that govern the design of the brace were applied, including the tensile strength of the elastic waistband, straps, and the supportive bones. For each design factor, three levels of values within the reasonable value ranges were assigned for the parametric analysis.

Since a complete factorial design requires numerous simulation trials ($3^4 = 81$) which translates into heavy computational time and effort, a more effective and feasible approach called fractional factorial design was used instead. According to Franciosa, Gerbino, Lanzotti & Silvestri (2012), the built-in Matlab function “rowexch” can generate design combinations based on the levels of three design factors called the D-optimal array. The design combinations are accomplished by minimising the covariance of the parameters estimated at each iteration while maintaining the effects of each design factor. To obtain the best D-optimal design matrix, the rowexch algorithm was calculated 200 times with different initial design selections and then best D-optimal design matrix was selected through these 9 trials.

The 9 design combinations were then imported into ABAQUS for the FEA and the corrective effect of each combination was calculated. The design combination that attained the highest in-brace correction was regarded as the optimal design. An analysis of variance (ANOVA) was then performed to determine the sensitivity of each design factor.

3.8 Summary

In this chapter, the research methods for optimising the wear comfort and corrective effect of an active bodysuit have been deliberated in detail. A study of the balance, posture and muscle activity and two-hours clinical study of the active bodysuit developed by Sit et al. (2020) have been conducted as a background study to offer a better understanding of the abnormalities of ADS patients and the limitations of this bodysuit respectively. The subjects underwent a radiographic examination to examine the effectiveness and biomechanics of the active bodysuit.

Regarding the optimisation of the active bodysuit, an FEM is established and validated by using the radiographic and pressure measurements obtained from the clinical study of the active bodysuit. The validated FEM can simulate the loading of the bodysuit on the torso and predict the changes in the measurements of the spinal and spinopelvic parameters after donning the active bodysuit. Subsequently, the brace components responsible for the corrective forces would be identified.

To enhance the perceived comfort of the active bodysuit, different materials are sourced from the market, and both the thermal comfort and mechanical properties such as the tensile strength, durability, thermal conductivity, and air and water vapour permeabilities are evaluated and compared to determine the most appropriate materials for the proposed active bodysuit. Different combinations of materials are then applied to the FEM to determine the optimal design of the active bodysuit via a D-optimal array.

CHAPTER 4: Evaluation of posture and muscle activity of ADS patients

4.1 Introduction

The studies in the literature review in Chapter 2 show that posture, balance, and muscle activity can be influenced by sensorimotor and cognitive functions. Due to the deteriorated proprioception and spinal deformity of ADS patients, they might have different static balance strategies and level of muscle activity compared to their asymptomatic counterparts. In order to investigate the static balance strategies of ADS patients, an experiment is carried out with 20 older adults (10 participants with ADS and 10 asymptomatic individuals) when performing balanced standing and sitting. In this chapter, the measurements of the COP, sEMG, and body angle of the two subject groups, as well as the convex and concave sides of the muscle activity of the ADS patients and flexion angle of the lower limbs will be analysed, and their significance evaluated.

In this study, it is hypothesised that (a) the postural steadiness of ADS subjects has deteriorated more than the asymptomatic subjects in habitual standing, (b) the body angles and muscle activity between the convex and concave sides of ADS subjects with spinal deformity are different, and (c) the body angles and muscle activity of ADS subjects are different compared to the asymptomatic subjects.

4.2 Subject recruitment

A screening programme was carried out at The Hong Kong Polytechnic University in 2020 and the target population was older adults between 50 and 70 years old. During the examination process, the participants were required to perform the Adam's forward bending test and a professional prosthetist and orthotist (P&O) measured the ATR of each participant by using a scoliometer. The participants with an ATR ≤ 3˚ were assigned to the asymptomatic group and 10 females were invited to participate in the study. Meanwhile, the participants with an ATR ≥ 5˚ were assigned to the potential scoliotic group. In total, 124 subjects were screened, and 23 were found to have an ATR ≥ 5˚.

The 23 individuals with an ATR ≥ 5˚ were then invited to undergo a radiographic examination at Hong Kong Advanced Imaging. After confirming the diagnosis of scoliosis and examining their spinal deformity through a radiographic examination, 10 participants with Cobb angle ≥ 20˚ who met the recruitment criteria (Section 3.3.1), were recruited for the study. The study was approved by the Human Ethics Committee of the Hong Kong Polytechnic University and all of the participants gave informed written consent prior to the participating in the experiment. Table 4.1 summarises the demographics of the participants. The mean demographic data of the two subject groups were calculated by using an independent t-test, in which the two subject groups show no significant difference in terms of age, height, weight and BMI. Table 4.2 shows the radiographic measurements of the recruited ADS subjects by using the SRS-Schwab classification.

Table 4.1 Demographic data of the participants

	ADS subjects (Mean ± SD)	Asymptomatic subjects (Mean ± SD)	t	df	*p*
Number of participants	10	10			
Age (years old)	59.9 ± 4.04	59.6 ± 5.15	0.145	18	0.886

Height (cm)	157.8 ± 7.52	155.5 ± 2.92	0.901	18	0.38
Weight (kg)	51.8 ± 8.66	51.8 ± 5	-0.016	18	0.988
BMI (kg/m²)	20.7 ± 2.59	21.4 ± 1.82	-0.688	18	0.5

Table 4.2 Radiographic measurements of recruited ADS subjects

SRS-Schwab curve type	Subject code	Cobb angle in thoracic region (˚)	Cobb angle in lumbar region (˚)	Convex side of the major curve	PI-LL (˚)	SVA (mm)	PT (˚)
L	s20002	-	34	Left lumbar	-10	-52 (+)	0
	s20003	29	31	Left lumbar	3	15	21 (+)
	s20008	-	72	Right lumbar	-19 (+)	-17	5
	s20009	16	33	Left lumbar	29 (++)	43 (+)	32 (++)
	s20010	-	42	Right lumbar	8	30	17
	Mean (SD)	9 (13.2)	42.4 (17.1)	-	0.2 (6.57)	5.6 (17.7)	15 (12.8)
D	s20004	30	48	Left lumbar	29 (++)	34	24 (+)

	s20005	36	40	Left lumbar	-25 (++)	2	-1
	s20007	33	60	Left lumbar	14 (+)	23	31 (++)
	Mean (SD)	33 (3)	49.3 (10.1)	-	-5.5 (27.6)	12.5 (14.8)	15 (22.6)
N	s20001	-	29	Left lumbar	10	11	18
	s20006	16	29	Right lumbar	-1	-3	16
	Mean (SD)	8 (11.3)	29 (0)	-	4.5 (7.78)	4 (9.9)	17 (1.41)
Mean (SD)	-	27.4 (21.3)	30.4 (18.7)	-	3.8 (18.2)	8.6 (28)	16.3 (11.74)

Notes: (+) = Moderate deformity, (++) = Marked deformity

4.3 Evaluation of the COP-related variables and body angles of ADS and asymptomatic groups

The experimental protocols were provided in Chapter 3, and the parameters of the COP displacement were calculated accordingly. The mean and standard deviation of each measured variable were collected from the two subject groups. As some of the COP data did not pass the Shapiro-Wilk test of normality ($p < 0.05$), the Mann-Whitney U test was used to compare the measured variables between the two groups during the habitual standing wear trial. The significance of the statistical analysis was set at $p < 0.05$. No significant difference was found between the two subject groups on the RMS distance, mean velocities of the COP in both the ML and AP directions and also the AREA-CC (Table 4.3).

Table 4.3 Mean and standard deviation of COP variables of the ADS and asymptomatic subjects in habitual standing posture

	ADS subjects	Asymptomatic subjects			
	Median	Median	U	Z	*p*
RDIST AP	3.92	4.21	45	-0.378	0.705
RDIST ML	2.07	2.21	49	-0.076	0.94
MVELO AP	13.3	13.6	39	-0.832	0.406
MVELO ML	20.4	21.2	44	-0.454	0.65
AREA-CC	28.3	35.4	46	-0.302	0.762

Note: *$p < 0.05$, **$p<0.01$, and *** $p<0.001$

The flexion angle of the lower limbs of the ADS patients during standing and sitting was grouped according to the convex and concave sides of their spinal deformity (Table 4.4). Through the use of the Wilcoxon signed rank test, the ADS patients were found to have a more flexed knee on the convex side of the spine compared to the concave side during habitual standing ($Z = -2.191$, $p = 0.028$). Significant differences were also found between the hip and knee angles during habitual sitting, in which the ADS subjects have larger hip ($Z = -1.58$, $p = 0.013$) and knee ($Z = -2.803$, $p = 0.005$) flexion angles on the convex side than the concave side of their spine. Meanwhile, the left and right sides of the flexion angles of the lower limbs of the asymptomatic subjects were also compared (Table 4.5), but no significant differences were found between the left and right angles of the hip, knee and ankle.

Table 4.4 Mean and standard deviation of flexion angle of lower limbs of ADS patients: convex vs. concave sides of spine

		Convex side	Concave side		
		Median	Median	*Z*	*p*
Standing	Hip angle (˚)	-7.9	-6.48	-1.58	0.114
	Knee angle (˚)	-1.5	-8.09	-2.191	0.028*
	Ankle angle (˚)	2.82	2.03	-1.58	0.114
Sitting	Hip angle (˚)	72.9	69.1	-1.58	0.013*
	Knee angle (˚)	81.8	74.6	-2.803	0.005**
	Ankle angle (˚)	2.24	-0.51	-2.497	0.114

Note: $^*p < 0.05$, $^{**}p<0.01$, and $^{***}p<0.001$

Table 4.5 Mean and standard deviation of flexion angle of lower limbs of asymptomatic patients: convex vs. concave sides of spine

		Left side	Right side		
		Median	Median	Z	*p*
Standing	Hip angle (˚)	-11.1	-12	-0.764	0.445
	Knee angle (˚)	-13.9	-11.4	-1.682	0.093
	Ankle angle (˚)	0.05	2.66	-1.682	0.093
Sitting	Hip angle (˚)	64.4	65.4	-0.459	0.646
	Knee angle (˚)	80.2	80.3	-0.153	0.878
	Ankle angle (˚)	2.66	3.16	-0.357	0.721

Note: $*p < 0.05$, $**p<0.01$, and $***p<0.001$

Moreover, the convex and concave sides of the flexion angle of the hip, knee and ankle, pelvis tilt, obliquity and rotation, and spinal tilt were compared between the two groups of subjects during habitual standing and sitting respectively: seen Table 4.6. The Mann-Whitney U test was used while the significance of the statistical analysis was set at $p < .05$. In comparing the mean angles of the hip, knee and ankle of the two groups, the convex side of the ADS subjects shows a relatively large flexion angle of the knee ($Z = -2.57$, $p = 0.01$) and dorsiflexion angle of the ankle ($Z = -2.117$, $p = 0.034$) during habitual standing and a larger spinal tilt angle ($Z = -3.704$, $p < 0.001$) during habitual sitting. The remaining differences of the body angles between the ADS and asymptomatic groups show no significance ($p > 0.05$).

Table 4.6 Comparison of body angles: ADS vs. asymptomatic subjects

			ADS subjects	Asymptomatic subjects			
			Median	Median	U	Z	*p*
Standing	Convex side	Hip angle (˚)	-7.9	-11.5	31	-1.436	0.151
		Knee angle (˚)	-1.5	-13	16	-2.57	0.01**
		Ankle angle (˚)	2.82	0.397	22	-2.117	0.034*
	Concave side	Hip angle (˚)	-6.48	-11.5	36	-1.058	0.29
		Knee angle (˚)	-8.09	-13	26	-1.814	0.07
		Ankle angle (˚)	2.03	0.397	45	-0.378	0.705
	Pelvis tilt (˚)		3.17	5.21	42	-0.605	0.545
	Pelvis obliquity (˚)		-0.897	-1.02	42	-0.605	0.545
	Pelvis rotation (˚)		1.24	-0.49	40	-0.756	0.45
	Spinal tilt (˚)		6.36	5.11	36	-1.058	0.29
Sitting	Convex side	Hip angle (˚)	72.9	65.4	33	-1.285	0.199
		Knee angle (˚)	81.8	80.3	43	-0.529	0.597
		Ankle angle (˚)	2.24	2.66	42	-0.605	0.545
		Hip angle (˚)	69.1	65.4	41	-0.68	0.496

Concave side	Knee angle (˚)	74.6	80.3	26	-1.814	0.07
	Ankle angle (˚)	-0.51	2.66	27	-1.739	0.082
Pelvis tilt (˚)		-4.06	-10.9	26	-1.814	0.07
Pelvis obliquity (˚)		-0.296	-0.034	44	-0.454	0.65
Pelvis rotation (˚)		0.227	-0.956	45	-0.378	0.705
Spinal tilt (˚)		10.4	2.28	1	-3.704	<0.001***

Note: $^{*}p < 0.05$, $^{**}p < 0.01$, $^{***}p < 0.001$

4.4 Evaluation of muscle activity of ADS and asymptomatic subjects

The sEMG values of the muscle pairs of the convex and concave sides of the ADS patients, as well as the left and right sides of the asymptomatic subjects were compared; see Tables 4.7 and 4.8 respectively. The results show that the muscle activity on the convex side of the ADS patients is higher than the concave side, as significant differences can be observed in the muscle pairs of the ES thoracic (Z = -2.803, p = 0.005), ES lumbar (Z = -2.803, p = 0.005), LM (Z = -2.803, p = 0.005) and TA (Z = -2.293, p = 0.022) during habitual standing. During sitting, the differences between the muscle pairs of the ES thoracic (Z = -2.803, p = 0.005), ES lumbar (Z = -2.803, p = 0.005), LM (Z = -2.803, p = 0.005) and RF (Z = -2.599, p = 0.009) are also significant based on the Wilcoxon signed ranks test. However, no significant differences can be found for the sEMG values between the left and right muscles of the asymptomatic subjects (p >0.05).

Table 4.7 Mean and standard deviation of sEMG values of muscles: convex vs. concave side of ADS patients

		Convex side	Concave side		
		Median	Median	Z	*p*
Standing	ES thoracic	0.093	0.038	-2.803	0.005**
	ES lumbar	0.071	0.037	-2.803	0.005**
	LM	0.097	0.051	-2.803	0.005**
	RF	0.027	0.019	-0.968	0.333
	TA	0.016	0.015	-2.293	0.022*
Sitting	ES thoracic	0.101	0.046	-2.803	0.005**
	ES lumbar	0.058	0.031	-2.803	0.005**
	LM	0.052	0.025	-2.803	0.005**
	RF	0.015	0.011	-2.599	0.009**
	TA	0.009	0.009	-1.580	0.114

Note: *$p < 0.05$, **$p<0.01$, and *** $p<0.001$

Table 4.8 Mean and standard deviation of sEMG values of muscles: left vs. right side of asymptomatic subjects

		Left side	Right side		
		Median	Median	Z	*p*
Standing	ES thoracic	0.043	0.062	-0.459	0.646
	ES lumbar	0.036	0.039	-0.866	0.386
	LM	0.043	0.046	-1.478	0.139
	RF	0.029	0.015	-1.58	0.114
	TA	0.010	0.018	-0.866	0.386
Sitting	ES thoracic	0.075	0.061	-0.459	0.646
	ES lumbar	0.032	0.034	-1.07	0.285
	LM	0.028	0.030	1.886	0.059
	RF	0.023	0.016	-0.968	0.333
	TA	0.011	0.009	-0.968	0.333

Note: $*p < 0.05$, $**p<0.01$, and $*** p<0.001$

As the sEMG values of the left and right sides of the asymptomatic group show no significance, the sEMG values of the muscle pairs were averaged. When comparing the sEMG values of the ADS patients vs. those of the asymptomatic group via the Mann-Whitney U test, the muscle activity of TA of the former on the convex side (Z = -2.495, p = 0.013) is significantly less than that of the asymptomatic group while the muscle activity of the LM of the ADS patients on the concave side (Z = -2.041, p = 0.041) is significantly higher during habitual standing. During sitting, the muscle activity of the ES lumbar (Z = -2.269, p = 0.023), LM (Z = -2.495, p = 0.013) and TA (Z = -3.326, p < 0.001) of the ADS patients on the convex side as well as the muscle activity of the ES lumbar on the concave side (Z = -2.117, p = 0.034) are significantly higher while the muscle activity of the ES thoracic (Z = -2.873, p < 0.004) and LM on the concave side (Z = -2.948, p = 0.003) are significantly lower compared to the asymptomatic group. An interesting observation is that the paraspinal muscles of the ADS subjects consume at least 30% more energy than the asymptomatic group, except for the ES thoracic region during sitting (Figure 4.1).

Table 4.9 Comparison of sEMG values between ADS and asymptomatic subjects

			ADS subjects	Asymptomatic subjects			
			Median	Median	U	Z	*p*
Standing	Convex side	ES thoracic	0.093	0.059	29	-1.587	0.112
		ES lumbar	0.071	0.037	49	-0.076	0.94
		LM	0.097	0.043	32	-1.361	0.174
		RF	0.027	0.021	37	-0.983	0.326
		TA	0.016	0.012	17	-2.495	0.013*
		ES thoracic	0.038	0.059	48	-0.151	0.88

	Concave side	ES lumbar	0.037	0.037	38	-0.907	0.364
		LM	0.051	0.043	23	-2.041	0.041*
		RF	0.019	0.021	37	-0.983	0.326
		TA	0.015	0.012	45	-0.378	0.705
Sitting	Convex side	ES thoracic	0.101	0.063	29	-1.587	0.112
		ES lumbar	0.058	0.034	20	-2.269	0.023*
		LM	0.052	0.029	17	-2.495	0.013*
		RF	0.015	0.017	31	-1.436	0.151
		TA	0.009	0.009	6	-3.326	<0.001***
	Concave side	ES thoracic	0.046	0.063	12	-2.873	0.004**
		ES lumbar	0.031	0.034	22	-2.117	0.034*
		LM	0.025	0.029	11	-2.948	0.003**
		RF	0.011	0.017	26	-1.814	0.07
		TA	0.009	0.009	48	-.151	0.88

Note: $*p < 0.05$, $**p<0.01$, and $*** p<0.001$

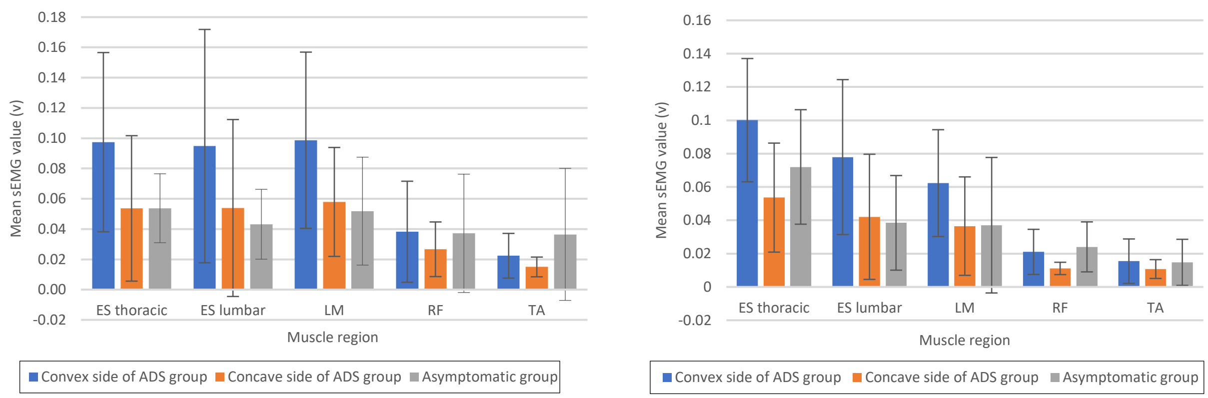

(a) (b)

Figure 4.1 Comparison of mean sEMG values of ADS and asymptomatic subjects during (a) habitual standing, and (b) habitual sitting

4.5 Discussion

In this study, habitual standing and sitting postures are used to assess the static balance control ability and muscle activity level of the concave and convex sides of the spinal deformity of ADS subjects, which are compared to those of the asymptomatic participants. However, the first hypothesis is not supported as the ADS group do not show more body sway and COP displacement compared to the asymptomatic group. The result is also different from the findings in Haddas and Lieberman (2019) and Yagi et al. (2016). A possible explanation might be due to the severity of the deformity of the recruited subjects. Postural steadiness and balance are highly correlated to the Cobb angle and spinopelvic parameters (Gottipati et al., 2018; Haddas et al., 2020). The radiographic spinopelvic parameters of the ADS patients in previous studies are much worse, even with recommendation for surgical procedures being followed (Wren et al., 2011). As some of the recruited subjects have a relatively smaller Cobb angle and no deformity in the sagittal modifier, their balance and postural control ability might not be significantly influenced.

The second aim of this study is to investigate the differences in the muscle activity and the body angles of the lower limbs in terms of the convex and concave sides. The findings show that the body angles of the lower limbs of the ADS patients might change because of their spinal deformity as they have a larger knee flexion in the standing posture and increased hip and knee flexion in the sitting posture on the convex side. Moreover, the paraspinal muscles and lower extremities on the convex side generally show increased muscle activity compared to the concave side. The findings are in agreement with those of previous research in that the ADS patients have asymmetrical muscles in which the elongated and stretched muscles on the convex side may require more energy expenditure and can withstood a higher tension load (Hyun et al., 2013; Mattei, 2013; Tecco et al., 2011). The imbalance in muscular activity may lead to higher possibility of fatigue or even lower back pain, and then discourage ADS patients from performing their daily activities.

The third aim of the study is to distinguish the differences in body angles and sEMG activity between the ADS and asymptomatic groups. During standing, the balancing pattern of the former changes to compensate for the shift of the gravity line caused by the spinal deformity (Barrey et al., 2011), with more knee flexion and ankle dorsiflexion compared to the latter. Meanwhile, the ADS group may need to maintain their sitting posture by leaning their torso forward as they have a larger spinal tilt angle during habitual sitting compared to the asymptomatic participants. As for the muscle activity, the findings show that the ADS patients have significant differences compared to the non-ADS subjects, especially their concave side during sitting. The findings also show that the torso of the ADS patients generally exert more muscular energy than their non-ADS counterparts (Mahaudens et al., 2009).

There are several limitations inherent in the work in this chapter. First, the sample size (N = 10) for each subject group) is relatively small, which may limit the statistical power of the study (power = 0.51). Secondly, the severity of the spinal deformity of the recruited ADS subjects varies, which might influence the effect of the parameters related to posture, balance and muscle activity, so the ADS patients with more severe spinopelvic parameters should be further investigated. Lastly, the tasks provided in this study is only to measure static balance, so different types of perturbations or assessments can be added to investigate the relationship between balance and sensorimotor factors of the ADS patients.

4.6 Conclusions

This study examines the posture and muscle activity of ADS and asymptomatic individuals. The results show that ADS subjects have more knee flexion and ankle dorsiflexion during standing and a larger spinal tilt angle during sitting as a compensatory mechanism for maintaining balance. Moreover, the muscle activity between the two groups with habitual sitting posture shows significant differences. The ADS patients also exert more energy in the paraspinal muscles to maintain their habitual posture which causes fatigue easily when performing daily activities. These findings enhance current knowledge on the balance strategies adopted by ADS patients, so the examination of posture and sEMG values might also be an appropriate means of differentiating between scoliotic and non-scoliotic individuals.

CHAPTER 5: Clinical study of existing active bodysuit

5.1 Introduction

In this chapter, two clinical studies of the active bodysuit developed in Sit et al. (2020) are conducted to evaluate its efficacy. One is 2 hours in length while the other is 3 months long. The purpose of these two preliminary clinical trials is to obtain detailed background information about this brace, investigate the deficiencies of the active bodysuit, and deliberate possible modifications to optimise the proposed active bodysuit. The participants are required to undergo a radiographic examination that would identify their spinal deformity, and the effect of the active bodysuit is evaluated by comparing the X-rays of the spine pre- and post-bracing treatment. Moreover, questionnaires are the secondary outcome measure used to access the effectiveness of the active bodysuit.

5.2 Subject recruitment

Participants between 50 and 70 years old were screened for ADS at The Hong Kong Polytechnic University by using the recruitment criteria outlined in Section 3.3.1 of Chapter 3. After confirming a diagnosis of scoliosis and examining the spinal deformity through a radiographic examination, a total of 10 ADS subjects were recruited to undergo the posture study as outlined in Chapter 4. Their spinal measurements are listed in Table 4.2. Among these 10 subjects, only 6 participated the 2-hour wear trial of the active bodysuit (mean age: 60 ± 3.74 years old, mean height: 157 ± 8.09 cm, mean weight: 54.8 ± 7.84 kg). Among these 6 subjects, 5 participated in the 3-month clinical study (mean age: 60.2 ± 4.07 years old, mean height: 160 ± 5.71 cm, mean weight: 56.9 ± 6.92 kg). The outbreak of Covid-19 and unwillingness to take repetitive X-rays were the reasons for participants to drop out the study.

5.3 Fit of active bodysuit by Sit et al. (2020)

A professional prosthetist and orthoptist (P&O) was recruited for the fitting session to adjust the placement of the buckle and tightness of the elastic waistband and straps while evaluating the shape of the supportive bones (Figure 5.1). The aim for adjusting the buckle, elastics and supportive bones was to ensure that the corrective forces was exerted onto the apex of the curve based on the three-point pressure system in which the elastic straps and elastics are responsible for holding the shoulder and pelvis in place respectively. The buckle and supportive bones are responsible for pushing the apex and helping the subject to maintain an upright posture.

Figure 5.1 Photos taken from brace fitting session

5.4 Two-hour wear trial study

After the 2-hour wear trial, in-brace radiographic images were taken and questionnaires on the psychological and physiological comfort were conducted with the subjects. The initial effect of wearing the brace on reduction of spinal curvature can be found by comparing the radiographic images of subject with brace donned versus doffed (Figure 5.2).

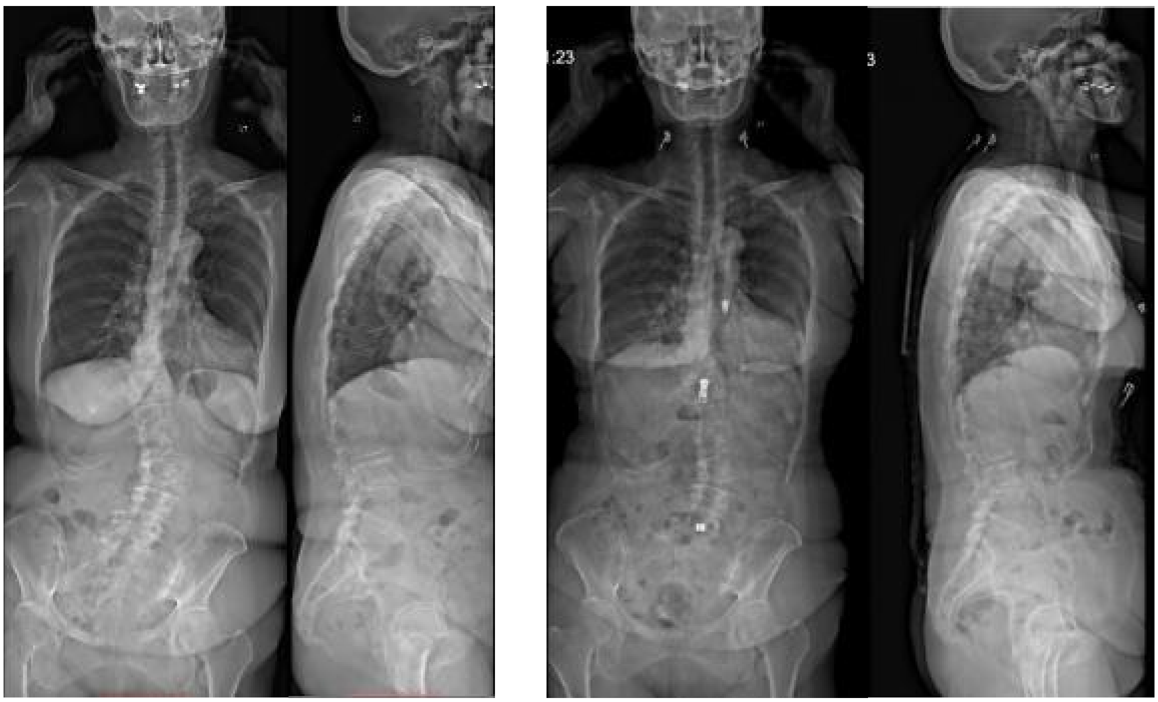

a b

Figure 5.2 Radiographic images of lateral plane (left side of x-ray) and sagittal plane (right side of x-ray): (a) brace doffed and (b) brace donned

5.4.1 Effect on controlling spinal curvature

Generally, older adults who have attained skeletal maturity, prevention of an increase of the mean Cobb angle or a reduction in the spinal curvature progression are regarded as positive results

(Schoutens et al., 2020). As shown in Table 5.1, the results show that only Subject s20009 has the largest reduction of 8˚ in the thoracic region while Subject s20004 has the highest reduction of 6˚ in the lumbar region. The remaining subjects (66.7%) experience a reduction of less than 5˚ of their Cobb angles. The Wilcoxon signed rank test indicated that only the Cobb angle of the lumbar region of the subjects shows a significant difference when the brace is not worn versus after 2 hours of bracing treatment ($Z = -2.032$, $p = 0.042$) but this is not true for the Cobb angle in the thoracic region ($Z = -1.604$, $p = 0.109$). For the sagittal modifiers, there is an increase in the median SVA of 13.5 mm, median PI-LL mismatch of 3˚ and decreasing mean PT of 0.5˚ after 2-hours of wearing the brace. There are no statistically significant differences among the SVA ($Z = -1.572$, $p = 0.116$), PI-LL mismatch ($Z = -0.674$, $p = 0.5$) and PT ($Z = -.412$, $p = 0.68$) between pre-intervention and post-intervention. Therefore, the results indicate that the active bodysuit did not offer a significant change to the in-brace Cobb's angle, the sagittal balance and spinopelvic parameters.

Table 5.1 Spinal measurements at pre-intervention and after 2 hours of brace wear

Spinal measurement	Subject code	Pre-intervention	After 2-hours of brace wear	In-brace reduction/increase of the measurements
Cobb angle in the thoracic region (˚)	s20002	-	-	-
	s20004	30	27	-3
	s20007	33	31	-2
	s20008	-	-	-

	s20009	24	16	-8
	s20010	-	-	-
	Median	30	27	-3
Cobb angle in the lumbar region (˚)	s20002	34	33	-1
	s20004	48	42	-6
	s20007	60	56	-4
	s20008	72	71	-1
	s20009	33	30	-3
	s20010	42	42	0
	Median	45	42	-2
SVA (mm)	s20002	-52	-37	+15
	s20004	34	20	-14
	s20007	23	33	+10
	s20008	-17	3	+20
	s20009	43	67	+24
	s20010	30	42	+12
	Median	26.5	26.5	13.5

PI-LL (˚)	s20002	-10	-11	+1
	s20004	29	21	-8
	s20007	14	14	0
	s20008	-19	-10	+9
	s20009	29	36	+7
	s20010	8	13	+5
	Median	11	13.5	3
PT (˚)	s20002	0	-1	-1
	s20004	24	25	+1
	s20007	31	27	-4
	s20008	5	5	0
	s20009	32	34	+2
	s20010	17	16	-1
	Median	20.5	20.5	-0.5

5.4.2 Wear Comfort

The subjects are required to complete two questionnaires after wearing the active bodysuit for 2 hours, including the SRS-22r and Oswestry Low Back Pain Disability Questionnaire to assess the health-related quality of life of the recruited subjects.

5.4.2.1 Oswestry Low Back Pain Disability Questionnaire

The Oswestry Low Back Pain Disability Questionnaire contains 10 questions to examine the influence of lower back pain on perceived ability in performing daily activities. The Oswestry Disability Index (ODI) is used to categorise the questionnaire scores into 5 levels of disability. The range of the ODI is 0% to 100%, in which a lower score indicates higher body functionality. Among the 6 subjects, 3 of them (50%) have moderate disability (21% - 40%) and the remaining 3 subjects (50%) are categorised as having minimal disability (0% - 20%) (Figure 5.3).

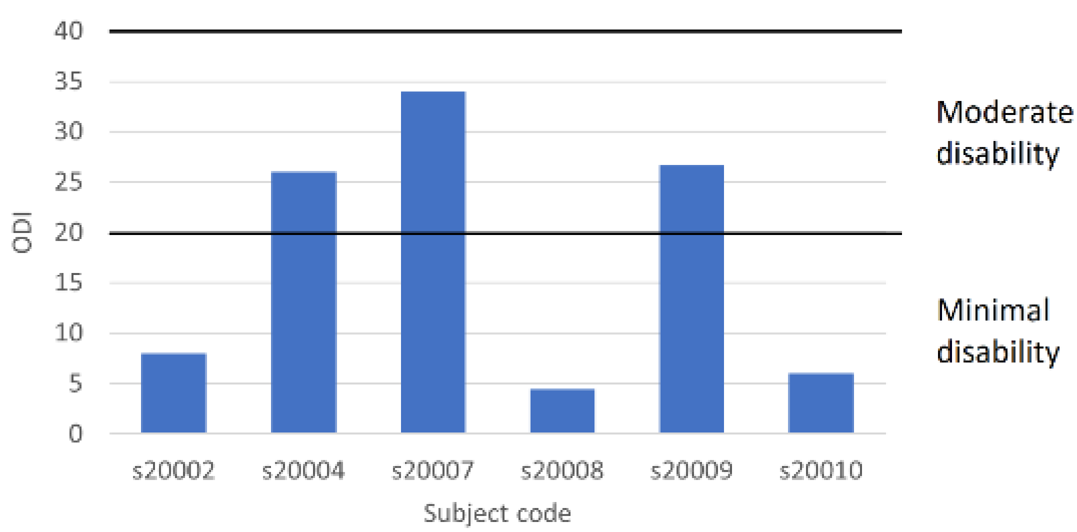

Figure 5.3 ODI scores of recruited ADS patients

5.4.2.2 Scoliosis Research Society 22-item Patient Questionnaire

The SRS-22r is commonly used to assess the functionality, level of pain, self-perceived image, mental health and satisfaction with treatment of scoliotic patients. The score for each domain ranges from 1 to 5, where 1 denotes the worst outcome and 5 denotes the best outcome. Figure 5.4 shows the SRS-22r score of each subject, with an overall average score of 3.45. Baldus et al. (2008) examined the quality-of-life outcomes of adult patients who receive conservative treatment for a deformity and a control population by using SRS-22r. In comparing all of the average SRS scores in each domain, the adult patients with a spinal deformity in Baldus et al. (2008) and the recruited subjects in this study have a similar quality-of-life outcome. Meanwhile, the average SRS-22r score of the control population in Baldus et al. (2008) is higher than that of the subjects in this study. This could be interpreted to mean that ADS patients have a lower health related quality of life than the non-scoliotic population and the active bodysuit does not deteriorate the quality of life of ADS patients.

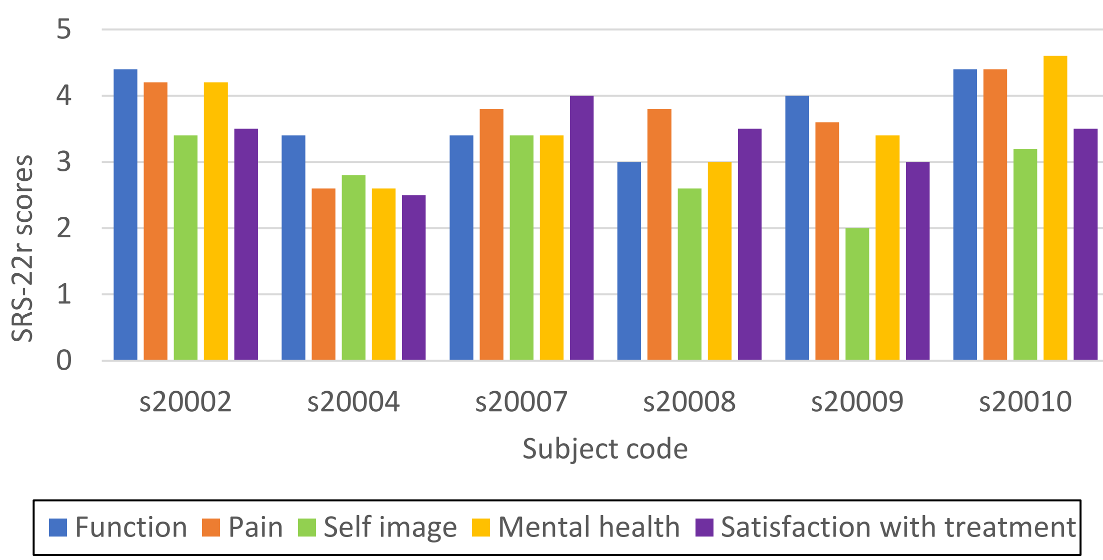

Figure 5.4 SRS-22R scores for each domain

Table 5.2 Comparison of mean SRS-22r score for each domain

	Subjects in this study	Population with spinal deformity (Baldus et al., 2008)	Control population (Baldus et al., 2008)
Function	3.77 (0.6)	3.5 (0.8)	4.3 (0.4)
Pain	3.73 (0.6)	3.3 (0.9)	4.3 (0.6)
Self-image	2.9 (0.5)	3.1 (0.8)	4.2 (0.6)
Mental health	3.53 (0.7)	3.7 (0.8)	4.1 (0.6)
Satisfaction with treatment	3.33 (0.5)	-	-

5.5 Three-month clinical study

To determine the short-term effect of the active bodysuit, 5 of the subjects who took part in the 2-hour trial wear agreed to participate in the 3-month clinical study. The subjects underwent another radiographic examination and completed a questionnaire to assess their health-related quality of life at the end of the 3-month clinical wear trial. The subjects wore the active bodysuit for an average of 3.2 hours ± 1.96 each day (Figure 5.5).

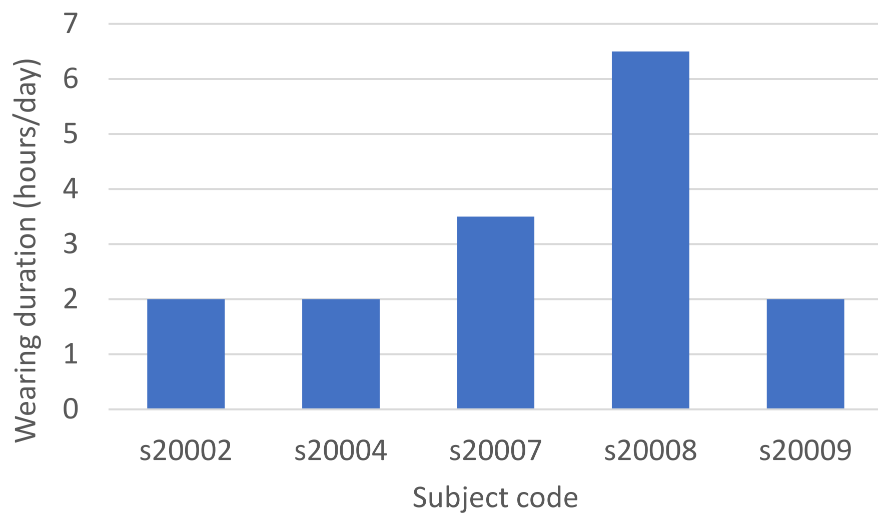

Figure 5.3 Self-reported length of brace wear

5.6 Effects on spinal measurements

After the 3-month wear trial, the participants showed an average reduction of 4° of the curvature in the thoracic region and 1.6° of the curvature in the lumbar region (Table 5.3). Moreover, 4 subjects experience a reduction of more than 5˚ of their Cobb angles and 1 subject has deteriorated lumbar curvature. However, there is no significant changes in the Cobb angles in the thoracic region ($Z = -1.633$, $p = 0.102$) and lumbar region ($Z = -0.73$, $p = 0.465$) between pre-intervention and after 3 months of the clinical trial. For the sagittal modifiers, the sagittal balance and PI-LL mismatch demonstrate an average increase of 17.4 mm and 0.6° respectively while the mean PT of the subjects shows a reduction of 1°. Only the sagittal balance (SVA) significantly changes after the 3-month clinical trial ($Z = -2.023$, $p = 0.043$), while the PI-LL mismatch ($Z = -0.412$, $p = 0.68$) and PT angle ($Z = -0.966$, $p = 0.334$) show similar results based on the measurements taken during pre-intervention.

To compare the spinal deformity changes between 2-hours and 3-months in-brace, 2 subjects experience a reduction of more than 5˚ of their Cobb angles in the lumbar region. However, there is no significant changes in the Cobb angles in the thoracic region (Z = -1.342, p = 0.18) and lumbar region (Z = -0.948, p = 0.343). Moreover, there is no significant changes between the sagittal modifiers of SVA (Z = -0.944, p = 0.345), PI-LL mismatch (Z = -0.542, p = 0.588) and PT angle (Z = -0.406, p = 0.684).

Table 5.3 Spinal measurements at pre-intervention and after 3-month wear trial

Spinal measurement	Subject code	Pre-intervention	3 month in-brace	In-brace reduction/increase of Cobb angle
Cobb angle in the thoracic region (˚)	s20002	-	-	-
	s20004	30	24	-6
	s20007	33	27	-6
	s20008	-	-	-
	s20009	24	16	-8
	Median	30	24	-6
	s20002	34	44	+10
	s20004	48	43	-5
	s20007	60	60	0

Cobb angle in the lumbar region (˚)	s20008	72	61	-11
	s20009	33	31	-2
	Median	48	44	-2
SVA (mm)	s20002	-52	-51	+1
	s20004	34	39	-5
	s20007	23	31	+8
	s20008	-17	16	+33
	s20009	43	93	+50
	Median	23	31	8
PI-LL (˚)	s20002	-10	-12	-2
	s20004	29	25	-4
	s20007	14	16	+2
	s20008	-19	-14	+5
	s20009	29	31	+2
	Median	14	16	2
PT (˚)	s20002	0	3	+3
	s20004	24	23	-1

s20007	31	28	-3
s20008	5	2	-3
s20009	32	31	-1
Median	24	23	-1

5.7 Effects on health-related quality of life

The participants completed both the ODI and SRS-22r at the end of the two hours and the third month of intervention. The results were compared by using the Wilcoxon signed rank test. The ODI of the subjects is similar between the two intervals ($Z = -0.135$, $p = 0.893$). Two of the subjects (s20007 and s20009) reduced their level of disability from moderate to minimum after 3-months of brace wear, 4 of the subjects (80%) have minimal disability after wearing the brace and only 1 subject (20%) was classified as moderately disabled.

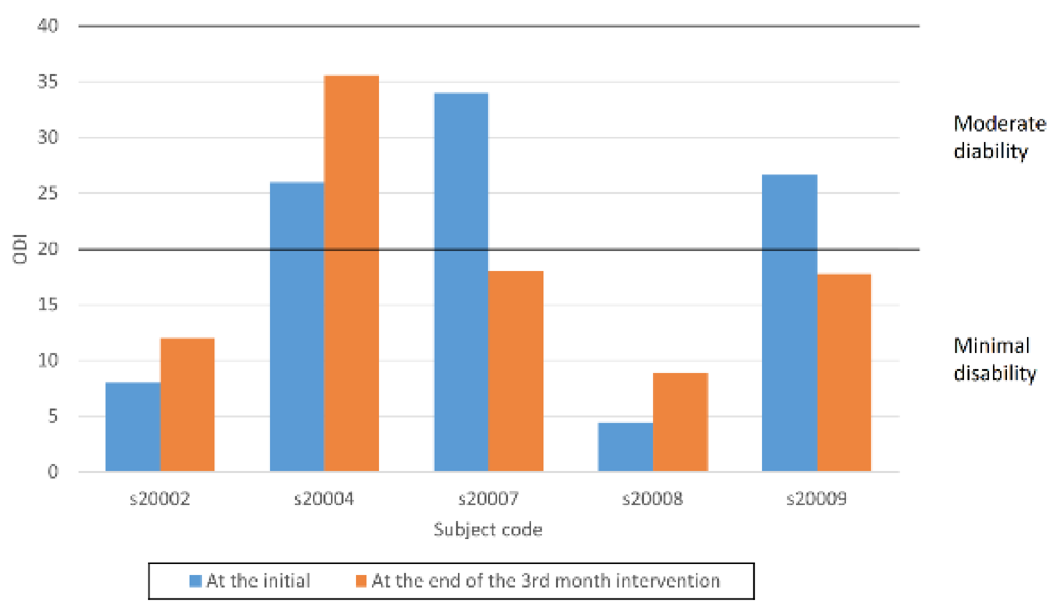

Figure 5.4 ODI score at end of the two hours and the third month of intervention

In comparing the SRS-22r scores between the 2-hours and 3-months wear trial, the total mean score is increased from 3.34 to 3.74. Figure 5.5 shows that the average score of each domain on the 3rd month of the intervention is relatively higher than those obtained in the pre-intervention stage. After conducting the Wilcoxon signed rank test, the result indicated that the pain score of the participants is significantly reduced ($Z = -2.032$, $p = 0.042$). Meanwhile the average score of function ($Z = -1.604$, $p = 0.109$), self-image ($Z = -0.54$, $p = 0.588$), mental health ($Z = -1.761$, $p = 0.078$) and satisfaction with treatment ($Z = -1.633$, $p = 0.102$) has not been affected after wearing the active bodysuit for 3 months.

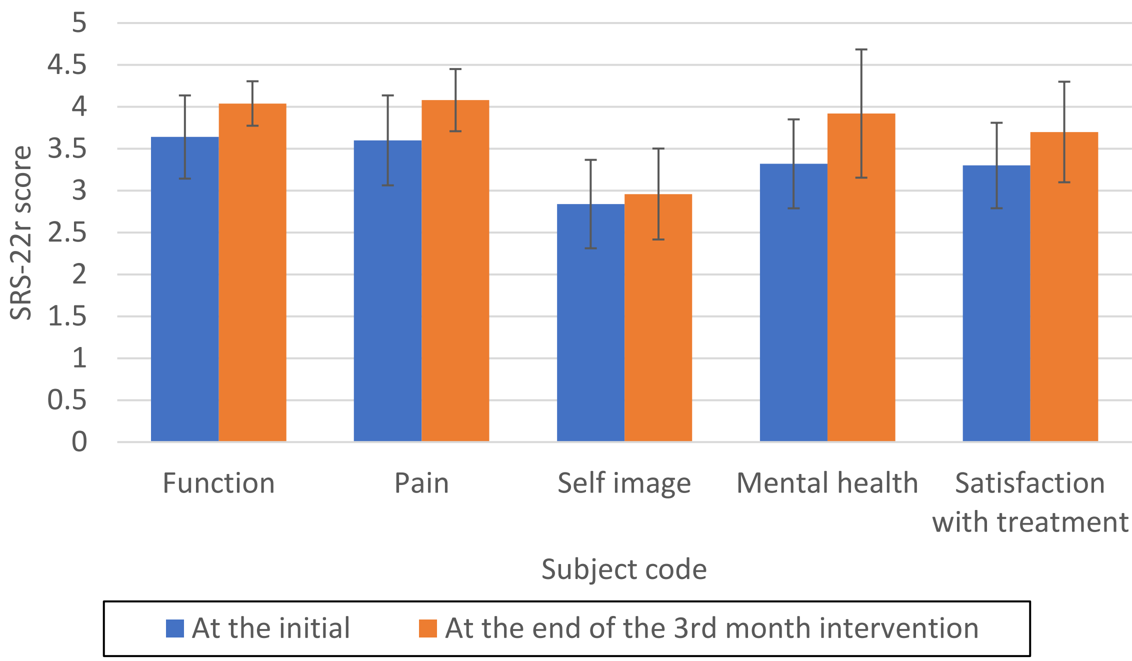

Figure 5.5 SRS-22R domain scores at end of the two hours and the third month of intervention

5.8 Subject feedback

Apart from the radiographic examination and the questionnaires, a short interview was also conducted to further investigate the limitations of the active bodysuit. The subjects reported that they feel uncomfortably warm when they wear the active bodysuit because the multiple layers of the bodysuit do not allow air to flow through, and the shoulder straps and waistband became loose after a certain period of time. Moreover, the design is quite complicated to don on and off. Therefore, it appears that the materials used might affect how the subject perceive and receive the bodysuit. To address these issues and optimise the bodysuit, materials with higher thermal comfort are recommended for the inner vest of the proposed active bodysuit, and woven materials with higher tensile strength and less stretchability are recommended to exert higher corrective forces through the shoulder straps and waistband to the spine of ADS patients.

5.9 Summary

The active bodysuit developed by Sit et al. (2020) is a flexible brace that has incorporated rigid materials to correct the body alignment and posture of ADS patients. However, its efficacy has not been confirmed and its corresponding biomechanics are uncertain. Therefore, a clinical study is conducted in this study to examine the functions of the active bodysuit through radiographic examination, questionnaires, and feedback from the users.

Although the 2-hour clinical study shows that there is a significant in-brace reduction of the Cobb angle, the average reduction of Cobb angle is less than 3 degrees. Meanwhile, the results of the 3-month clinical study are not statistically significant, but 4 out of 5 subjects experienced more than 5 degrees reduction of their Cobb angle. The in-brace corrective effect might have been influenced by the low compliance rate with the treatment and the materials of the active bodysuit based on the feedback from the subjects.

As for the questionnaires, the recruited ADS subjects present a statistically higher score in the pain domain after 3-months of brace wear while the ODI and the remaining SRS-22r subdomain scores are similar. The result shows that the active bodysuit has potential for preventing the progression of spinal curvature, relieving pain, as well as maintaining the ability of ADS patients to perform daily activities. At the same time, the thermal discomfort and corrective effect of the existing active bodysuit need to be addressed.

There are some limitations in this part of the study. Firstly, the sample size of the two-hours (N = 6) and three-months (N = 5) clinical trial is inadequate to obtain a high statical power. Secondly, the duration of the study is relatively short, and the study is not able to trace the physical and psychological effects of the active bodysuit towards ADS patients in long term. Thirdly, there is no standardised posture for patients in taking radiographic images which the posture variability may affect the accuracy of the spinal measurements. For future study, a larger sample size (N >10) and a longer period (6 months) of clinical trial should be conducted, with a designated posture adopted in taking X-rays, and more statical analysis can be conducted such as the relationship between spinal curvature correction and low back pain.

CHAPTER 6: Design and development of active bodysuit

6.1 Introduction

The active bodysuit in Sit et al. (2020) has a low compliance rate due to thermal discomfort and lack of material durability as reported by the recruited subjects in a clinical wear trial. As the material parameters are highly correlated to the brace performance in their study, the different brace components should have different selection requirements. To address the above problems, materials with higher thermal conductivity, water vapor and air permeabilities, dimensional stability and better mechanical performance are chosen for the proposed active bodysuit.

6.2 Design criteria

The proposed active bodysuit aims to optimise the corrective forces exerted and performance of flexible braces as well as address the drawbacks of the design in Sit et al. (2020). The design criteria of the active bodysuit are listed in Table 6.1 for the functional, expressive and aesthetic aspects which are related to utility, symbolic meaning and appearance of the brace respectively.

Table 6.6.1 Design criteria of the active bodysuit

Design Aspect	Design requirement	Interpretation
Functional	Posture, spinal control and pain relief	To exert sufficient corrective forces onto the subject to correct posture, body alignment, and relieve pain.

	Durability	To withstand long durations of wear and laundering.
	Mobility	To maintain body movement of the subject during bracing treatment.
	Comfort	To maintain optimal microclimate between the proposed bodysuit and body.
	User accessibility	To ensure the design allows ease of donning and doffing, and ADS patients can adjust fit by themselves.
Expressive	Garment form	To give a distinct appearance of a flexible brace to avoid association with rigid orthoses.
	Light in weight	To emphasise its use as a functional garment instead of a heavy and rigid brace.
Aesthetics	Minimalist	To avoid a bulky appearance and allow focus to be on the markings on the brace.
	Light achromatic colours	To conceal proposed bodysuit underneath everyday garments.

In terms of the functional aspect, the primary outcome of the active bodysuit is to reduce the Cobb angle of the ADS patients as well as improve their body alignment which can be evaluated by the degree of in-brace correction after the bodysuit is worn for 2 hours. The proposed active bodysuit should provide adequate corrective forces through the shoulder straps, supportive bones and waistband (Figure 6.1). Moreover, the bodysuit needs to be convenient to wear, durable and breathable without restricting body movement so as to maintain the quality of life of the ADS patients and thus enhance the compliance rate with bracing treatment.

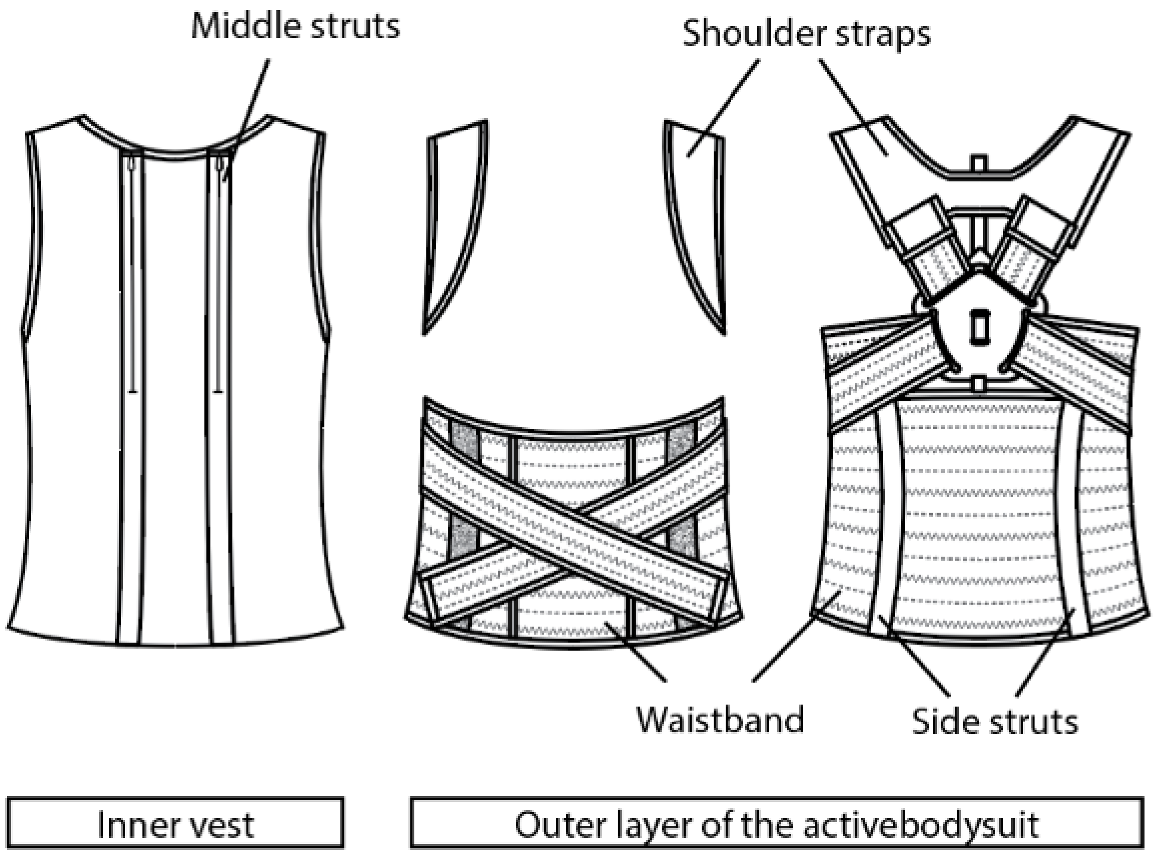

Figure 6.1 Corrective components of active bodysuit

As conventional hard braces are heavy and bulky, ADS patients find it difficult to conceal or cover the brace during bracing treatment which has negative psychological impacts on them, such as low self-esteem and feeling useless. To reduce the negative psychological mindset of ADS patients towards bracing treatment, the proposed active bodysuit should be similar in appearance to a functional garment and light in weight to avoid any association between the proposed brace and traditional orthoses.

Finally, a minimalist brace design and light colour should be used for the aesthetics of the proposed active bodysuit. The minimalism design is to retain a simple brace design with only the essential elements, a monochromatic colour scheme, and emphasise certain design elements. Moreover, ADS patients may experience psychological barriers and antipathy towards the bulky appearance of the traditional hard brace, so it is important to ensure that the proposed brace design is camouflaged and covered by outerwear.

6.3 Material selection

The physical properties of textiles are very much correlated with the functional criteria for the proposed active bodysuit, i.e., the control of posture and body alignment, durability and wear comfort. Hence, the mechanical performance, dimensional stability and thermal comfort of different materials were tested. For the inner vest (Figure 6.2), high dimensional stability and thermal comfort are required for withstanding laundering and maintaining thermoregulation of the body during the long duration of the bracing treatment. To determine the thermal comfort and durability of the textiles, several tests were conducted, including for stretch and recovery, thermal conductivity, air and water vapor permeabilities and dimensional stability after laundering. A total of 13 textiles with different compositions were sourced and then compared with the two original materials used in Sit et al. (2020). Finally, the materials with the best performance were used to fabricate the proposed active bodysuit. Tables 6.2 and 6.3 provide the material specifications, including the fabric structure, thickness, weight and density, material composition, and microscopic view of the technical face and back of the material.

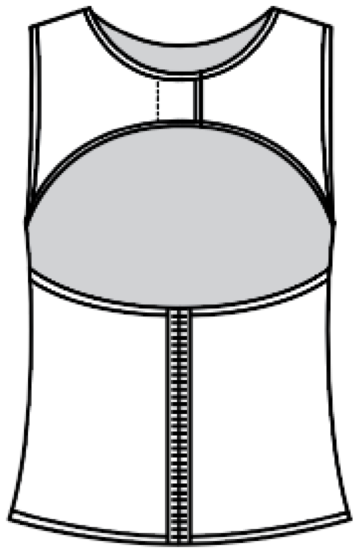

Figure 6.2 Inner vest of the proposed active bodysuit

Table 6.2 Specifications of tested materials

Code	Material Composition	Fabric Structure	Technical face view	Technical back view
F1	85% Nylon 15% Spandex	Single Jersey		

F2	100% polyester	Single Jersey	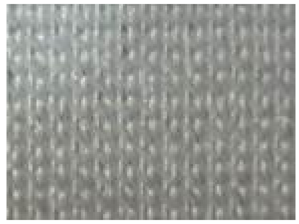	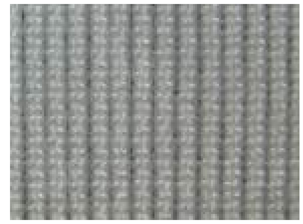
F3	89% Polyester 11% Lycra	Single Jersey	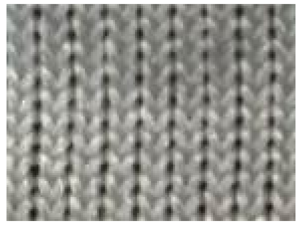	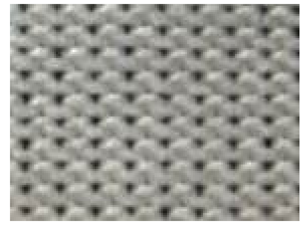
F4	73% Nylon 27% Spandex	Tricot	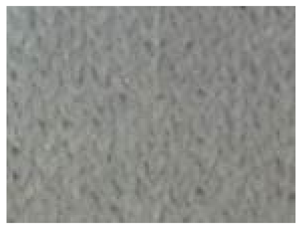	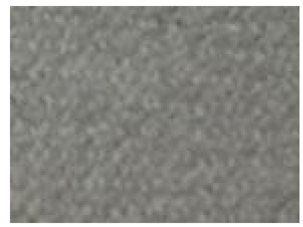
F5	90% Nylon 10% Spandex	Tricot	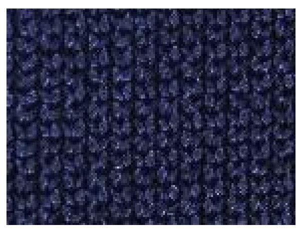	
F6	85% Polyester 15% Spandex	Interlock	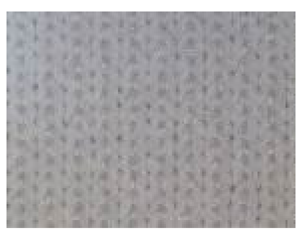	
F7	95% Cotton 5% Polyurethane	Single Jersey		

M1	83% Nylon 17% Spandex	Powernet	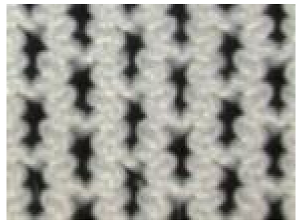	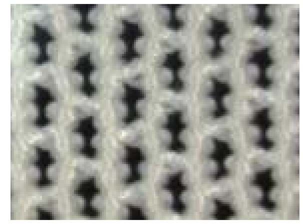
M2	76% Nylon 24% Spandex	Powernet		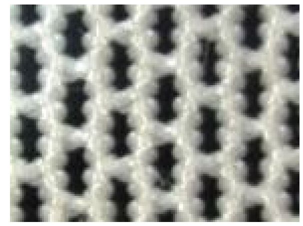
M3	88% Nylon 12% Spandex	Satinnet	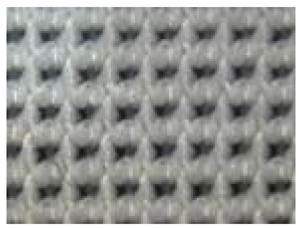	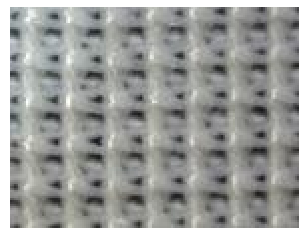
M4	90% Nylon 10% Spandex	Powernet	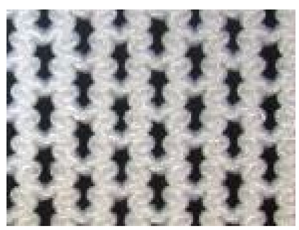	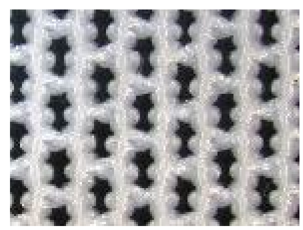
M5	80% Polyester 20% Spandex	Powernet	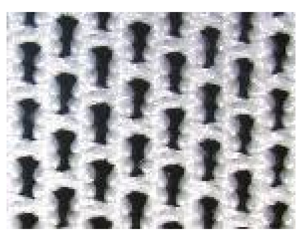	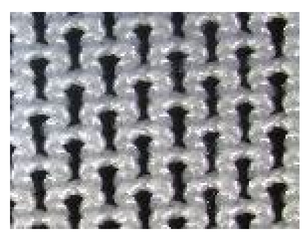
M6	85% Nylon 15% Spandex	Powernet	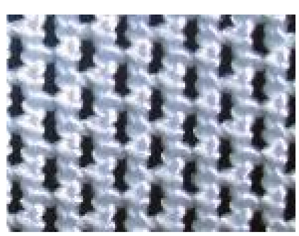	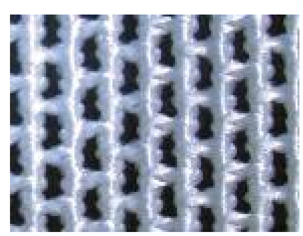

O1	82% Polyamide 18% Elastane	Tricot		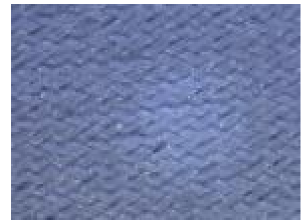
O2	77% Polyamide 23% Elastane	Powernet	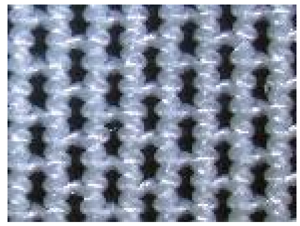	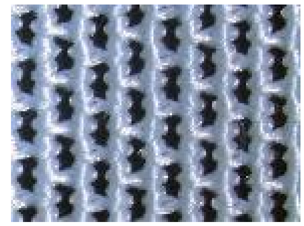

Notes: O1 and O2 denote the original fabric used in the active bodysuit

Table 6.3 Thickness and weight of the tested fabrics

Code	Fabric thickness (mm)	Fabric weight (g/m^2)	Fabric density (wales per inch × courses per inch)
F1	0.46	156.6 ± 1.8	76 × 44
F2	0.46	127.3 ± 1.0	90 × 83
F3	0.32	109.5 ± 0.7	77 × 51
F4	0.44	144.2 ± 1.1	78 × 64
F5	0.54	219.4 ± 2.9	102 × 76
F6	0.77	325.0 ± 4.6	102 × 64
F7	0.43	198.2 ± 3.1	115 × 69
M1	0.46	200.3 ± 2.5	26 × 38

M2	0.42	162.2 ± 2.5	22 × 23
M3	0.54	225.4 ± 1.3	32 × 38
M4	0.44	185.0 ± 2.2	25 × 19
M5	0.42	164.5 ± 1.8	19 × 19
M6	0.42	182.6 ± 0.1	25 × 36
O1	0.76	238.3 ± 0.6	114 × 75
O2	0.41	160.8 ± 3.0	25 × 32

6.3.1 Stretch and recovery test

As flexible braces are tightly fitting garments, the primary types of fabrics used for flexible braces are also important as they are subjected to stretching during normal wear and loading from the corrective components. Due to the use of elastic straps and waistband, the elastics were only elongated in the weft direction while the main fabric samples were subjected to four-way stretching. Hence, the stretch and growth percentage of elastics were tested in the weft direction only and the stretch and growth percentage of the fabric were tested in both warp and course directions, respectively, which are shown in Table 6.4.

Table 6.4 Test results of stretching properties of main fabric samples

	Warp direction		Course direction	
	Stretch (%)	Growth (%)	Stretch (%)	Growth (%)
F1	118.605 ± 4.731	9.490 ± 2.079	132.055 ± 1.421	7.480 ± 0.113
F2	113.505 ± 1.916	3.490 ± 1.174	84.255 ± 2.397	5.660 ± 1.174
F3	76.360 ± 0.707	3.985 ± 1.393	124.910 ± 2.333	3.070 ± 0.099
F4	129.265 ± 5.508	7.790 ± 6.152	124.195 ± 1.464	14.425 ± 4.603
F5	113.890 ± 1.372	10.195 ± 0.078	79.160 ± 0.000	7.205 ± 1.252
F6	61.810 ± 0.636	2.870 ± 0.014	69.060 ± 0.707	3.865 ± 0.375
F7	122.860 ± 0.566	7.605 ± 0.403	107.500 ± 4.144	6.125 ± 1.011
M1	106.915 ± 2.044	3.215 ± 0.049	63.100 ± 0.806	4.675 ± 0.021
M2	96.815 ± 1.761	3.115 ± 0.389	71.965 ± 0.559	3.040 ± 0.523
M3	26.065 ± 2.114	2.420 ± 0.792	98.870 ± 0.990	5.525 ± 0.361
M4	97.045 ± 2.383	4.300 ± 0.919	59.760 ± 0.000	5.335 ± 0.007
M5	84.560 ± 0.000	5.670 ± 0.141	83.970 ± 3.394	3.250 ± 4.978
M6	108.410 ± 1.061	9.780 ± 6.350	69.110 ± 0.495	6.930 ± 0.057
O1	99.560 ± 0.283	9.505 ± 5.353	105.460 ± 2.121	10.125 ± 0.078

O2	130.710 ± 2.475	3.655 ± 0.092	94.905 ± 2.906	4.080 ± 0.792

The percentage of stretch describes the ability of the fabric to extend at a designated load. A higher stretch rate means greater extensibility of the fabric. The fabric growth rate indicates the resistance to elongation of the fabric. A higher growth rate denotes greater elongation after stretching. For the main fabric samples used, the original mesh fabric (O2) used in the active bodysuit has the highest stretchability of 130.7% or more while M3 is the least stretchable with a stretchability of 26.1% in the warp direction. In the course direction, F1 can stretch up to 132% of its original length which is the highest percentage of stretch. M1 is the least stretchable among the 15 fabric samples. For the percentage of fabric growth, F5 shows the highest fabric growth rate of 10.2% after extension and M3 has the lowest fabric growth rate of 2.4% in the warp direction. F4 has the highest fabric growth rate of 14.4% and F3 has the lowest fabric growth rate in the weft direction. by combining the percentages of stretch and growth in both the warp and weft directions (Figures 6.3 and 6.4), F4 has the highest stretchability and growth rate. Meanwhile, M3 has the lowest fabric growth rate and the lowest elasticity among the 15 fabric samples.

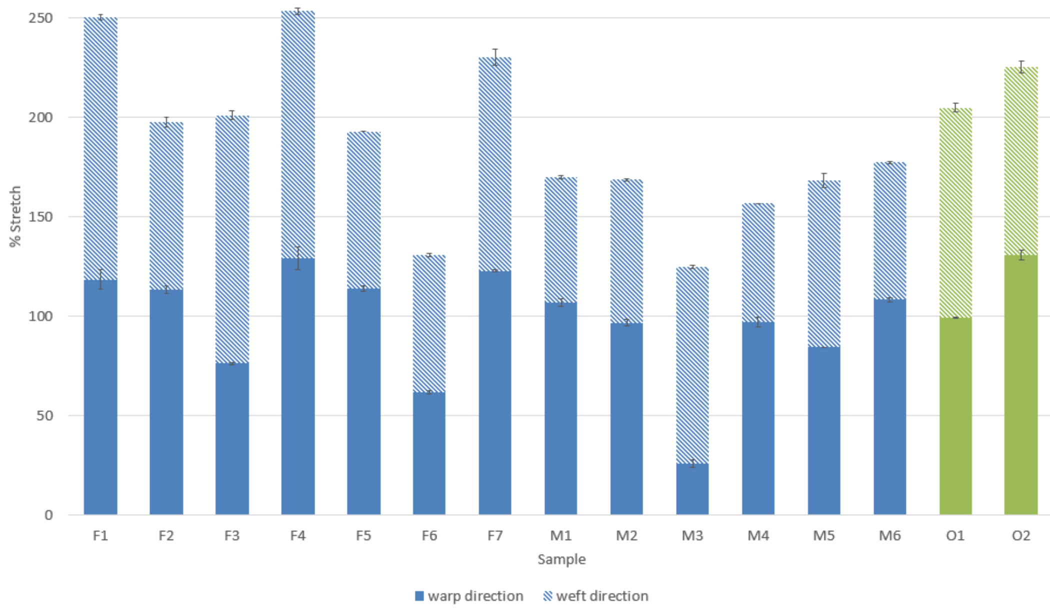

Figure 6.3 Stretch percentage of main fabric samples in warp and course directions

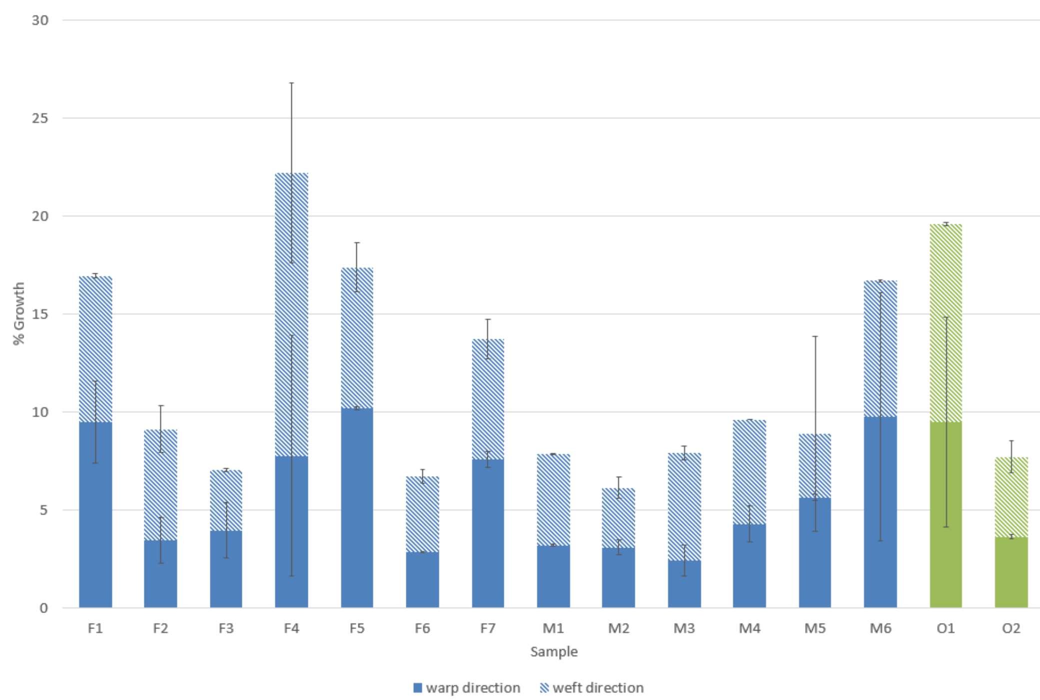

Figure 6.4 Growth percentage of main fabric samples in warp and course directions

6.3.2 Water vapor permeability test

Water vapor permeability is highly correlated to the thermal comfort of flexible braces. Therefore, the related experiment in this study shows the ability of the fabric sample to wick perspiration away from the surface of skin to the technical face of the garment, which eliminates the feeling of wearing a damp or wet garment, and then transmits the vapour to the external environment. A higher water vapour transmission (WVT) rate results in higher wear comfort of the fabric. The water vapor permeability is related to the fibre content and morphology. yarn structure and fabric density (Karthikeyan et al., 2016; Onal & Yildirim, 2012). For example, hydrophilic fibres with a hollow or channel cross section, and high yam twist, tension and fabric density allow faster capillary flow. As shown in Figure 6.5, all of the fabric samples have a higher WVT than O2 used for the active bodysuit (Sit et al., 2020) while M1 provides the best wear comfort with the highest WVT.

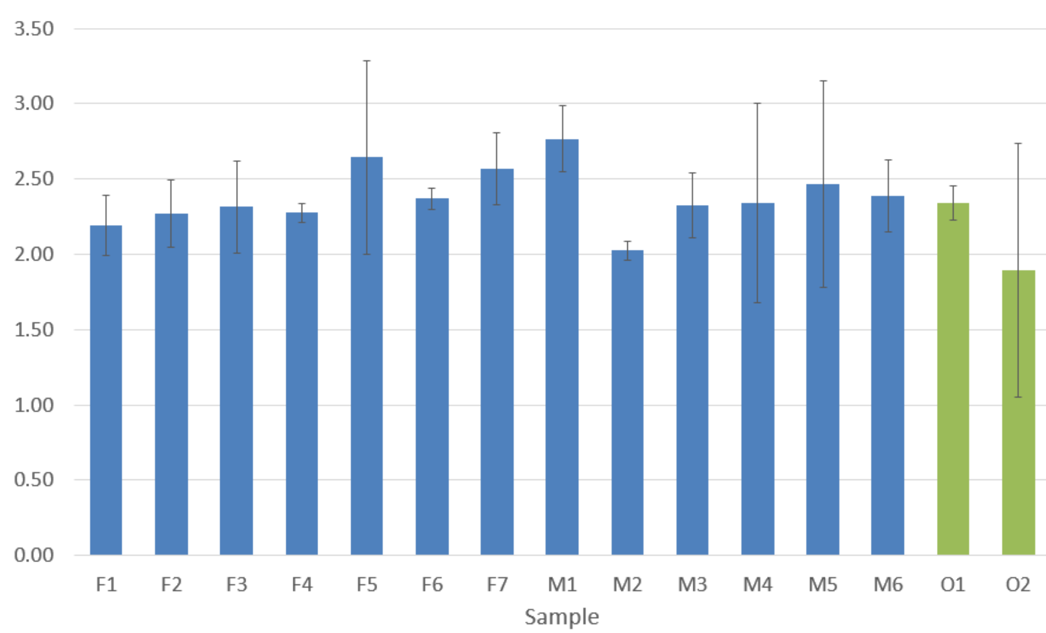

Figure 6.5 Water vapor permeability of the 15 samples

6.3.3 Air permeability test

Air permeability is described as the breathability of a material which is determined by measuring the amount of air flow that passes between two surfaces under a designated air pressure difference for a certain amount of time. Air permeability can be affected by the fabric structure, porosity, thickness and density (Zhu et al., 2015; Zupin et al., 2011). Air resistance has a negative correlation with air permeability. That is, a higher air resistance results in lower air permeability of materials. Hence, materials with higher air permeability are suitable for the proposed active bodysuit as the heat generated from the body can be easily transferred to the external environment. In Figure 6.6, M2 has the lowest air resistance and F6 has the highest air resistance. The highest air resistance of the latter is due to its large thickness which makes it difficult for air to pass through the other side of the fabric. Meanwhile, the mesh fabrics (M1 to M6, and O2) have a significantly higher air permeability compared to fabrics with a denser structure (F1 to F7, and O1). The result in this study shows that air permeability is significantly correlated with fabric thickness.

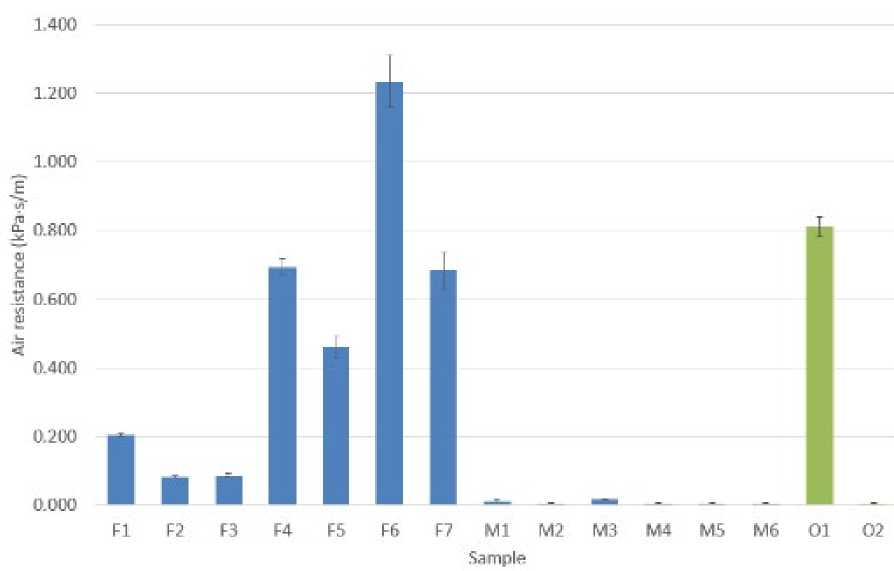

Figure 6.6 Air permeability of 15 samples

6.3.4 Thermal conductivity test

Thermal conductivity determines the microclimate of the human skin and fabric as it measures the amount of body heat that is dissipated from the skin to the external environment through the garment. A higher thermal conductivity indicates that the fabric is capable of transmitting more heat away from the skin. The possible influential factors of thermal conductivity are fibre composition, fabric structure, thickness porosity and finishing treatment done on the fabric (Karthikeyan et al., 2016). In the experiment, F5 has the highest thermal conductivity compared to the original fabrics used for the active bodysuit in Sit et al. (2020). The high conductivity value of F5 is related to the coating imparted onto the fabric surface which enhances its cooling effect (Figure 6.7). In contrast, F2 has the lowest thermal conductivity which might be due to its high density in both the wale and course directions.

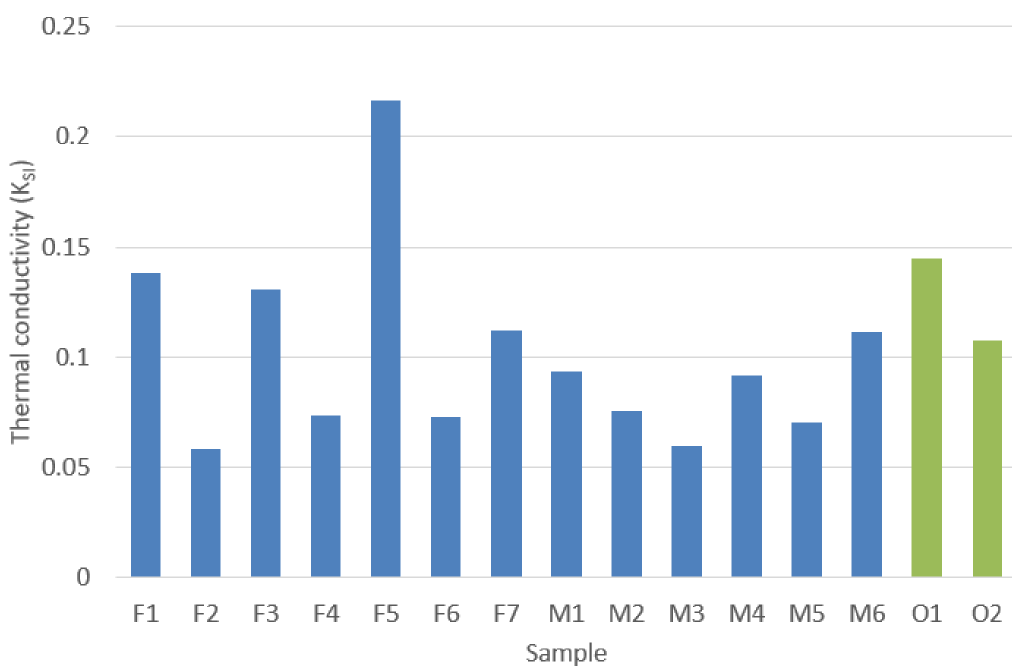

Figure 6.7 Thermal conductivity of 15 samples

6.3.5 Dimensional changes from laundering test

Dimensional stability is one of the critical factors that influences the durability of the materials when used for the proposed active bodysuit and its fit. A lower value of the dimensional changes means higher dimensional stability of the fabric. A maximum tolerance of 5% towards the dimensional changes of elastic fabric to laundering is acceptable according to ASTM D7019-14 Standard Performance Specification for Brassiere, Slip, Lingerie and Underwear Fabrics. Figures 6.8 and 6.9 show that M3 exceeds the 5% tolerance of dimensional changes in the warp direction while the other fabrics have good dimensional stability after laundering with dimensional changes within 5% in the warp and weft directions. However, F7 and M3 exceed the maximum tolerance after considering the dimensional changes in both the wale and course directions (Figure 6.10). Among the 15 fabric samples, F4 shows the lowest dimensional change which is potentially due to the use of highly twisted yarn and the dense fabric structure.

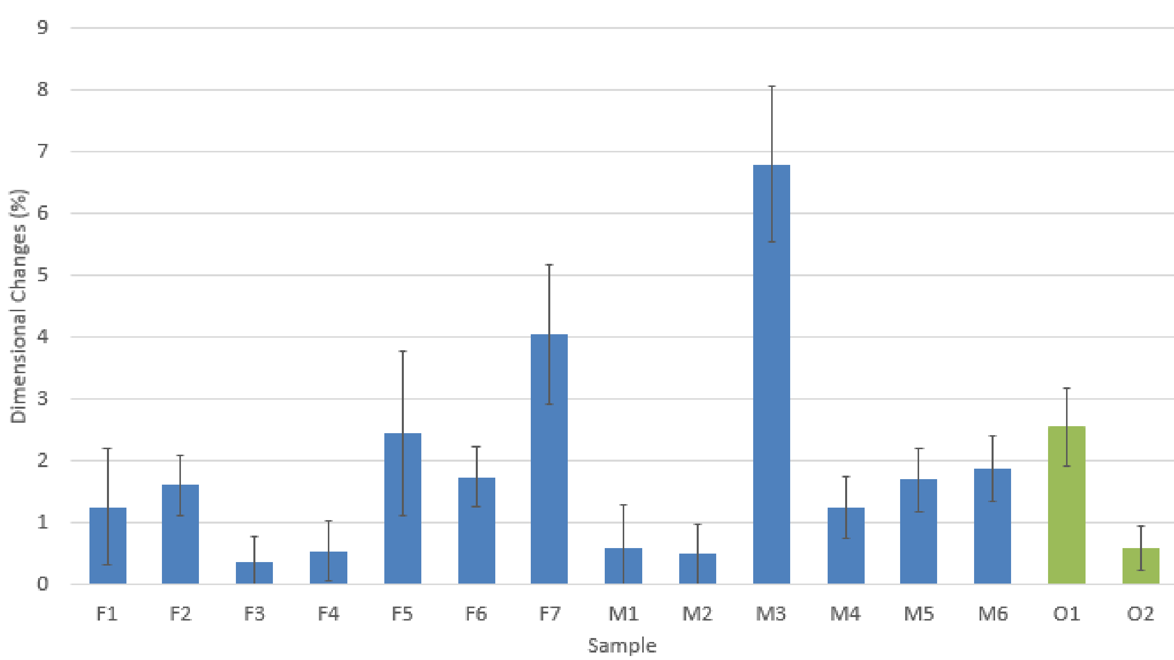

Figure 6.8 Dimensional changes of main fabric samples in warp direction

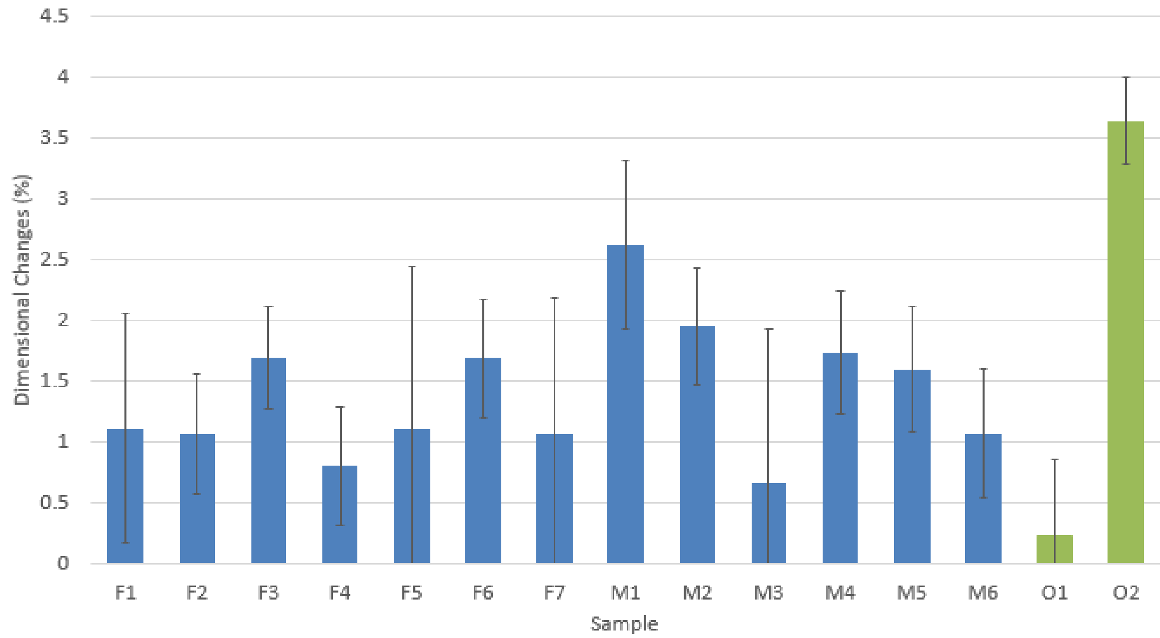

Figure 6.9 Dimensional changes of main fabric samples in weft direction

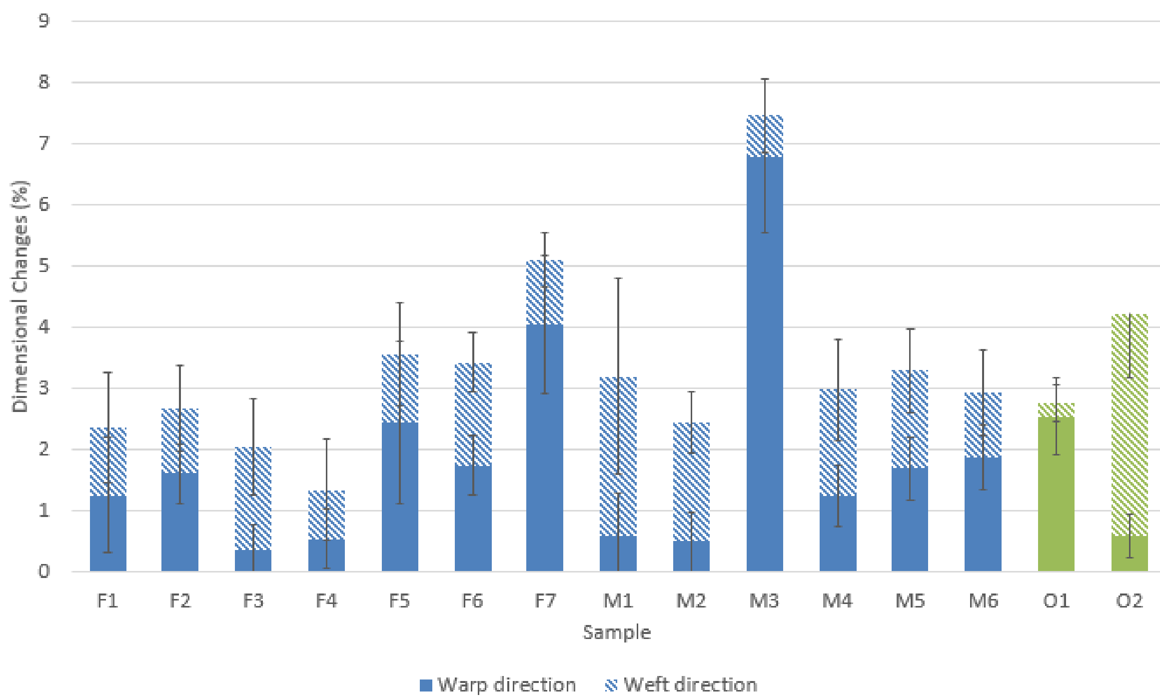

Figure 6.10 Dimensional changes of main fabric samples in both warp and weft directions

6.3.6 Overall evaluation of testing results

To select the most appropriate materials for the proposed active bodysuit, the testing results related to the design criteria of durability, wear comfort and light in weight are taken into consideration, including dimensional stability, air and water vapor permeabilities, thermal conductivity, and fabric stretch, growth and weight. The tested fabrics for each parameter are ranked from 1 to 15 according to the test result. A higher score indicates that the fabric has a better performance in the corresponding experiment, and the total score of the tested main fabric samples are provided in Table 6.5. F3 has the highest overall ranking among the 15 fabric samples, followed by M2 while F4 and O1 have the worst performance (Figure 6.11). Therefore, F3 can be used as the inner layer of the active bodysuit to offer good dimensional stability and thermal conductivity and M2 as the lining fabric of the inner layer of the proposed bodysuit because it has higher air permeability and contributes to an inner vest that is more stretchable and has better recovery.

Table 6.5 Total score of 15 main fabric samples

	Dimensional stability	Air permeability	Water vapor permeability	Thermal conductivity	Fabric stretch	Fabric growth	Fabric weight	Total score
F1	13	6	3	13	2	4	12	53
F2	11	8	4	1	7	8	14	53
F3	14	7	6	12	6	13	15	73
F4	15	3	5	5	1	1	13	43
F5	4	5	14	15	8	3	4	53

F6	5	1	10	4	14	14	1	49
F7	2	4	13	11	3	6	6	45
M1	7	10	15	8	10	11	5	66
M2	12	15	2	6	11	15	10	71
M3	1	9	7	2	15	10	3	47
M4	8	14	9	7	13	7	7	65
M5	6	14	12	3	12	9	9	65
M6	9	14	11	10	9	5	8	66
O1	10	2	8	14	5	2	2	43
O2	3	14	1	9	4	12	11	54

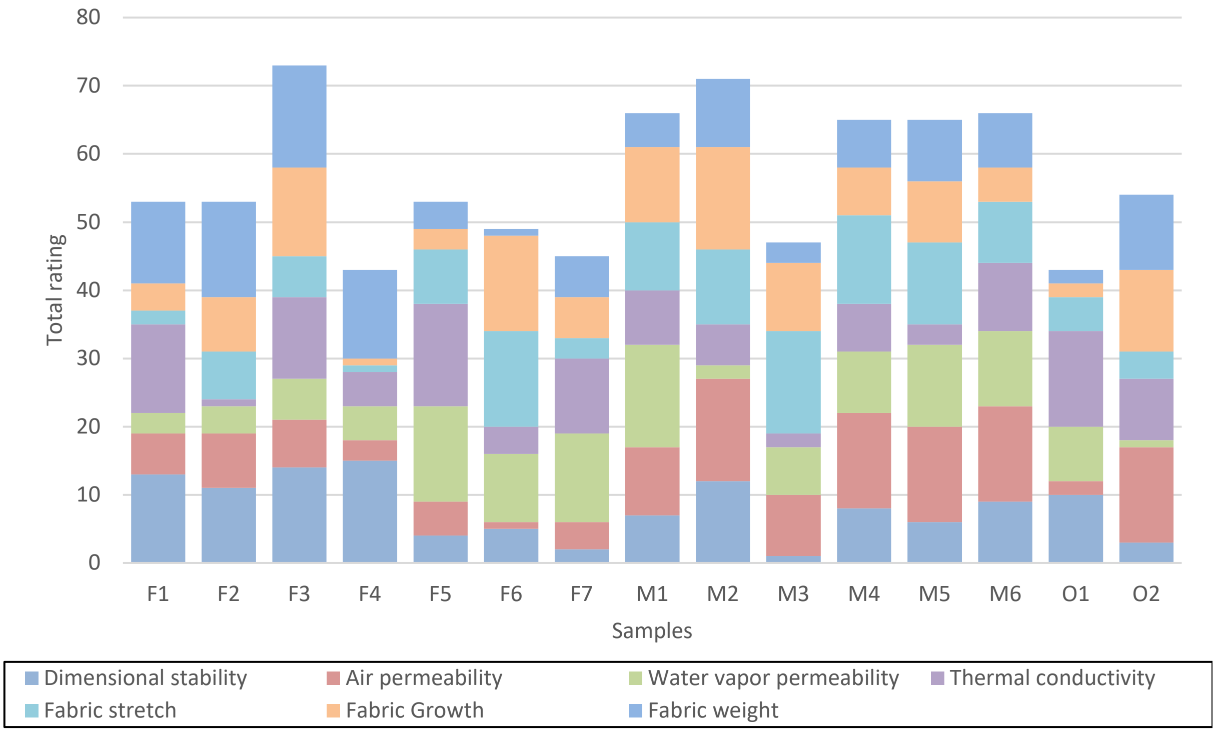

Figure 6.11 Overall ranking of the 15 main fabric samples

6.4 Summary

In this chapter, the design criteria and material selection process for the proposed active bodysuit have been discussed. Material testing related to the design criteria for a durable, light weight and comfortable bodysuit is carried out, including thermal conductivity, stretch and recovery, air and water vapor permeabilities, dimensional stability and fabric specifications, to determine the most appropriate materials for use as the inner vest. Based on the laboratory test results, a tricot fabric F3 is selected as the shell fabric of the inner vest while a powernet fabric M2 is selected as the lining fabric of the inner vest of the proposed active bodysuit.

CHAPTER 7: Formulation of Finite Element Model

7.1 Introduction

Finite element analysis (FEA) is one of the most common numerical computational methods in engineering and physics. The application of FEA has now been extended to other fields such as construction and medicine, especially to simulate the effectiveness of different orthopaedic devices and optimise brace designs. FEAs can objectively evaluate orthopaedic devices without the involvement of human subjects which minimises their exposure to harmful radiation from repetitive radiographic examinations, reduces the cost of producing a number of trial braces and eliminates the time duration required for a wear trial. Therefore, FEAs are a safe, reasonable and efficient method to evaluate the effectiveness of the existing active bodysuit in Sit et al. (2020). In this chapter, a biomechanical model is developed to simulate the in-brace spinal correction of the active bodysuit.

7.2 FE model construction

The simulation model mainly consists of three major components, including the torso geometry, skeletal structure and model of the active bodysuit in Sit et al. (2020). A female subject who is 64 years old and diagnosed with ADS (subject code: s20009) was recruited to construct the FEM for which she had taken X-rays to develop the skeleton model, undergone 3D scanning to develop the torso model, participated in a fitting session to create the brace model and provide the interface pressure for validation through the FEM later. Both the demographic information and spinal deformity measurements are listed in Table 7.1.

Table 7.1 Demographic information of scoliotic subject and corresponding spinal deformity measurements

Subject code	Age	Height (cm)	Weight (cm)	BMI	Curve Type	Curve level	Apex	Cobb angle (˚)	SVA (mm)	PT (˚)	PI-LL (˚)
s20009	64	158	61.7	24.72	Right thoracic	T5 to T12	T7	24	43	32	29
					Left lumbar	L1 to L5	L3	30			

7.2.1 Geometric models

7.2.1.1 Construction of skeletal model

The skeletal model was developed by using SolidWorks 2012 x64 Edition SP04 (Dassault Systèmes SolidWorks Corp., USA) which consisted of vertebrae C7 to L5, intervertebral discs, sacrum, pelvis, and femoral head. The skeletal structure was first created by using the standard skeletal model that is shown in Figure 7.1, and the vertebrae were built by using an extrusion model through an oval shaped surface which reduces the computational time and file size for the FEA. The alignment of the skeletal model was then rotated, deformed, and scaled according to the lateral and sagittal radiographic images of the subject. Then intervertebral discs were built between two consecutive vertebral bodies via extrusion while the sacrum, pelvis and femoral head were created as regular geometric shapes to reduce the computation time for the numerical simulation process (Figure 7.2). After that, the skeletal model was imported into Abaqus/CAE 6.144 (Dassault Systèmes Simulia Corp., USA) which is shown in Figure 7.3.

Figure 7.1 Standard skeletal model

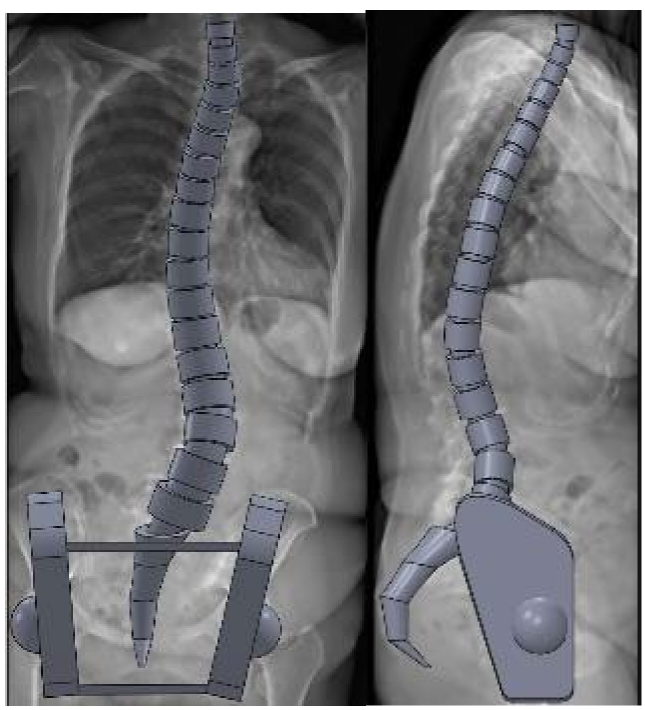

Figure 7.2 Skeletal model developed according to bi-planar radiographic images

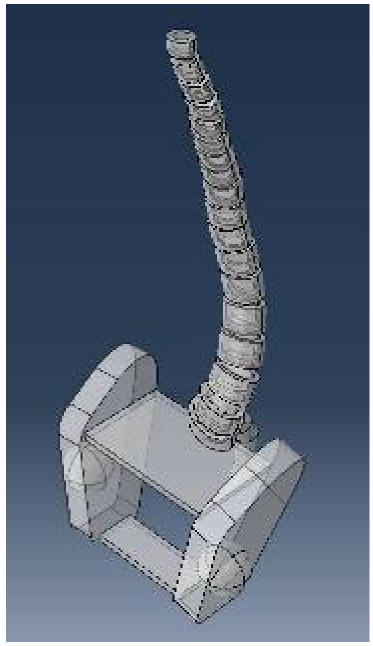

Figure 7.3 Skeletal model imported into Abaqus/CAE 6.144

7.2.1.2 Construction of the torso model

The contours of the torso were attained with the use of a Vitus Smart XXL 3D body scanner (Human Solutions GmbH, Germany). Geomagic Studio 2012 (Geomagic Inc., USA) software was used to convert the 3D scanned images from point cloud data into a geometric model of the human torso. To minimise errors or noise obtained during the scanning process, the locations of the points were corrected and made uniform. The points were then transformed into a polygon object by wrapping them around a mesh, and the polygon object was then smoothened by filling in the holes and removing spikes for individual points. Contour lines were drawn on the surface of the polygon object while patch boundaries were mapped from the contours and boundary lines. After creating an ordered u-v grid in every patch, a non-uniform rational B-spline (NURBS) surface was produced on the surface of the object. Figure 7.4 shows the procedure for developing the torso model.

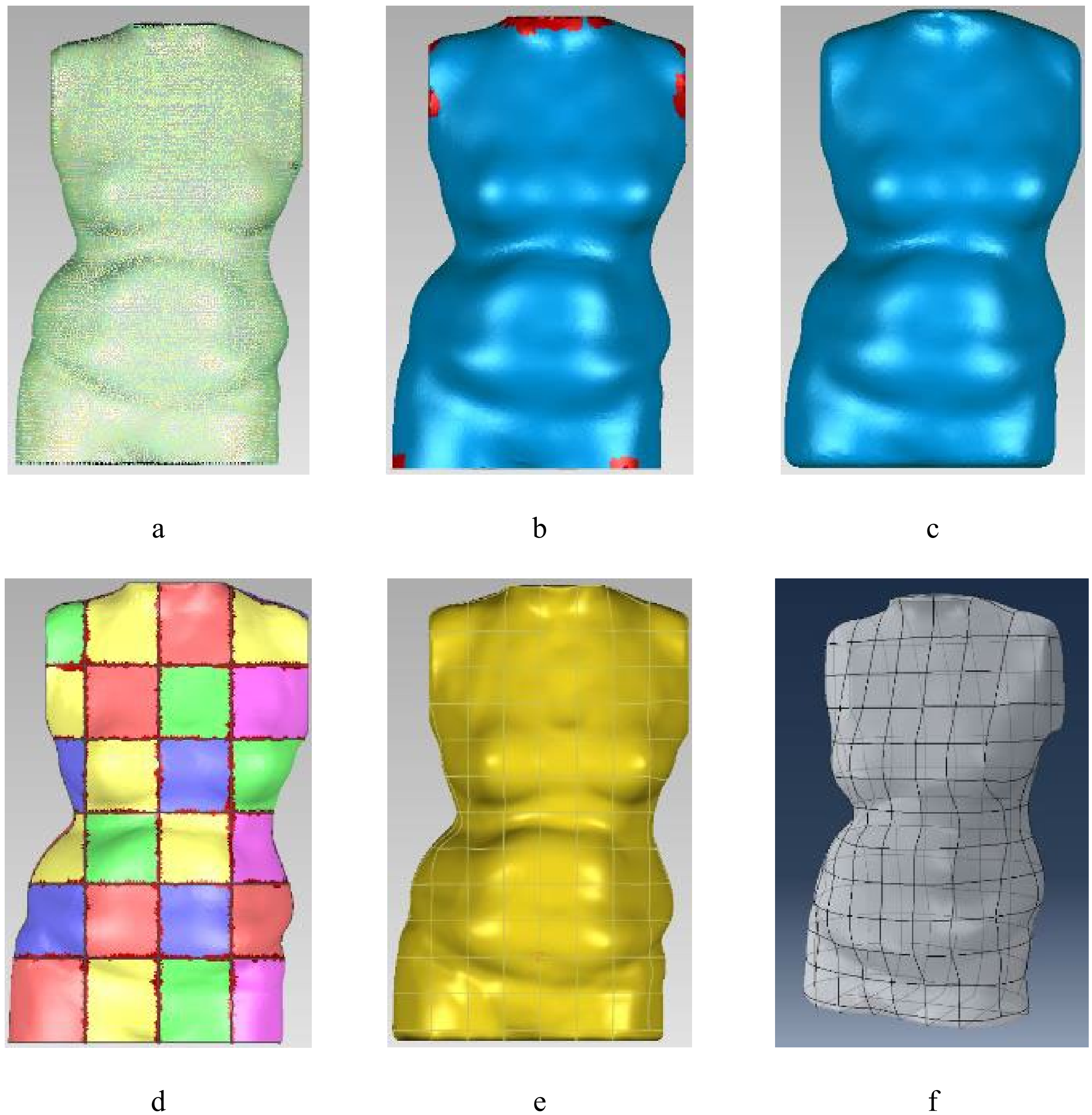

Figure 7.4 Development of torso model: (a) points of the 3D scanned image, (b) polygon object before processing, (c) polygon object after smoothening, (d) patches mapped and contours identified, (e) NURBS surface generated on surface of the torso, and (f) final geometry of the torso model in Abaqus/CAE 6.144

7.2.1.3 Construction of the active bodysuit

The model of the active bodysuit was built by importing the torso model into SolidWorks 2012 x64 Edition SP04. The “Shell” feature was used to hollow the solid geometric model of the torso based on the selected faces and a thin layer was created for the active bodysuit. Then, the unnecessary parts were trimmed based on the photos captured during the fitting session with the subject. The final model of the active bodysuit was divided into two components, the shoulder straps and the waistband as shown in Figure 7.5 and the model was set to a thickness of 3 mm.

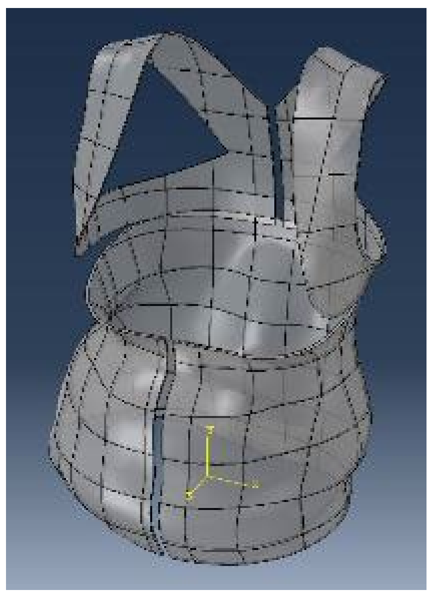

Figure 7.5 Geometric model of the active bodysuit

Apart from the shoulder straps and waistband of the active bodysuit, the supportive bones at the back were also extracted from the geometric model of the torso with the same thickness of 3 mm in accordance with the elastic materials of the bodysuit (Figure 7.6). To create the supportive bones, an axis was generated at the centre of the torso model and the position of the supportive struts was defined by the angles from the photos taken in the fitting session. After identifying the position of the struts, the remaining parts were then trimmed and deleted. After formulating both the supportive bones and active bodysuit model in SolidWorks 2012 x64 Edition SP04 the models were merged in Abaqus/CAE 6.144. The intersecting of the supportive bones in the bodysuit was then removed and the supportive bones were added into the active bodysuit (Figure 7.7) where the material properties of these brace components can be defined separately and allow better integration of the brace components. One opening was placed at the front of the waistband and the back of the shoulder straps respectively in the biomechanical model to simulate the process of tightening the corrective components.

Figure 7.6 Geometric model of the supportive bones

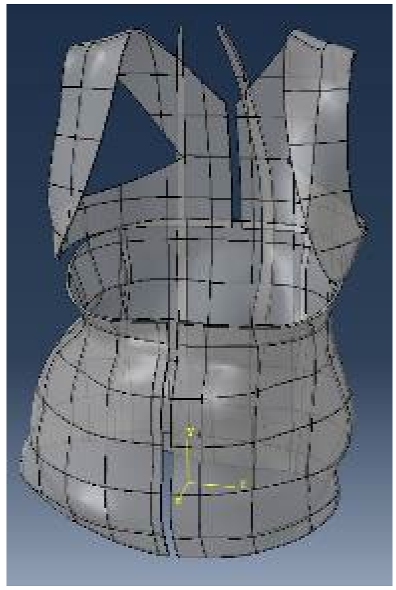

Figure 7.7 Integrated model of the supportive bones and active bodysuit

7.3 Defining material properties

In this study, the biomechanical model has seven material components: the torso, bones, intervertebral disc, waistband, shoulder straps, and the middle and side struts. All of the models were assumed to be isotropic and linearly elastic. The Young's modulus and Poisson's ratio of the torso, vertebrae, and intervertebral disc were defined by using the parameters in previous research done by Pawlaczyk et al. (2013), Xu et al. (2019), Wang et al. (2016) and Chan (2019). For the waistband, shoulder strap (Figure 7.8) and the middle strut (Figure 7.9), the Young's modulus was determined from the stress-strain curve of these materials while the Poisson's ratio was defined by using the information in previous studies (Fok, 2020; Zhou et al., 2010). The material properties used in the biomechanical model are listed in Table 7.2.

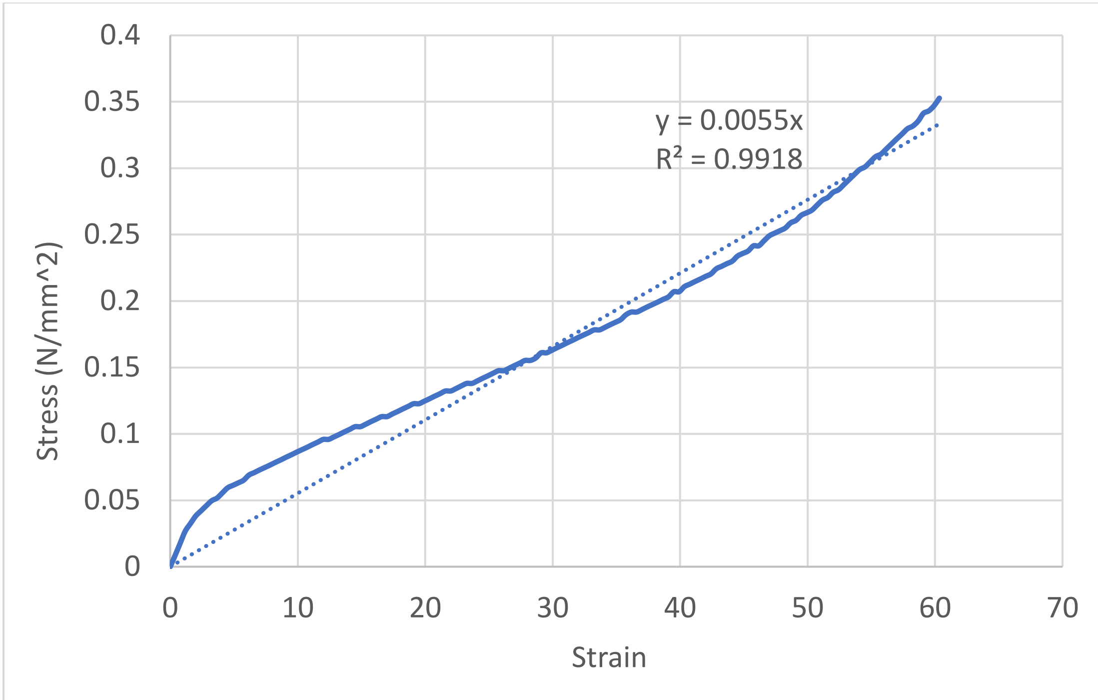

Figure 7.8 Plotted tensile stress-strain for elastic used in waistband and shoulder strap

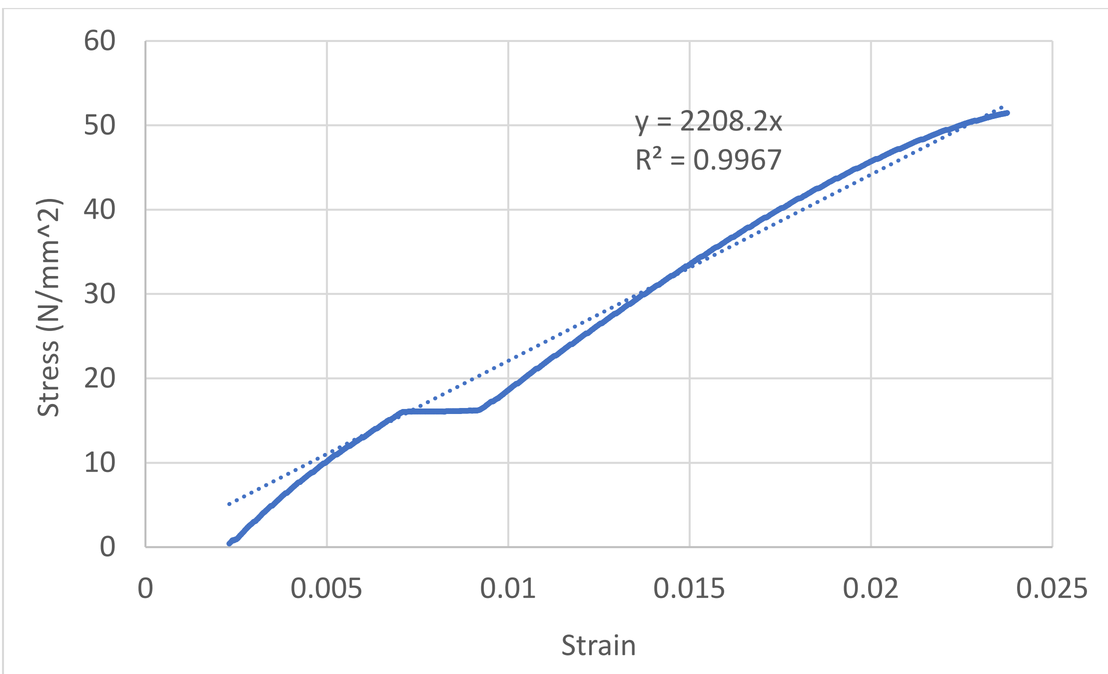

Figure 7.9 Plotted tensile stress-strain for middle strut

Table 7.2 Material properties used in the biomechanical model

	Young's modulus (MPa)	Poisson's ratio
Torso	1.6	0.3
Vertebrae	12,000	0.3
Intervertebral disc	0.8	0.3
Waistband and shoulder straps	0.59	0.4
Middle struts	2400	0.4
Side struts	1450	0.3

7.4 Defining mesh element type

The mesh elements used for the skeletal, torso and active bodysuit model are linear quadratic tetrahedral elements with 10-nodes and three degrees of freedom at each node (C3D10) (Figure 7.10). The biomechanical model consisted of 23,952 elements in total; the mesh size and number of elements in each component are listed in Table 7.3. Figures 7.11 and 7.12 show the meshed model of the scoliotic torso and active bodysuit, respectively.

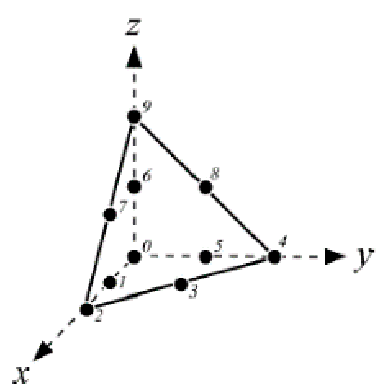

Figure 7.10 Quadratic tetrahedral element with 10 nodes

Table 7.3 Mesh size and number of elements in each component

	Mesh size	Number of elements
Torso body		10,825
Vertebra	180	2,605
Intervertebral disc		1,071
Waistband and shoulder strap	21	8,093
Supportive bone		1,358

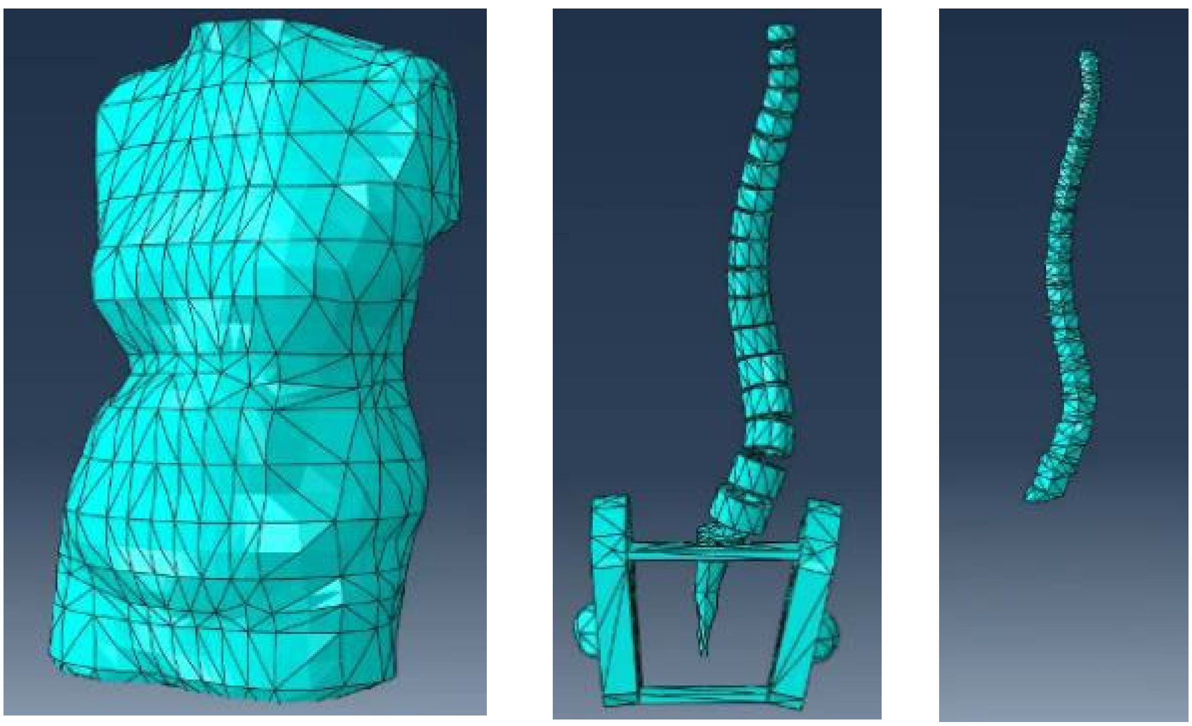

a b c

Figure 7.11 Meshed model of (a) scoliotic torso body, (b) skeletal structure and (c) intervertebral disc

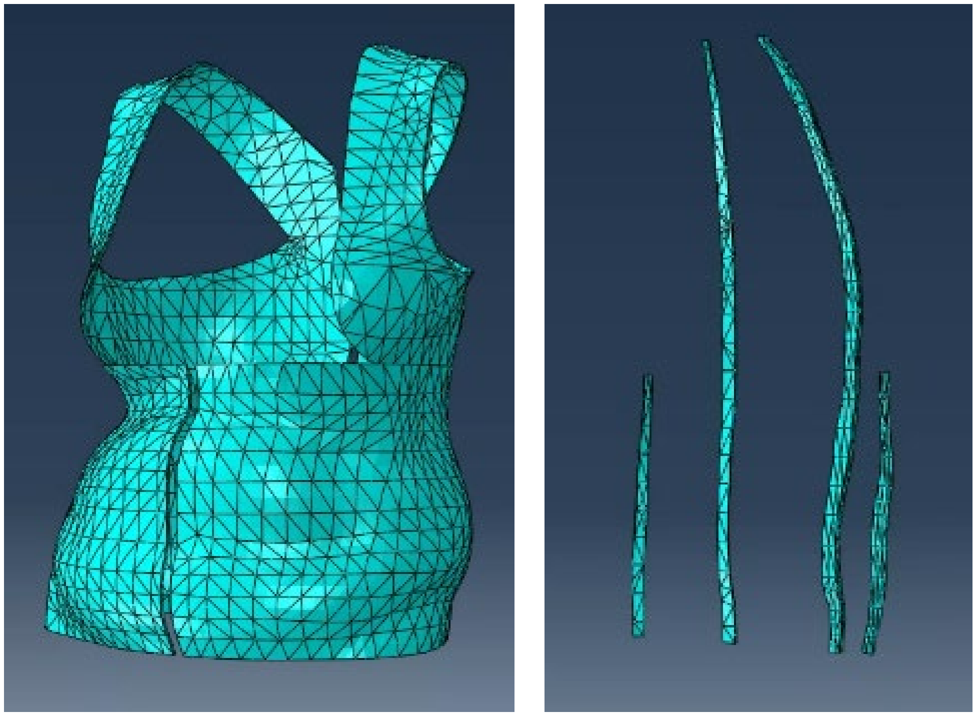

a b

Figure 7.12 Meshed model of (a) active bodysuit and (b) supportive bones

7.5 Simulation process of the biomechanical model

In the initial stage of the wear process, the scoliotic torso model and active bodysuit model were aligned by using the same relative coordinate system without any contact between the two models. Surface-to-surface contact was applied to simulate the interaction between the surface of the two models. When the models were forced to come into contact with each other, the inner side of the active bodysuit model was set as the master surface while the surface of the deformable scoliotic torso body was set as the slave surface to avoid penetration (Figure 7.13).

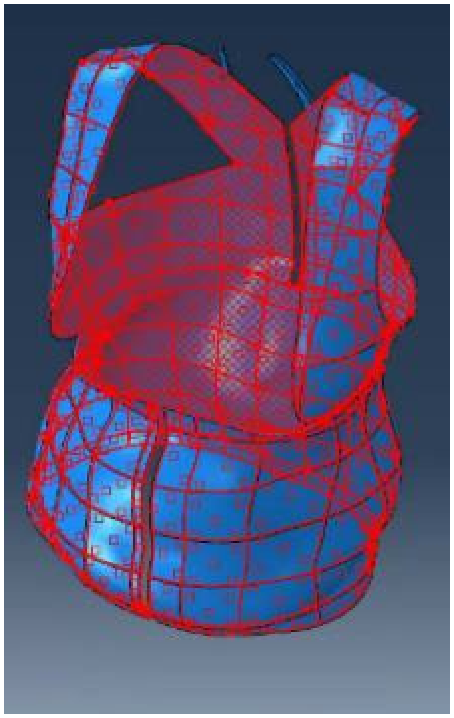

a

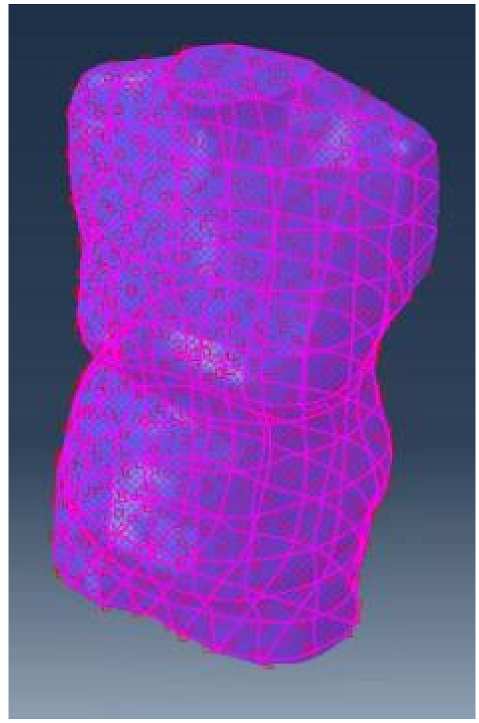

b

Figure 7.13 (a) Master and (b) slave surface for surface-to-surface interaction

The boundary conditions for the biomechanical model were defined based on the actual donning situation. To investigate the in-brace spinal effect of the active bodysuit, the model only included the torso, skeletal structure of the thoracic and lumbar spines, sacrum, pelvis and femoral head. An assumption was made in that the corrective forces applied onto the torso through the active bodysuit do not cause any displacement of the lower limbs. Therefore, the bottom surface of the torso body was fixed by restricting any translations in x, y and z plane (U1, U2, U3) and rotations in directions of x, y,and z (UR1, UR2 and UR3). Then, translation displacement of U2 was applied at the edge of the waistband and shoulder straps to simulate the tightening forces given by the corrective components. During the analysis, both the left and right edges of the waistband and shoulder straps were moved towards the midline of the body. Meanwhile, the rotations and U2 displacement of the middle struts were fixed at the back of the active bodysuit (Figure 7.14)

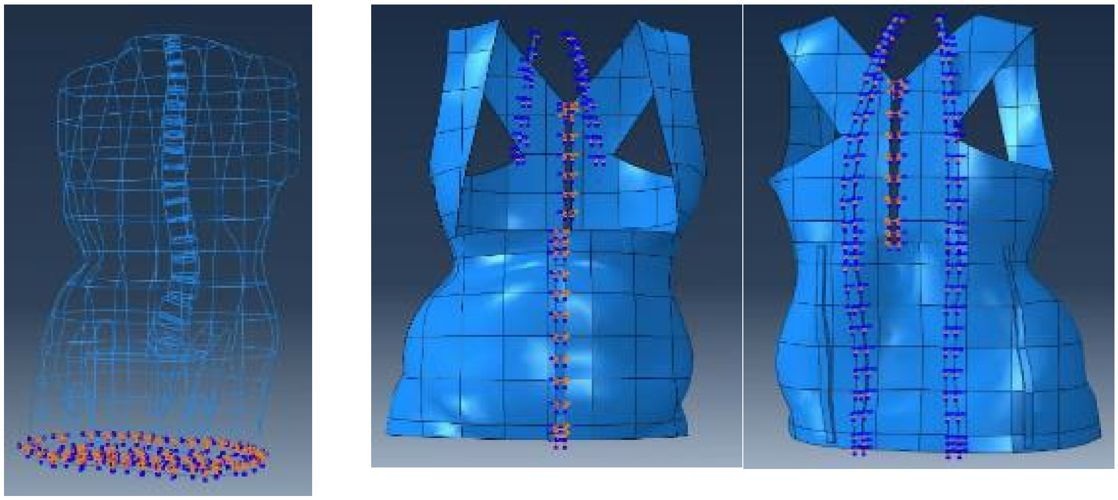

a b

Figure 7.14 Boundary conditions of the (a) base and (b) tightening process of the corrective components

7.6 Evaluation of the pressure distribution of the FEM

The stress levels of the FEM were created with different colours, with red representing the highest stress and blue the lowest stress applied. Figure 7.15 shows the stress distribution of the torso model after the analysis stage in which a relatively high stress level could be observed at the right side of the waist, the centre of the back and the pelvis area. Similar to the stress distribution captured in Figure 7.16, the bodysuit exerted a larger amount of force to the convex side of the spine which indicates that the body contours may influence the pressure distribution given by the active bodysuit. For the skeletal model, the lumbar and pelvis regions showed higher stress compared to the thoracic region (Figure 7.17) which implies a higher corrective effect to the lumbar spine. It was also found that the skeletal model can withstand higher levels of stress than the torso model, which shows that the pressure induced by the active bodysuit is distributed from the skin surface, to the muscles and then towards the spine.

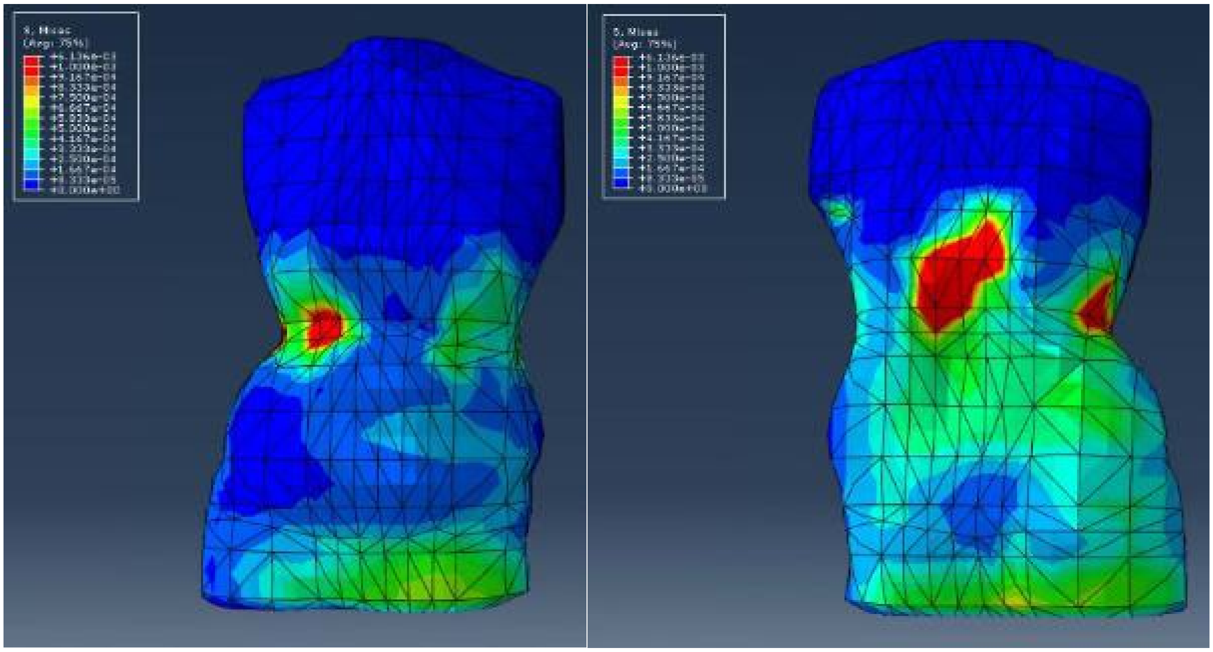

Figure 7.15 Stress distribution of the torso model after analysis

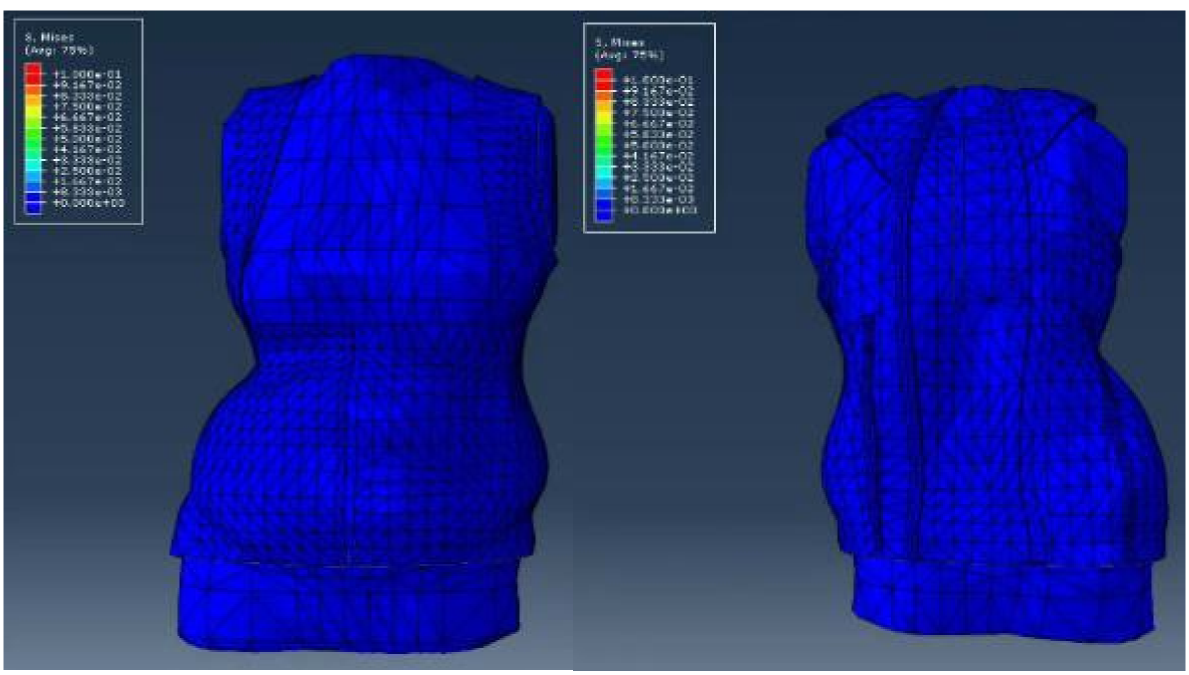

a

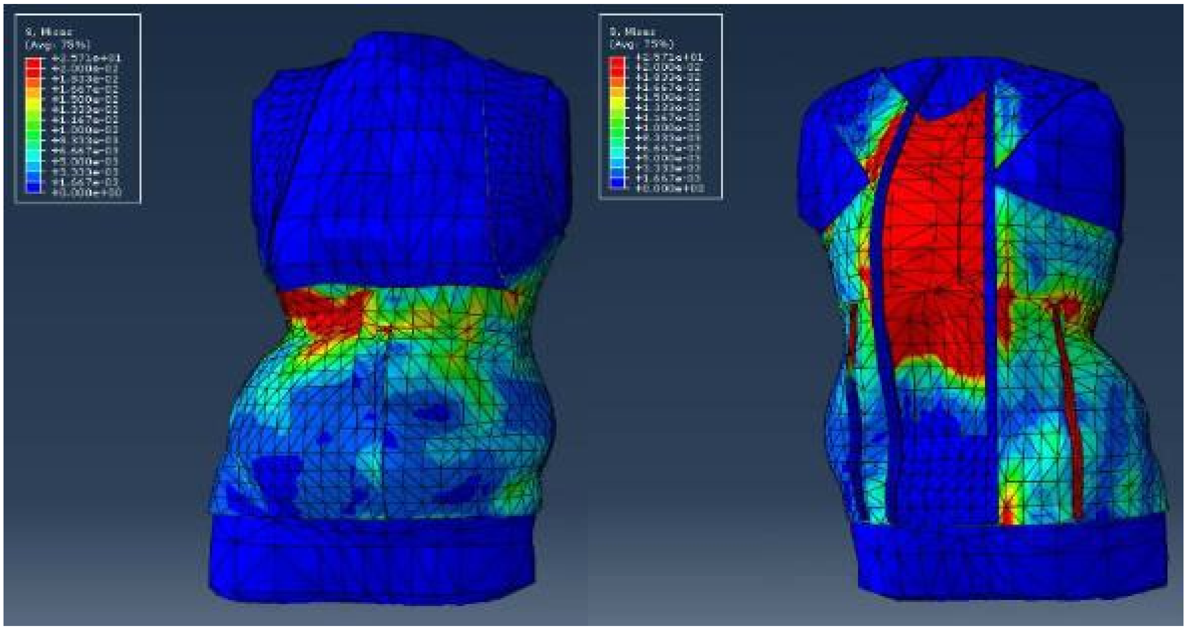

b

Figure 7.16 FEM (a) initial stage and (b) after analysis

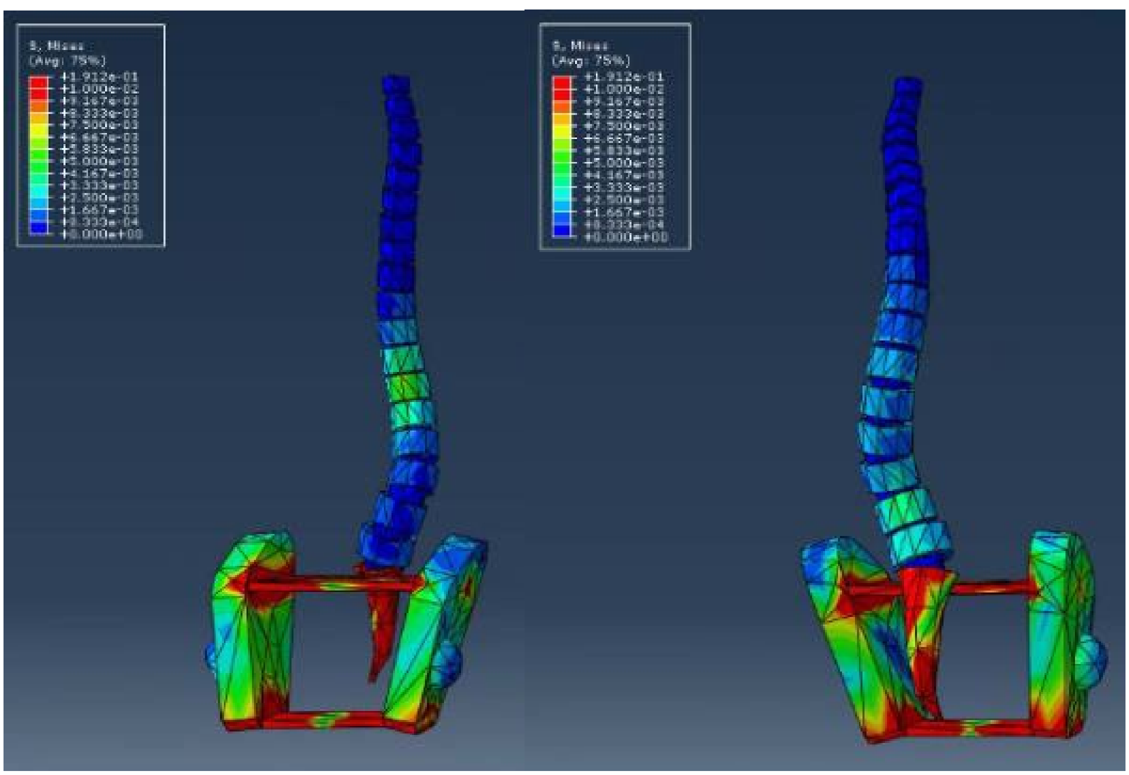

Figure 7.17 Stress distribution of the skeletal model after analysis

Finally, the displacement of the skeletal model was represented by using arrows, in which the red arrows refer to larger deformation and the blue arrows to less displacement. Figure 7.18 shows that the C7 vertebrae has the largest displacement, followed by the thoracic vertebrae, lumbar vertebrae and the pelvic region, which all had an upward and leftward shift. Nevertheless, it is surprising that the shoulder straps only exert a small amount of stress to the shoulder and bust region, which may be due to the gap between the torso, shoulder straps and middle struts. Due to the limited amount of corrective force exertion, the C7 and the upper thoracic vertebrae also have limited corrective forces which may facilitate the corresponding region to move forward and result in high levels of displacement. As the result, the scoliotic spine tends to be straightened while the sagittal imbalance of the patient would increase.

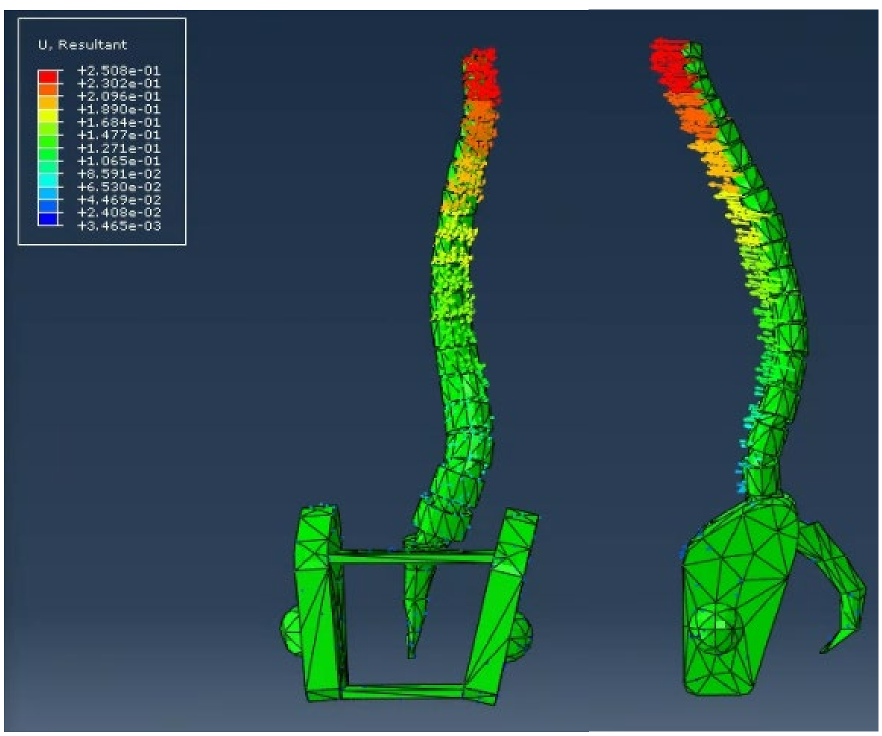

Figure 7.18 Displacement of the skeletal model

7.7 Validation of in-brace spinal correction

As for the validation of the FEM, Figure 7.19 plots the displacement of the coronal and sagittal planes of the spinal curves obtained from the simulation process, and that from the actual in-brace radiographic images and images without the use of the brace. The vertebrae position from C7 to L5 obtained from the FEA and actual in-brace radiographic images of the subject were examined by using Pearson correlation coefficients. For the coronal plane, the movement of the vertebral bodies for both in-brace and the predicted spinal curves shifts to the left, with a significantly positive correlation between them ($r = .799$, $p = < .001$). However, the FEM underestimated the magnitude of displacement of the vertebras; there is also a greater difference between the magnitude of the displacement of the thoracic vertebras than that of the vertebral bodies of the lumbar spine region. For the sagittal plane, the movement of the spine in-brace and FE estimated spinal curvature shifts to the left while their magnitude of displacement is very significantly and positively correlated ($r = .995$, $p = < .001$).

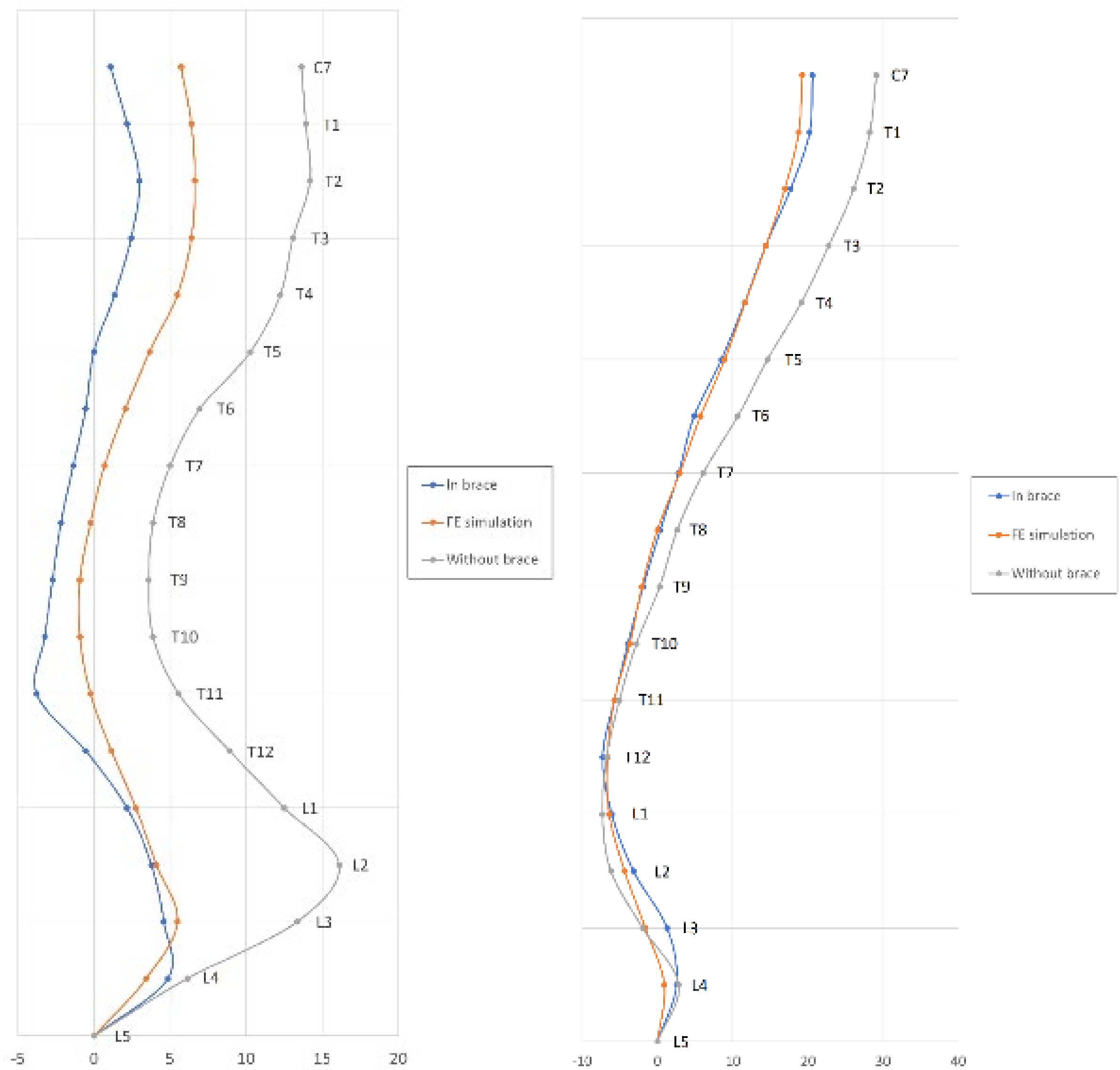

(a) (b)

Figure 7.19 Magnitude of displacement of vertebral bodies measured from radiographic images and FEM in (a) coronal plane and (b) sagittal plane

Spinal measurements from the in-brace radiographic images and the skeletal model were compared to further validate the FEM (Table 7.4). The FEM revealed a reduction of the Cobb angles but an increase in the spinopelvic values. The difference between the in-brace spinal values and those of the FE simulation is less than 5 degrees tolerance, in which the Cobb angle in thoracic region and PT from the FE simulation are slightly larger than the values derived in-brace. The result shows that the FEM underestimates the spinal corrective effect of the active bodysuit which is similar to the result of the displacement of the vertebral bodies. A possible reason for the deviation between the FEA and clinical results is that the geometry of the FEM greatly influences the force and displacement response of the numerical models (Dallard et al., 2018; Niemeyer et al., 2012). The FEM developed in this study has simplified the geometry of the torso, skeletal and active bodysuit models, like excluding the rib cage and the posterior elements of the vertebrae, sharp edges and meshes of the model, thus affecting the outputted calculation of the spinal measurements and displacements.

Table 7.4 Spinal measurements from radiographic images and FEM

	Without brace	In brace	FE simulation
Cobb angle in thoracic region (°)	24	16	20.4
Cobb angle in lumbar region (°)	33	30	29.2
PT (°)	32	34	37
PI-LL (°)	29	36	34.8

7.8 Design optimisation through D-optimal design

The developed biomechanical model was validated and intended to predict the initial in-brace corrective ability of the proposed active bodysuit. Thus, the major Cobb angle was defined as the objective function of the design optimisation process. The ‘optimal’ design of the proposed active bodysuit is one with the highest reduction in the major Cobb angle while pressure measurement of the torso and spinopelvic measurements in the sagittal plane are not included in the objective function. In order to describe different design combinations and evaluate their effect on the spinal curvature, four design factors were considered which are the material properties of the shoulder straps (P1), elastic waistband (P2), and middle (P3) and side struts (P4) respectively. The descriptions of the design factors are provided in Table 7.5. Each design factor is assigned three levels of values (L1-L3) as per previous literature which includes Chan (2019), Fok (2020) and the Cambridge University Engineering Department (2003).

Table 7.5 Design factors and their levels for design optimisation

Factor ID	Design factor	Level 1 (L1)	Level 2 (L2)	Level 3 (L3)
P1	Shoulder straps (MPa, v)	243, 0.4	695, 0.4	763, 0.4
P2	Waistband (MPa, v)	0.38, 0.4	0.45, 0.4	0.59, 0.4
P3	Middle struts (MPa, v)	Cast acrylic (3020, 0.4)	6061 Aluminium alloy (75,000, 0.3)	Carbon fibre reinforced polymer (100,000, 0.2)
P4	Side struts (MPa, v)	Resin bone (1449, 0.3)	Polyoxymethylene (3750, 0.4)	Shape memory alloy (50328, 0.3)

The design of experiments is a systematic method for multi-parameter designs to evaluate the effect and level of each design variable (Sharma et al., 2016). A full factorial design generates all possible factor combinations but requires a long computation time and resources to simulate a large number of trials ($4^3 = 81$). So, a D-optimal design is adopted in this study to find the most effective design combination and optimise the corrective effect of the proposed active bodysuit. A total of 9 design combinations (T1-T9) of four 3-level design factors was generated (Table 7.6) through a MATLAB function by using row exchange. To enhance the possibility of obtaining the global maximum, the algorithm was repeated 100 times to generate designs from random starting sets of input.

Table 7.6 Nine design combinations (T1-T9) generated by using D-optimal design for the 3-level design factors (P1-P4)

	P1	P2	P3	P4
T1	1	1	2	2
T2	3	2	2	3
T3	3	1	3	1
T4	1	2	1	1
T5	1	3	3	3
T6	2	2	3	2
T7	2	1	1	3
T8	3	3	1	2
T9	2	3	2	1

The material properties of the validated FEM were then modified according to the 9 design combinations, and the major Cobb angle was predicted for each design combination. The mean effects of each level of the design factors towards the major Cobb angle were determined. For example, the mean response of the shoulder strap (P1) at Level 1 is obtained by averaging the major Cobb angle of T1, T4 and T5. The sum of squares related to each factor was calculated by using the following equation:

$$SS_j = \sum_{i=1}^{N_l}(R_i - R_m) \qquad \forall j = 1, \dots, N_f$$

where:

SS_j = sum of squares of design factor *j,*

N_l = number of levels,

N_f = number of factors,

R_i = the mean response of factor *j* at level *I, and*

R_m = the overall mean response of the 9 design combinations.

7.8.1 Results and discussion

The FE predicted results of the 9 design combinations are presented in Table 7.7, in which T3 has the lowest in-brace correction (33°) and T6 has the highest in-brace correction (29.8°). The mean response of each level of the 4 design factors is shown in Figure 7.20. Among the four design factors, the shoulder strap (P1) with less stiffness results in a higher in-brace reduction of the Cobb angle. The optimal material for the waistband (P2), middle strut (P3) and side struts (P4) is elastic with a Young's Modulus of 0.45 MPa, 6061 aluminium alloy and polyoxymethylene respectively.

Figure 7.20 shows that the level with the lowest Cobb angle for each factor is chosen for the optimal design in which the optimal design combination for P1 to P4 is 1-2-2-2. An FEA was then done to evaluate the performance of the optimal design combination on spinal curvature reduction. The predicted Cobb angle is 27°, which is smaller than the results of the 9 design combinations. When compared with the predicted Cobb angle of the validated FEM, the optimal design can reduce the Cobb angle by 2.2°.

Table 7.7 FE predicted in-brace Cobb angle of the 9 design combinations

Design treatment	Major Cobb angle (°)
T1	30.7
T2	30.4
T3	33
T4	31
T5	30.4
T6	29.8
T7	32
T8	32
T9	31.9

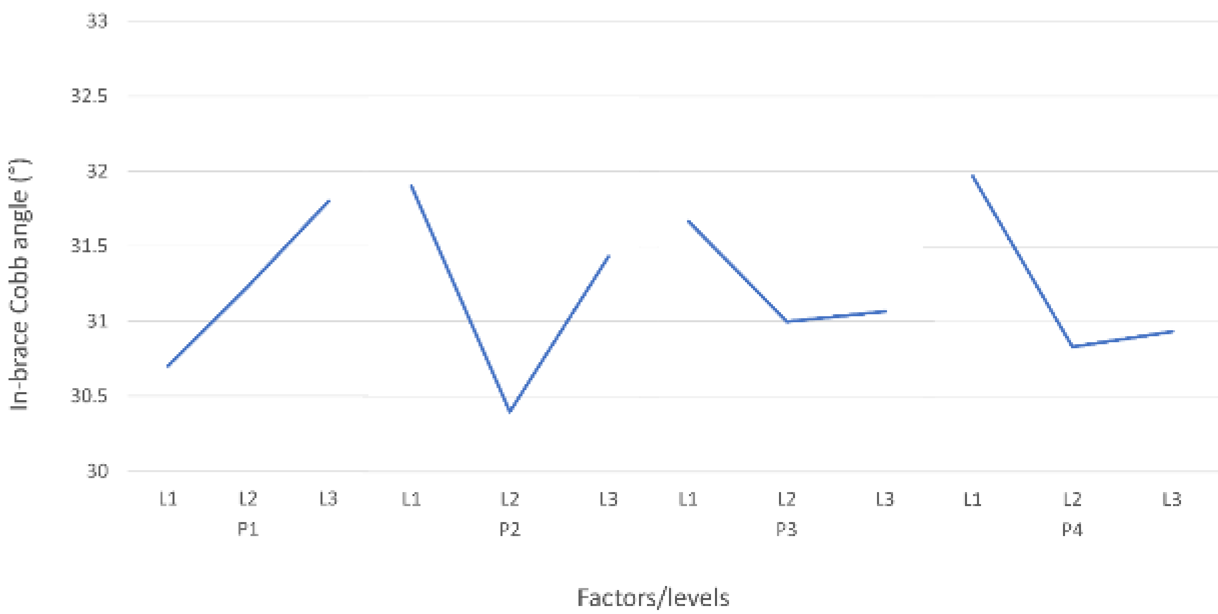

Figure 7.20 Mean responses of all levels of design factors

The sum of the squares (SS) describes the sensitivity of each design factor on in-brace spinal curvature reduction (Table 7.8). A higher SS value means higher sensitivity of the design factor. The stiffness of the waistband (P2) is regarded as the most important factor in changing the Cobb angle (SS = 1.18), followed by stiffness of the side struts (SS = 0.79), shoulder straps (SS = 0.61) and lastly, the middle strut (SS = 0.27).

Table 7.8 Sum of squares of the four design factors

Factor ID	Factor	Sum of squares (SS) (°)
P1	Shoulder straps	0.61
P2	Waistband	1.18
P3	Middle strut	0.27
P4	Side struts	0.79

7.9 Summary

In this chapter, an FEM is constructed to simulate the wear process of the active bodysuit through the torso of an ADS patient which demonstrates its biomechanics and corrective effect. The FEM comprises the scoliotic skeletal model, a torso model and the bodysuit model. The FEM simulations show that a relatively high level of pressure is exerted onto the right side of the waist, centre of the back and pelvis region of the torso and also the lumbar spine and pelvis of the skeletal model. The in-brace radiographic images of a recruited subject are then compared with the simulated spinal curves. A similar trend can be found between the actual and simulated spinal curves which validates the developed FEM.

To optimise the design and corrective effect of the proposed active bodysuit, a D-optimal design is adopted to modify the materials of the shoulder straps, waistband, and middle and side struts. Each design factor has a total of 3 levels, with a total of 81 combinations that can be produced. Only nine design combinations are generated and simulated by using a D-optimal array. Based on the result, shoulder straps with less stiffness may further reduce the major Cobb angle. The result also shows that the waistband is the most critical component for correcting the spinal curvature, followed by the side struts, shoulder straps and finally the middle strut. To optimise the design of the proposed active bodysuit, woven shoulder straps with a Young's Modulus of 243 MPa, waistband with a Young's Modulus of 0.45 MPa, 6061 aluminium alloy middle struts and polyoxymethylene side struts should be used to reduce the predicted in-brace Cobb angle from 29.2° to 27°.

There are limitations for this chapter in the study. First of all, only one FEM is developed and validated which limits the generalisability of the model. Secondly, the optimal design identified by the simulation model has not been applied to the patients, which the actual effect of the proposed active bodysuit has not yet to be determined. Future research can be conducted to enhance the generalisability of this method such as developing and validating more FEM with different curve type and conducting actual wear trial to evaluate the actual effect of the proposed active bodysuit.

CHAPTER 8: Conclusions and Suggestions for Future Research

8.1 Conclusions

Scoliosis is defined as the 3D deformity of the spine and trunk in both the coronal and sagittal planes. ADS, a condition of the ageing population caused by a degenerative functional spinal unit, has become more prevalent as people become more aware of their health in general with age and advancements in medical science. Patients with ADS can receive treatment based on the measurements of their spinal deformity, type of spinal curvature, age and acceptance of calculated risks. Bracing treatment is one of most traditional and conservative treatments that exert external corrective forces to the spine and torso. However, the efficacy of soft bracing is not yet fully validated due to the low treatment compliance rate and uncertain duration of brace wear.

The active bodysuit developed by Sit et al. (2020) is a flexible brace that corrects the body alignment and posture of ADS patients. Yet, the corrective effect and thermal comfort of this bodysuit is ambiguous. In order to optimise the brace design and exert sufficient corrective forces to improve the posture and spinal alignment of patients, the research objectives of this study are: (1) conduct background research on ADS, review different treatments, mechanisms involved for determining the textiles and materials suitable for the active bodysuit, (2) understand the posture and muscle activity of ADS patients, (3) investigate the performance of the active bodysuit in Sit et al. (2020) through a clinical trial, (4) conduct material testing to improve the thermal comfort of the proposed active bodysuit and (5) develop and validate a FEM that optimises the corrective effect of the proposed active bodysuit. The objectives have been completed and the results are summarised as follows.

First, detailed background information of scoliosis such as its definition, diagnosis methods, classification of ADS as well as the operative and conservative treatments for ADS has been obtained through a literature review. Moreover, the design, materials, mechanism, purpose of different types of rigid and flexible bracing treatments and their limitations have been identified. Furthermore, previous studies on the posture, balance, muscle activity and FEA for ADS have been consulted, which facilitate the planning of the methodology of this study.

Secondly, a comparative study of the posture, standing balance and muscle activity between ADS patients and asymptomatic people has been conducted by using a 3D motion capture system. The results reveal that ADS patients have more knee flexion and ankle dorsiflexion during habitual standing, with a larger spinal tilt angle during habitual sitting in order to maintain balance. ADS patients have imbalanced muscle activity so they would exert more energy in the paraspinal muscles and demonstrate different muscle activity patterns compared with the asymptomatic group. Therefore, the spinal deformities of ADS patients might increase the need to maintain proper posture and perform daily activities to inhibit the spinal issues.

Thirdly, a 2-hour and a 3-month clinical study of the active bodysuit have been conducted to investigate its biomechanics and efficacy in controlling the spinal curvature and improving the health-related quality of life of ADS patients respectively. The result allows a better understanding of the current designs of braces and hence determine the optimal modifications for the proposed active bodysuit. The study demonstrates that the active bodysuit can reduce the in-brace Cobb angle in the 3-month clinical trial, prevent progression of the spinal deformity, relieve pain and increase ability of ADS subjects to perform daily activities. However, the active bodysuit cannot provide sufficient in-brace correction in the 2-hour wear trial due to the materials used and the low compliance rate with the bodysuit. Thus, modifying the accessories and materials of the brace might potentially increase compliance and the corrective effect of the proposed active bodysuit.

Lastly, different material tests have been conducted to improve the thermal comfort and a biomechanical model is formulated to optimise the corrective effect of the proposed active bodysuit. The biomechanical model comprises the torso, skeletal and brace models. An ADS subject is recruited to validate the model by comparing the actual and predicted spinal curves. The stimulated model shows a similar trend with the actual spinal curvature of the recruited subject. After the validation of the FEM, a D-optimal design is used to examine the effect of the different materials of the proposed bodysuit towards spinal correction. A total of 4 design factors with 3 levels are applied in the study, including the shoulder straps, waistband, and middle and side struts. The results show that the waistband is the most critical component for reducing the in-brace Cobb angle and the optimal corrective effect is realised by using woven shoulder straps with a Young's Modulus of 243 MPa, elastics with a Young's Modulus of 0.45 MPa for the waistband, 6061 Aluminium alloy for the middle struts and polyoxymethylene for the side struts. The predicted model shows that the proposed active bodysuit provides a higher degree of spinal curvature correction than the active bodysuit.

8.2 Limitations of the study

Some of the limitations of this study that limit the generalisability of the results are as follows:

1. Previous studies in the literature show that the severity of spinal deformities might have impacts on the posture and balance of ADS patients. However, it is difficult to reach out to ADS patients and recruit them for the study. The target population is also reluctant to join the study because of the ongoing COVID-19 pandemic (at the time of this study).

2. Due to limited instrumentation, the tasks in this study can only be used to measure the static standing balance of the recruited subjects, while the sensorimotor factors of the ADS patients have not been examined. Investigation of the sensorimotor factors of the ADS patients would have allowed a better understanding towards the relationship between the sensorimotor system and balance control.
3. Due to limited resources, there is no clinical trial conducted and develop only one biomechanical model for the proposed active bodysuit. Although the design and materials of the proposed active bodysuit have been improved by conducting material testing and a FEA, the actual corrective effect of the proposed active bodysuit for ADS patients has yet to be determined.

8.3 Recommendations for future work

Based on the established research findings and limitations, the recommendations for future work are as follows:

1. Sensorimotor function assessment, and external perturbations are not included in the study. To gain a better understanding of the balance control strategies adopted by ADS patients, further research work is required.
2. A torso model with organs, ligaments, tendons, muscles and skin and skeletal model with rib cage and posterior elements should be developed in the future. Moreover, FE simulations with more design factors such as the thickness of the materials can be carried out to predict their performance for in-brace spinal curvature reduction.
3. A randomised controlled trial with a large sample size for the proposed active bodysuit is recommended to evaluate the actual efficacy of the proposed active bodysuit which the

subjects are randomly assigned to wear the existing active bodysuit and the proposed active bodysuit for 1 year. Moreover, monitoring devices like temperature loggers or IMU sensors can be embedded in the active bodysuit to check the compliance rate.

Appendix I Radiographic images of the recruited ADS subjects

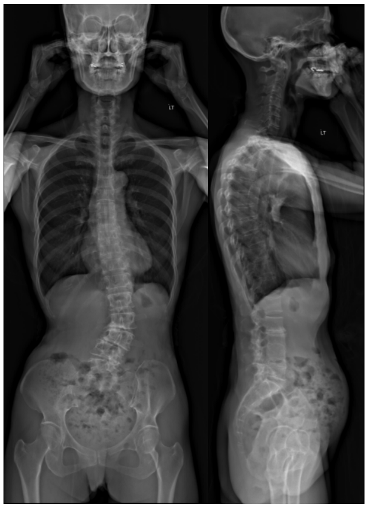

s20001

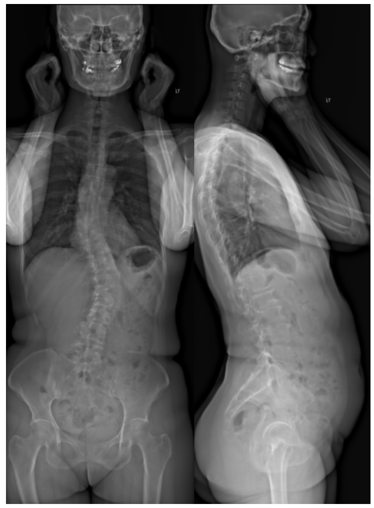

s20002

s20003

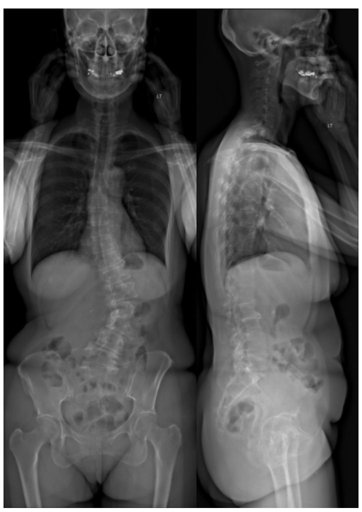

s20004

s20005

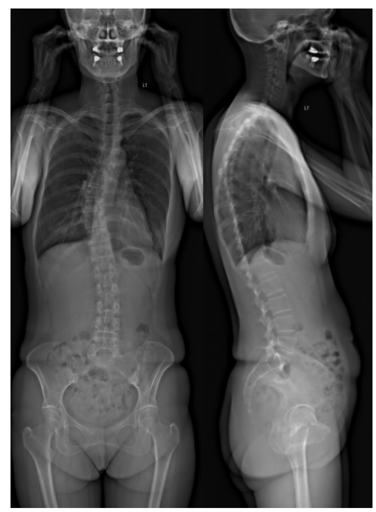

s20006

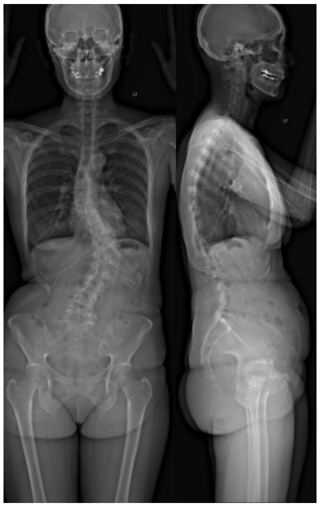

s20007

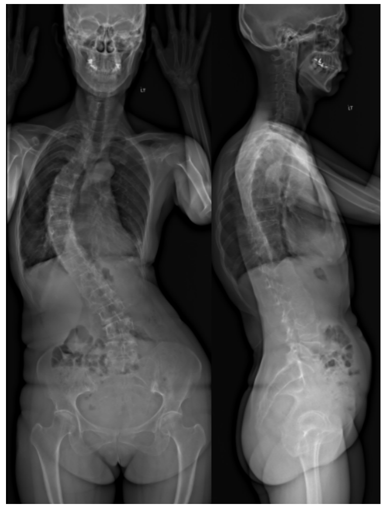

s20008

s20009

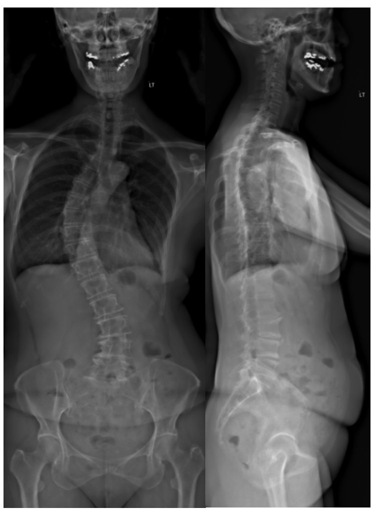

s20010

References

Aebi, M. (2005). The adult scoliosis. Eur Spine J, 14(10), 925-948. https://doi.org/10.1007/s00586-005-1053-9

Alanazi, M. H., Parent, E. C., & Dennett, E. (2018). Effect of stabilization exercise on back pain, disability and quality of life in adults with scoliosis: a systematic review. European journal of physical and rehabilitation medicine, 54(5), 647. https://doi.org/10.23736/S1973-9087.17.05062-6

Anatomy Note (2019). Hip Muscle And Ligament Anterior View. https://www.anatomynote.com/human-anatomy/muscle-system/hip-muscle-and-ligament-anterior-view-and-posterior-view/

Anders, C., Patenge, S., Sander, K., Layher, F., Biedermann, U., & Kinne, R. W. (2017). Detailed spatial characterization of superficial hip muscle activation during walking: A multi-electrode surface EMG investigation of the gluteal region in healthy older adults. PLoS One, 12(6), e0178957. https://doi.org/10.1371/journal.pone.0178957

Antoine, L., Nathan, D., Laure, M., Briac, C., Jean-François, M., & Corinne, B. (2020). Compliance with night-time overcorrection bracing in adolescent idiopathic scoliosis: Result from a cohort follow-up. Med Eng Phys, 77, 137-141. https://doi.org/10.1016/j.medengphy.2020.01.003

Baldus, C., Bridwell, K. H., Harrast, J., Edwards, C. I., Glassman, S., Horton, W., Lenke, L. G., Lowe, T., Mardjetko, S., Ondra, S., Schwab, F., & Shaffrey, C. (2008). Age-Gender Matched Comparison of SRS Instrument Scores Between Adult Deformity and Normal

Adults: Are All SRS Domains Disease Specific? Spine, 33(20), 2214-2218. https://doi.org/10.1097/BRS.0b013e31817c0466

Barrey, C., Roussouly, P., Perrin, G., & Le Huec, J.-C. (2011). Sagittal balance disorders in severe degenerative spine. Can we identify the compensatory mechanisms? Eur Spine J, 20(S5), 626-633. https://doi.org/10.1007/s00586-011-1930-3

Benka Wallén, M., Sorjonen, K., Löfgren, N., & Franzén, E. (2016). Structural Validity of the Mini-Balance Evaluation Systems Test (Mini-BESTest) in People With Mild to Moderate Parkinson Disease. Phys Ther, 96(11), 1799-1806. https://doi.org/10.2522/ptj.20150334

Benzel, E. C. (2012). Spine surgery: techniques, complication avoidance, and management (3rd ed.. ed.). Churchill Livingstone.

Berven, S., Kamper, S., Germscheid, N., Dahl, B., Shaffrey, C., Lenke, L., Lewis, S., Cheung, K., Alanay, A., Ito, M., Polly, D., Qiu, Y., & Kleuver, M. (2018). An international consensus on the appropriate evaluation and treatment for adults with spinal deformity. Eur Spine J, 27(3), 585-596. https://doi.org/10.1007/s00586-017-5241-1

Bess, S. S., Protopsaltis, P. T., Lafage, S. V., Lafage, S. R., Ames, S. C., Errico, S. T., & Smith, S. J. (2016). Clinical and Radiographic Evaluation of Adult Spinal Deformity. Clinical Spine Surgery, 29(1), 6-16. https://doi.org/10.1097/BSD.0000000000000352

Birknes, K. J., Harrop, S. J., White, P. A., Albert, J. T., & Shaffrey, I. C. (2008). ADULT DEGENERATIVE SCOLIOSIS: A REVIEW. Neurosurgery, 63(3 Suppl), A94-A103. https://doi.org/10.1227/01.NEU.0000325485.49323.B2

Boos, N., & Aebi, M. (2008). Spinal Disorders: Fundamentals of Diagnosis and Treatment. https://doi.org/10.1007/978-3-540-69091-7

Burger, E. (2014). General considerations for spine surgery including consent and preparation. general surgical principles, guidelines for informed consent, patient positioning for surgery, equipment needed, and postoperative considerations. https://doi.org/10.1007/978-3-642-34126-7_6

Callisaya, M. L., Blizzard, L., McGinley, J. L., Schmidt, M. D., & Srikanth, V. K. (2009). Sensorimotor Factors Affecting Gait Variability in Older People—A Population-Based Study. J Gerontol A Biol Sci Med Sci, 65A(4), 386-392. https://doi.org/10.1093/gerona/glp184

Cambridge University Engineering Department, U. o. C. (2003). Materials Data Book.

Case, B. (2016). Stand tall, don't fall: improve your strength, balance, flexibility and posture. United States: Bill Case.

Cattagni, T., Scaglioni, G., Laroche, D., Gremeaux, V., & Martin, A. (2016). The involvement of ankle muscles in maintaining balance in the upright posture is higher in elderly fallers. Exp Gerontol, 77, 38-45. https://doi.org/10.1016/j.exger.2016.02.010

Chalmers, E., Lou, E., Hill, D., Zhao, V. H., & Man-Sang, W. (2012). Development of a Pressure Control System for Bracing treatment of Scoliosis. TNSRE, 20(4), 557-563. https://doi.org/10.1109/TNSRE.2012.2192483

Chan, W.Y. (2019). Evaluation and enhancement of thermal and mechanical performance of posture correction girdle for adolescent idiopathic scoliosis (AIS). Hong Kong Polytechnic University.

Chao, T.-C., & Jiang, B. C. (2017). A comparison of postural stability during upright standing between normal and flatfooted individuals, based on COP-based measures. Entropy (Basel, Switzerland), 19(2), 76. https://doi.org/10.3390/e19020076

Chen, X., Cai, H., Zhang, G., Zheng, F., Wu, C., & Lin, H. (2020). The construction of the scoliosis 3D finite element model and the biomechanical analysis of PVCR orthopaedy. Saudi J Biol Sci, 27(2), 695-700. https://doi.org/10.1016/j.sjbs.2019.12.005

Cheung, J. P. Y. (2020). The importance of sagittal balance in adult scoliosis surgery. Annals of translational medicine, 8(2), 35-35. https://doi.org/10.21037/atm.2019.10.19

Cho, K. J., Kim, Y. T., Shin, S. H., & Suk, S. I. (2014). Surgical treatment of adult degenerative scoliosis. Asian Spine J, 8(3), 371-381. https://doi.org/10.4184/asj.2014.8.3.371

Cho, K.-J., Kim, Y.-T., Seo, B., & Shin, J. (2016). Radiological Evaluation and Classification of Adult Spinal Deformity. J Korean Orthop Assoc, 51(1), 1. https://doi.org/10.4055/jkoa.2016.51.1.1

Claus, A. P., Hides, J. A., Moseley, G. L., & Hodges, P. W. (2018). Different ways to balance the spine in sitting: Muscle activity in specific postures differs between individuals with and without a history of back pain in sitting. Clin Biomech (Bristol, Avon), 52, 25-32. https://doi.org/10.1016/j.clinbiomech.2018.01.003

Clin, J., Aubin, C.-É., Lalonde, N., Parent, S., & Labelle, H. (2011). A new method to include the gravitational forces in a finite element model of the scoliotic spine. Med Biol Eng Comput, 49(8), 967-977. https://doi.org/10.1007/s11517-011-0793-4

Clin, J., Aubin, C.-E., Parent, S., Sangole, A., & Labelle, H. (2010). Comparison of the biomechanical 3D efficiency of different brace designs for the treatment of scoliosis using a finite element model. Eur Spine J, 19(7), 1169-1178. https://doi.org/10.1007/s00586-009-1268-2

Cox, J. M. (2011). Lower back pain: mechanism, diagnosis, and treatment (7th ed.). Wolters Kluwer Health/Lippincott Williams & Wilkins.

Dagdia, L., Kokabu, T., & Ito, M. (2019). Classification of adult spinal deformity: Review of current concepts and future directions. Spine Surgery and Related Research, 3(1), 17-26. https://doi.org/10.22603/ssrr.2017-0100

Dallard, J., Duprey, S., & Merlhiot, X. (2018). SIMPLIFIED VERSUS REAL GEOMETRY FINGERTIP MODELS: A FINITE ELEMENT STUDY TO PREDICT FORCE–DISPLACEMENT RESPONSE UNDER FLAT CONTACT COMPRESSION. Journal of mechanics in medicine and biology, 18(4), 1850048. https://doi.org/10.1142/S0219519418500483

de Mauroy, J. C., Lecante, C., Barral, F., & Pourret, S. (2016a). Bracing in adult with scoliosis: experience in diagnosis and classification from a 15-year prospective study of 739 patients. Scoliosis and spinal disorders, 11. https://doi.org/10.1186/s13013-016-0090-y de Mauroy, J. C., Lecante, C., Barral, F., & Pourret, S. (2016b). Prospective study of 158 adult scoliosis treated by a bivalve polyethylene overlapping brace and reviewed at least 5 years after brace fitting. Scoliosis and spinal disorders, 11(Suppl 2), 28. https://doi.org/10.1186/s13013-016-0091-x

Debenham, M. I. B., Smuin, J. N., Grantham, T. D. A., Ainslie, P. N., & Dalton, B. H. (2021). Hypoxia and standing balance. Eur J Appl Physiol, 121(4), 993-1008. https://doi.org/10.1007/s00421-020-04581-5

Del Campo, A. (2010). Physical therapy in the treatment of adult and paediatric spinal deformities: the Spinecor method. Scoliosis, 5(Suppl 1), O31. https://doi.org/10.1186/1748-7161-5-S1-O31

Donzelli, S., Zaina, F., & Negrini, S. (2015). Compliance monitor for scoliosis braces in clinical practice. J Child Orthop, 9(6), 507-508. https://doi.org/10.1007/s11832-015-0703-7

Eguchi, Y., Suzuki, M., Yamanaka, H., Tamai, H., Kobayashi, T., Orita, S., Yamauchi, K., Suzuki, M., Inage, K., Fujimoto, K., Kanamoto, H., Abe, K., Aoki, Y., Toyone, T., Ozawa, T., Takahashi, K., & Ohtori, S. (2017). Associations between sarcopenia and degenerative lumbar scoliosis in older women. Scoliosis Spinal Disord, 12(1), 9. https://doi.org/10.1186/s13013-017-0116-0

Eguchi, Y., Toyoguchi, T., Inage, K., Fujimoto, K., Orita, S., Suzuki, M., Kanamoto, H., Abe, K., Norimoto, M., Umimura, T., Sato, T., Koda, M., Furuya, T., Aoki, Y., Nakamura, J., Akazawa, T., Takahashi, K., & Ohtori, S. (2019). Analysis of skeletal muscle mass in women over 40 with degenerative lumbar scoliosis. Eur Spine J, 28(7), 1618-1625. https://doi.org/10.1007/s00586-018-5845-0

Epstein, N. E. (2019). Review of Risks and Complications of Extreme Lateral Interbody Fusion (XLIF). Surgical neurology international, 10, 237. https://doi.org/10.25259/SNI_559_2019

Everett, R. C., & Patel, K. R. (2007). A Systematic Literature Review of Nonsurgical Treatment in Adult Scoliosis. Spine, 32(19 Suppl), S130-S134. https://doi.org/10.1097/BRS.0b013e318134ea88

Faldini, C., Martino, A., Borghi, R., Perna, F., Toscano, A., & Traina, F. (2015). Long vs. short fusions for adult lumbar degenerative scoliosis: does balance matters? (Report). European Spine Journal, 24(7), 887.

Faldini, C., Martino, A., Fine, M., Miscione, M., Calamelli, C., Mazzotti, A., & Perna, F. (2013). Current classification systems for adult degenerative scoliosis. Musculoskelet Surg, 97(1), 1-8. https://doi.org/10.1007/s12306-013-0245-4

Fok, L. H. (2020). Functional intimate apparel for adolescents with scoliosis. Hong Kong Polytechnic University.

Franciosa, P., Gerbino, S., Lanzotti, A., & Silvestri, L. (2012). Improving comfort of shoe sole through experiments based on CAD-FEM modeling. Med Eng Phys, 35(1), 36-46. https://doi.org/10.1016/j.medengphy.2012.03.007

Freedman, A. B., Horton, C. W., Rhee, M. J., Edwards, C. C., & Kuklo, R. T. (2009). Reliability Analysis for Manual Radiographic Measures of Rotatory Subluxation or Lateral Listhesis in Adult Scoliosis. Spine, 34(6), 603-608. https://doi.org/10.1097/BRS.0b013e31819a841e

Fu, G. K.-M., Rhagavan, I. P., Shaffrey, R. C., Chernavvsky, S. D., & Smith, S. J. (2011). Prevalence, Severity, and Impact of Foraminal and Canal Stenosis Among Adults With Degenerative Scoliosis. Neurosurgery, 69(6), 1181-1187. https://doi.org/10.1227/NEU.0b013e31822a9aeb

Gallo, D. (2014). Case reports: orthotic treatment of adult scoliosis patients with chronic back pain. Scoliosis, 9(1), 18-18. https://doi.org/10.1186/1748-7161-9-18

Garfin, S. R., Eismont, F. J., Bell, G. R., Fischgrund, J. S., & Bono, C. M. (2018). Rothman-Simeone and Herkowitz's the spine (Seventh edition ed.). Elsevier, Inc.

Global Burden of Disease Collaborative Network. (2018). Global Burden of Disease Study 2017 (GBD 2017). Seattle, United States: Institute for Health Metrics and Evaluation (IHME).

Godi, M., Franchignoni, F., Caligari, M., Giordano, A., Turcato, A. M., & Nardone, A. (2013). Comparison of reliability, validity, and responsiveness of the mini-BESTest and Berg Balance Scale in patients with balance disorders. Phys Ther, 93(2), 158-167. https://doi.org/10.2522/ptj.20120171

Godzik, J., Frames, C. W., Smith Hussain, V., Olson, M. C., Kakarla, U. K., Uribe, J. S., Lockhart, T. E., & Turner, J. D. (2020). Postural Stability and Dynamic Balance in Adult Spinal Deformity: Prospective Pilot Study. World Neurosurg, 141, e783-e791. https://doi.org/10.1016/j.wneu.2020.06.010

Gottipati, P., Stine, R., Ganju, A., & Fatone, S. (2018). The effect of positive sagittal spine balance and reconstruction surgery on standing balance. Gait Posture, 62, 227-234. https://doi.org/10.1016/j.gaitpost.2018.03.024

Graham, B. R., Sugrue, A. P., & Koski, R. T. (2016). Adult Degenerative Scoliosis. Clinical Spine Surgery, 29(3), 95-107. https://doi.org/10.1097/BSD.0000000000000367

Haddas, H. R., & Lieberman, H. I. (2019). The Change in Sway and Neuromuscular Activity in Adult Degenerative Scoliosis Patients Pre and Post Surgery Compared With Controls. Spine, 44(15), E899-E907. https://doi.org/10.1097/BRS.0000000000003009

Haddas, R., & Lieberman, I. H. (2018). A method to quantify the "cone of economy". Eur Spine J, 27(5), 1178-1187. https://doi.org/10.1007/s00586-017-5321-2

Haddas, R., Hu, X., & Lieberman, I. H. (2020). The Correlation of Spinopelvic Parameters With Biomechanical Parameters Measured by Gait and Balance Analyses in Patients With Adult Degenerative Scoliosis. Clin Spine Surg, 33(1), E33-E39. https://doi.org/10.1097/BSD.0000000000000939

Haddas, R., Lieberman, I. H., & Block, A. (2018). The Relationship Between Fear-Avoidance and Neuromuscular Measures of Function in Patients With Adult Degenerative Scoliosis. Spine (Phila Pa 1976), 43(23), E1412-E1421. https://doi.org/10.1097/BRS.0000000000002719

Haddas, R., Xu, M., & Lieberman, I. (2019). Finite Element Based-Analysis for Pre and Post Lumbar Fusion of Adult Degenerative Scoliosis Patients. Spine Deformity, 7. https://doi.org/10.1016/j.jspd.2018.11.008

Haddas, R., Xu, M., Lieberman, I., & Yang, J. (2016). Finite Element-Based Adjacent Level Analysis of Pre- and Postlumbar Fusion for Scoliosis in Comparison to Healthy Spines. Spine Journal, The, 16(10), S159-S159. https://doi.org/10.1016/j.spinee.2016.07.057

Hallager, W. D., Hansen, V. L., Dragsted, R. C., Peytz, R. N., Gehrchen, R. M., & Dahl, R. B. (2016). A Comprehensive Analysis of the SRS-Schwab Adult Spinal Deformity Classification and Confounding Variables: A Prospective, Non-US Cross-sectional Study in 292 Patients. Spine, 41(10), E589-E597. https://doi.org/10.1097/BRS.0000000000001355

Harrop, J. S., Vaccaro, A. R., & Awad, A. J. (2015). Adult degenerative scoliosis: coronal and sagittal deformities: treatment and management (First ed.). Jaypee Brothers Medical Publishers (P) Ltd.

Hatton, A. L., Dixon, J., Rome, K., & Martin, D. (2011). Standing on textured surfaces: Effects on standing balance in healthy older adults. Age Ageing, 40(3), 363-368. https://doi.org/10.1093/ageing/afr026

Heary, R. F., & Albert, T. J. (2014). Spinal deformities: the essentials (Second ed.). Thieme.

Hiyama, A., Katoh, H., Sakai, D., Sato, M., Tanaka, M., Nukaga, T., & Watanabe, M. (2018). Correlation analysis of sagittal alignment and skeletal muscle mass in patients with spinal degenerative disease. Sci Rep, 8(1), 15492-15498. https://doi.org/10.1038/s41598-018-33867-0

Houston Family Chiropractic. (2021). About Scoliosis & Braces. https://www.houstonfamilychiropractic.com/about-scoliosis-braces/

Houten, J. K., & Nasser, R. (2013). Symptomatic progression of degenerative scoliosis after decompression and limited fusion surgery for lumbar spinal stenosis. Journal of Clinical Neuroscience, 20(4), 613-615. https://doi.org/10.1016/j.jocn.2012.06.002

Human Solutions GmbH. (2015). The perfectly precise one for size & fit perfectionists. http://www.humansolutions.com/fashion/front_content.php?idcat=139&lang=7

Hyun, S.-J., Bae, C.-W., Lee, S.-H., & Rhim, S.-C. (2013). Fatty degeneration of paraspinal muscle in patients with the degenerative lumbar kyphosis: A new evaluation method of quantitative digital analysis using MRI and CT scan. Clin Spine Surg, 29(10), 441-447. https://doi.org/10.1097/BSD.0b013e3182aa28b0

Iwamoto, Y., Takahashi, M., & Shinkoda, K. (2017). Muscle co-contraction in elderly people change due to postural stability during single-leg standing. J Physiol Anthropol, 36(1), 43-47. https://doi.org/10.1186/s40101-017-0159-1

Jeon, C. H., Park, J. U., Chung, N. S., Son, K. H., Lee, Y. S., & Kim, J. J. (2013). Degenerative retrolisthesis: is it a compensatory mechanism for sagittal imbalance? The bone & joint journal, 95-b(9), 1244-1249. https://doi.org/10.1302/0301-620X.95B9.31237

Karthikeyan, G., Nalankilli, G., Shanmugasundaram, O. L., & Prakash, C. (2016). Thermal comfort properties of bamboo tencel knitted fabrics. International journal of clothing science and technology, 28(4), 420-428. https://doi.org/10.1108/ijcst-08-2015-0086

Kebaish, K. M., Neubauer, P. R., Voros, G. D., Khoshnevisan, M. A., & Skolasky, R. L. (2011, Apr 20). Scoliosis in adults aged forty years and older: prevalence and relationship to age, race, and gender. Spine (Phila Pa 1976), 36(9), 731-736. https://doi.org/10.1097/BRS.0b013e3181e9f120

Kim, H., Lee, C.-K., Yeom, J. S., Lee, J. H., Cho, J. H., Shin, S. I., Lee, H.-J., & Chang, B.-S. (2013). Asymmetry of the cross-sectional area of paravertebral and psoas muscle in patients with degenerative scoliosis. Eur Spine J, 22(6), 1332-1338. https://doi.org/10.1007/s00586-013-2740-6

Kim, Y. E., & Choi, H. W. (2015). Effect of disc degeneration on the muscle recruitment pattern in upright posture: a computational analysis. Comput Methods Biomech Biomed Engin, 18(15), 1622-1631. https://doi.org/10.1080/10255842.2014.936858

Konieczny, M. R., Hieronymus, P., & Krauspe, R. (2017). Time in brace: where are the limits and how can we improve compliance and reduce negative psychosocial impact in patients with scoliosis? A retrospective analysis. Spine J, 17(11), 1658-1664. https://doi.org/10.1016/j.spinee.2017.05.010

Kooistra, R. D., de Ruiter, C. J., & de Haan, A. (2008). Knee angle-dependent oxygen consumption of human quadriceps muscles during maximal voluntary and electrically evoked contractions. Eur J Appl Physiol, 102(2), 233-242. https://doi.org/10.1007/s00421-007-0573-x

Kraft, R., & Wozniak, S. (2011, 10/01). A Review of Computational Spinal Injury Biomechanics Research and Recommendations for Future Efforts.

Kuklo, T. R. (2007). Radiographic Evaluation of Spinal Deformity. Neurosurgery Clinics of North America, 18(2), 215-222. https://doi.org/10.1016/j.nec.2007.01.009

Kurra, S., Lavelle, W. F., Silverstein, M. P., Savage, J. W., & Orr, R. D. (2018). Long-term outcomes of transforaminal lumbar interbody fusion in patients with spinal stenosis and degenerative scoliosis. The Spine Journal, 18(6), 1014-1021. https://doi.org/10.1016/j.spinee.2017.10.063

Lamb, J. M., & Kallal, M. J. (2016). A Conceptual Framework for Apparel Design. Clothing and textiles research journal, 10(2), 42-47. https://doi.org/10.1177/0887302x9201000207

Law, D., Cheung, M.-c., Yip, J., Yick, K.-L., & Wong, C. (2017). Scoliosis brace design: influence of visual aesthetics on user acceptance and compliance. ERGONOMICS, 60(6), 876-886. https://doi.org/10.1080/00140139.2016.1227093

Lee, S., Lee, J. S., Kim, J. P., Kim, K., Hwang, C. H., & Koo, K. I. (2018). Precise Cobb Angle Measurement System Based on Spinal Images Merging Function. IRBM, 39(5), 343-352. https://doi.org/10.1016/j.irbm.2018.09.002

Lemmers, G., Lankveld, W., Westert, G., Wees, P., & Staal, J. (2019). Imaging versus no imaging for lower back pain: a systematic review, measuring costs, healthcare utilization and absence from work. Eur Spine J, 28(5), 937-950. https://doi.org/10.1007/s00586-019-05918-1

Liu, C. T., Chen, K., & Chiu, E. (2009). Adult Degenerative Scoliosis Treated by Acupuncture. J. Altern. Complement Med., 15(8), 935-937. https://doi.org/10.1089/acm.2008.0515

Liu, Y., Liu, Z., Zhu, F., Qian, B.-P., Zhu, Z., Xu, L., Ding, Y., & Qiu, Y. (2013). Validation and Reliability Analysis of the New SRS-Schwab Classification for Adult Spinal Deformity. Spine, 38(11), 902-908. https://doi.org/10.1097/BRS.0b013e318280c478

Lo, D. (2015). Finite element mesh generation. CRC Press.

Lord, S. R., Delbaere, K., & Sturnieks, D. L. (2018). Chapter 10 - Aging. In B. L. Day & S. R. Lord (Eds.), Handbook of clinical neurology (Vol. 159, pp. 157-171). Elsevier. https://doi.org/https://doi.org/10.1016/B978-0-444-63916-5.00010-0

Lou, E., Hill, D. L., & Raso, J. V. (2010). A wireless sensor network system to determine biomechanics of spinal braces during daily living. Med Biol Eng Comput, 48(3), 235-243. https://doi.org/10.1007/s11517-010-0575-4

Lowe, H. T., Berven, J. S., Schwab, H. F., & Bridwell, H. K. (2006). The SRS Classification for Adult Spinal Deformity: Building on the King/Moe and Lenke Classification Systems. Spine, 31(19S Suppl), S119-S125. https://doi.org/10.1097/01.brs.0000232709.48446.be

Luhmann, J. S., Sucato, J. D., Johnston, E. C., Richards, S. B., & Karol, A. L. (2016). Radiographic Assessment of Shoulder Position in 619 Idiopathic Scoliosis Patients: Can T1 Tilt Be Used as an Intraoperative Proxy to Determine Postoperative Shoulder Balance? Journal of Pediatric Orthopaedics, 36(7), 691-694. https://doi.org/10.1097/BPO.0000000000000519

Ma, H.-H., Tai, C.-L., Chen, L.-H., Niu, C.-C., Chen, W.-J., & Lai, P.-L. (2017). Application of two-parameter scoliometer values for predicting scoliotic Cobb angle. Biomedical engineering online, 16(1), 136-136. https://doi.org/10.1186/s12938-017-0427-7

MacRae, C. S., Critchley, D., Lewis, J. S., & Shortland, A. (2018). Comparison of standing postural control and gait parameters in people with and without chronic low back pain: a cross-sectional case–control study. BMJ Open Sport Exerc Med, 4(1), e000286. https://doi.org/10.1136/bmjsem-2017-000286

Mahaudens, P., Banse, X., Mousny, M., & Detrembleur, C. (2009). Gait in adolescent idiopathic scoliosis: kinematics and electromyographic analysis. Eur Spine J, 18(4), 512-521. https://doi.org/10.1007/s00586-009-0899-7

Marcotte, L. (2010). SpineCor in the treatment of adult scoliosis. Scoliosis, 5(Suppl 1), O47-O47. https://doi.org/10.1186/1748-7161-5-S1-O47

Marques, A. P., Almeida, S. M., Carvalho, J. M., Cruz, J. P., Oliveira, A. M., & Jácome, C. P. (2016). Reliability, Validity, and Ability to Identify Fall Status of the Balance Evaluation Systems Test, Mini–Balance Evaluation Systems Test, and Brief–Balance Evaluation Systems Test in Older People Living in the Community. Arch Phys Med Rehabil, 97(12), 2166-2173.e2161. https://doi.org/10.1016/j.apmr.2016.07.011

Mataliotakis, G., Tsirikos, A. I., & Mohammad, S. (2017). Adult degenerative deformity: principles of sagittal balance, classification and surgical management. Orthopaedics and Trauma, 31(6), 370-377. https://doi.org/10.1016/j.mporth.2017.09.008

Mattei, T. A. M. D. (2013). Do not miss it: paraspinal muscle atrophy in the concave side of the curve in patients with adult degenerative scoliosis. Spine J, 13(8), 987-988. https://doi.org/10.1016/j.spinee.2013.03.052

McAviney, J., Mee, J., Fazalbhoy, A., Du Plessis, J., & Brown, B. T. (2020). A systematic literature review of spinal brace/orthosis treatment for adults with scoliosis between 1967 and 2018: clinical outcomes and harms data. BMC Musculoskeletal Disorders, 21(1), 1. https://doi.org/10.1186/s12891-020-3095-x

Menezes, C.M., Lima, R.S., Falcon, R.S., & de Souza Junior R.E. ((2019). THE IMPORTANCE OF CLAVICLE ANGLE AND HEIGHT OF THE CORACOID PROCESS IN IDIOPATHIC SCOLIOSIS. Coluna/Columna, 18(3), 196-199. https://doi.org/10.1590/s1808-185120191803196866

Michell, A. W. (2013). Understanding EMG. Oxford University Press.

Minas, T., Ogura, T., Headrick, J., & Bryant, T. (2018). Autologous Chondrocyte Implantation "Sandwich" Technique Compared With Autologous Bone Grafting for Deep Osteochondral Lesions in the Knee. The American Journal of Sports Medicine, 46(2), 322-332. https://doi.org/10.1177/0363546517738000

Modi, H. N., Suh, S.-W., Hong, J.-Y., Song, S.-H., & Yang, J.-H. (2010). Intraoperative blood loss during different stages of scoliosis surgery: A prospective study. Scoliosis, 5(1), 16. https://doi.org/10.1186/1748-7161-5-16

Morningstar, M. W. (2011). Outcomes for adult scoliosis patients receiving chiropractic rehabilitation: a 24-month retrospective analysis. Journal of Chiropractic Medicine, 10(3), 179-184. https://doi.org/10.1016/j.jcm.2011.01.006

Morningstar, M. W., Stitzel, C., Dovorany, B., & Siddiqui, A. (2017). Clinical outcomes of a scoliosis activity suit worn by patients with chronic post-fusion pain: 6-month case-controlled results. Medical Research Archives, 5.

Muscolino, J. E. (2015). Manual therapy for the low back and pelvis: a clinical orthopedic approach (First edition.. ed.). Wolters Kluwer Health/Lippincott Williams & Wilkins.

Niemeyer, F., Wilke, H.-J., & Schmidt, H. (2012). THE IMPACT OF UNCERTAIN GEOMETRY PARAMETERS ON THE RELIABILITY OF NUMERICAL SIMULATIONS OF THE LUMBAR SPINE. Journal of biomechanics, 45, S599-S599. https://doi.org/10.1016/S0021-9290(12)70600-0

Novak, J. S. (2006). Janice Novak's posture, get it straight (2nd . ed.). Andover, Minn. : Expert Publishing, Inc.

Ohyama, S., Hoshino, M., Terai, H., Toyoda, H., Suzuki, A., Takahashi, S., Hayashi, K., Tamai, K., Hori, Y., & Nakamura, H. (2019). Sarcopenia is related to spinal sagittal imbalance in patients with spinopelvic mismatch. Eur Spine J, 28(9), 1929-1936. https://doi.org/10.1007/s00586-019-06066-2

Onal, L., & Yildirim, M. (2012). Comfort properties of functional three-dimensional knitted spacer fabrics for home-textile applications. Textile research journal, 82(17), 1751-1764. https://doi.org/10.1177/0040517512444331

Osoba, M. Y., Rao, A. K., Agrawal, S. K., & Lalwani, A. K. (2019). Balance and gait in the elderly: A contemporary review: Balance and Gait in the Elderly. Laryngoscope investigative otolaryngology, 4(1), 143-153. https://doi.org/10.1002/lio2.252

O'Sullivan, P. B., Grahamslaw, K. M., Kendell, M., Lapenskie, S. C., MÖLler, N. E., & Richards, K. V. (2002). The effect of different standing and sitting postures on trunk muscle activity in a pain-free population. Spine (Phila Pa 1976), 27(11), 1238-1244. https://doi.org/10.1097/00007632-200206010-00019

O'Sullivan, P. B., Smith, A. J., Beales, D. J., & Straker, L. M. (2011). Association of Biopsychosocial Factors With Degree of Slump in Sitting Posture and Self-Report of Back Pain in Adolescents: A Cross-Sectional Study. Phys Ther, 91(4), 470-483. https://doi.org/10.2522/ptj.20100160

Paillard, T., & Noé, F. (2015). Techniques and Methods for Testing the Postural Function in Healthy and Pathological Subjects. Biomed Res Int, 2015, 891390-891315. https://doi.org/10.1155/2015/891390

Palazzo, C., Montigny, J.-P., Barbot, F., Bussel, B., Vaugier, I., Fort, D., Courtois, I., & Marty-Poumarat, C. (2017). Effects of Bracing in Adult With Scoliosis: A Retrospective Study. Archives of Physical Medicine and Rehabilitation, 98(1), 187-190. https://doi.org/10.1016/j.apmr.2016.05.019

Palou, E. (2014). Spinal Osteotomy – Indications and Techniques. In (pp. 609-624). https://doi.org/10.1007/978-3-642-34746-7_223

Park, A., Ling, J., & Bettany Saltikov, J. (2016). Living with scoliosis and wearing a soft back brace: an explorative study of older adults. Physiotherapy, 102, e214-e214. https://doi.org/10.1016/j.physio.2016.10.264

Pasma, J. H., Engelhart, D., Schouten, A. C., van der Kooij, H., Maier, A. B., & Meskers, C. G. M. (2014). Impaired standing balance: The clinical need for closing the loop. Neuroscience, 267, 157-165. https://doi.org/10.1016/j.neuroscience.2014.02.030

Pawlaczyk, M., Lelonkiewicz, M., & Wieczorowski, M. (2013). Age-dependent biomechanical properties of the skin. Postepy Dermatol Alergol, 30(5), 302-306. https://doi.org/10.5114/pdia.2013.38359

Ploumis, A., Transfeldt, E. E., Gilbert, T., Mehbod, A. A., Dykes, D. C., & Perra, J. (2006). Degenerative lumbar scoliosis - Radiographic correlation of lateral rotatory olisthesis with neural canal dimensions. Spine, 31(20), 2353-2358.

Ravindra, V. M., Senglaub, S. S., Rattani, A., Dewan, M. C., Härtl, R., Bisson, E., Park, K. B., & Shrime, M. G. (2018). Degenerative Lumbar Spine Disease: Estimating Global Incidence and Worldwide Volume. Global Spine Journal, 8(8), 784-794. https://doi.org/10.1177/2192568218770769

Reimann, H., Ramadan, R., Fettrow, T., Hafer, J. F., Geyer, H., & Jeka, J. J. (2020). Interactions Between Different Age-Related Factors Affecting Balance Control in Walking. Front Sports Act Living, 2, 94-94. https://doi.org/10.3389/fspor.2020.00094

Roy, S., Grünwald, A. T. D., Alves-Pinto, A., Maier, R., Cremers, D., Pfeiffer, D., & Lampe, R. (2019). A Noninvasive 3D Body Scanner and Software Tool towards Analysis of Scoliosis. Biomed Res Int, 2019, 1-15. https://doi.org/10.1155/2019/4715720

Sardjono, A. T., Wilkinson, F. M. H., Veldhuizen, G. A., Van Ooijen, A. P. M., Purnama, E. K., & Verkerke, J. G. (2013). Automatic Cobb Angle Determination From Radiographic Images. Spine, 38(20), E1256-E1262. https://doi.org/10.1097/BRS.0b013e3182a0c7c3

Sarwahi, V., Wendolowski, S., Gecelter, R., Amaral, T. D., & Thornhill, B. (2016). P122 - T1 Tilt and Clavicle Angle are the Best Predictors of Postoperative Shoulder Balance. The Spine Journal, 16(10), S346-S346. https://doi.org/10.1016/j.spinee.2016.07.448

Scheufler, K.-M., Cyron, D., Dohmen, H., & Eckardt, A. (2010). Less Invasive Surgical Correction of Adult Degenerative Scoliosis, Part I: Technique and Radiographic Results. Neurosurgery, 67(3), 696-710. https://doi.org/10.1227/01.NEU.0000377851.75513.FE

Schlenstedt, C., Brombacher, S., Hartwigsen, G., Weisser, B., Möller, B., & Deuschl, G. (2016). Comparison of the Fullerton Advanced Balance Scale, Mini-BESTest, and Berg Balance

Scale to Predict Falls in Parkinson Disease. Phys Ther, 96(4), 494-501. https://doi.org/10.2522/ptj.20150249

Schoutens, C., Cushman, D. M., McCormick, Z. L., Conger, A., Van Royen, B. J., & Spiker, W. R. (2020). Outcomes of Nonsurgical Treatments for Symptomatic Adult Degenerative Scoliosis: A Systematic Review. Pain Med, 21(6), 1263-1275. https://doi.org/10.1093/pm/pnz253

Schwab, F., Farcy, J.-P., Bridwell, K., Berven, S., Glassman, S., Harrast, J., & Horton, W. (2006). A Clinical Impact Classification of Scoliosis in the Adult. Spine, 31(18), 2109-2114. https://doi.org/10.1097/01.brs.0000231725.38943.ab

Schwab, F., Ungar, B., Blondel, B., Buchowski, J., Coe, J., Deinlein, D., Dewald, C., Mehdian, H., Shaffrey, C., Tribus, C., & Lafage, V. (2012). Scoliosis Research Society—Schwab Adult Spinal Deformity Classification: A Validation Study. Spine, 37(12), 1077-1082. https://doi.org/10.1097/BRS.0b013e31823e15e2

Scoliosis Research Society Terminology Committee. (1976). A glossary of scoliosis terms. Spine, 1, 57-8.

Sharma, O. P., Patel, V., & Mehta, T. (2016). Design of experiment approach in development of febuxostat nanocrystal: Application of Soluplus® as stabilizer. Powder technology, 302, 396-405. https://doi.org/10.1016/j.powtec.2016.09.004

Shivanna, K. H., Tadepalli, S. C., & Grosland, N. M. (2010). Feature-based multiblock finite element mesh generation. Comput Aided Des, 42(12), 1108-1116. https://doi.org/10.1016/j.cad.2010.07.005

Silva, F. E., & Lenke, L. G. (2010). Adult degenerative scoliosis: evaluation and management. Neurosurgical focus, 28(3), E1-E1. https://doi.org/10.3171/2010.1.FOCUS09271

Sit, Y.L., Yip, J., & Kwan, Y.H. (2020). A New Concept for Adult Degenerative Scoliosis: Posture Training Bracewear. ISERD - 779th International Conference on Medical and Health Sciences (ICMHS), Zurich, Switzerland.

Slattery, C., & Verma, K. (2018). Classification in Brief: SRS-Schwab Classification of Adult Spinal Deformity. Clinical Orthopaedics and Related Research, 476(9), 1890-1894. https://doi.org/10.1007/s11999.0000000000000264

Slobodyanyuk, K., Poorman, C. E., Smith, J. S., Protopsaltis, T. S., Hostin, R., Bess, S., Mundis, G. M., Schwab, F. J., & Lafage, V. (2014). Clinical improvement through nonoperative treatment of adult spinal deformity: Who is likely to benefit? Neurosurgical focus, 36(5). https://doi.org/10.3171/2014.3.FOCUS1426

Smith, S. J., Klineberg, I. E., Schwab, P. F., Shaffrey, G. C., Moal, G. B., Ames, G. C., Hostin, G. R., Fu, G. K.-M., Burton, G. D., Akbarnia, G. B., Gupta, G. M., Hart, G. R., Bess, G. S., Lafage, G. V., & International Spine Study Group, G. (2013). Change in Classification Grade by the SRS-Schwab Adult Spinal Deformity Classification Predicts Impact on Health-Related Quality of Life Measures: Prospective Analysis of Operative and Nonoperative Treatment. Spine, 38(19), 1663-1671. https://doi.org/10.1097/BRS.0b013e31829ec563

Smith, S. J., Shaffrey, I. C., Glassman, D. S., Berven, H. S., Schwab, J. F., Hamill, L. C., Horton, C. W., Ondra, L. S., Sansur, A. C., & Bridwell, H. K. (2011). Risk-Benefit Assessment of

Surgery for Adult Scoliosis: An Analysis Based on Patient Age. Spine, 36(10), 817-824. https://doi.org/10.1097/BRS.0b013e3181e21783

Smith-Ray, R. L., Hughes, S. L., Prohaska, T. R., Little, D. M., Jurivich, D. A., & Hedeker, D. (2015). Impact of Cognitive Training on Balance and Gait in Older Adults. J Gerontol B Psychol Sci Soc Sci, 70(3), 357-366. https://doi.org/10.1093/geronb/gbt097

Soares, M. M., & Rebelo, F. (2012). Advances in Usability Evaluation Part I. Baton Rouge: Taylor & Francis Group.

Souron, R., Farabet, A., Millet, G. Y., & Lapole, T. (2016). Reliability of the functional measures of the corticospinal pathways to dorsiflexor muscles during maximal voluntary contractions. J Neurol Sci, 369(11), 368-374. https://doi.org/10.1016/j.jns.2016.09.003

Staudenmann, D., Roeleveld, K., Stegeman, D. F., & van Dieën, J. H. (2010). Methodological aspects of SEMG recordings for force estimation – A tutorial and review. J Electromyogr Kinesiol, 20(3), 375-387. https://doi.org/10.1016/j.jelekin.2009.08.005

Sullivan, B. T., Jain, A., Aziz, K. T., & Khanna, A. J. (2017). Clinical and radiographic evaluation of adult spinal deformities. Seminars in Spine Surgery, 29(4), 166-174. https://doi.org/10.1053/j.semss.2017.08.001

Tambe, A. D., & Michael, A. L. R. (2011). (iii) Adult degenerative scoliosis. Orthopaedics and Trauma, 25(6), 413-424. https://doi.org/10.1016/j.mporth.2011.11.006

Tecco, S., Mummolo, S., Marchetti, E., Tetè, S., Campanella, V., Gatto, R., Gallusi, G., Tagliabue, A., & Marzo, G. (2011). sEMG activity of masticatory, neck, and trunk muscles during the treatment of scoliosis with functional braces. A longitudinal controlled study. J Electromyogr Kinesiol, 21(6), 885-892. https://doi.org/10.1016/j.jelekin.2011.08.004

The Spine Center (2021). Lateral Lumbar Interbody Fusion. https://www.thespinesurgerycenter.com/lateral-lumbar-interbody-fusion.html

Vera-Garcia, F. J., Moreside, J. M., & McGill, S. M. (2010). MVC techniques to normalize trunk muscle EMG in healthy women. J Electromyogr Kinesiol, 20(1), 10-16. https://doi.org/10.1016/j.jelekin.2009.03.010

Vergari, C., Ribes, G., Aubert, B., Adam, C., Miladi, L., Ilharreborde, B., Abelin-Genevois, K., Rouch, P., & Skalli, W. (2015, 2015/01/01/). Evaluation of a Patient-Specific Finite-Element Model to Simulate Conservative Treatment in Adolescent Idiopathic Scoliosis. Spine Deformity, 3(1), 4-11. https://doi.org/https://doi.org/10.1016/j.jspd.2014.06.014

VICON Documentation (2021). Attach Plug-in Gait markers to a patient. https://docs.vicon.com/display/Nexus28/Attach+Plug-in+Gait+markers+to+a+patient

Wang, C. M., Laud, W. P., Macias, B. M., & Nattinger, B. A. (2011). Utility of a Combined Current Procedural Terminology and International Classification of Diseases, Ninth Revision, Clinical Modification Code Algorithm in Classifying Cervical Spine Surgery for Degenerative Changes. Spine, 36(22), 1843-1848. https://doi.org/10.1097/BRS.0b013e3181f7a943

Wang, L., Zhang, B., Chen, h., Lu, X., Li, Z., & Guo, Q. (2016). A Validated Finite Element Analysis of Facet Joint Stress in Degenerative Lumbar Scoliosis. World Neurosurgery, 95, 126-133. https://doi.org/10.1016/j.wneu.2016.07.106

Wang, M. Y., Lu, Y., Anderson, D. G., & Mummaneni, P. V. (2014). Minimally invasive spinal deformity surgery: an evolution of modern techniques. Springer.

Weinreb, J. H., Bianco, K. L., Lafage, V., & Schwab, F. (2014). Indications for Adult Spinal Deformity Surgery. https://doi.org/10.1007/978-3-7091-1407-0_3

Weiss, H.-R., & Werkmann, M. (2009). Treatment of chronic lower back pain in patients with spinal deformities using a sagittal re-alignment brace. Scoliosis, 4(1), 7-7. https://doi.org/10.1186/1748-7161-4-7

Widmer, J., Fornaciari, P., Senteler, M., Roth, T., Snedeker, J., & Farshad, M. (2019). Kinematics of the Spine Under Healthy and Degenerative Conditions: A Systematic Review. Annals of Biomedical Engineering, 47(7), 1491-1522.

Wren, T. A. L., Gorton, G. E., Õunpuu, S., & Tucker, C. A. (2011). Efficacy of clinical gait analysis: A systematic review. Gait Posture, 34(2), 149-153. https://doi.org/10.1016/j.gaitpost.2011.03.027

Wu, W., Liang, J., Du, Y., Tan, X., Xiang, X., Wang, W., Ru, N., & Le, J. (2014). Reliability and reproducibility analysis of the Cobb angle and assessing sagittal plane by computer-assisted and manual measurement tools. BMC Musculoskeletal Disorders, 15(1). https://doi.org/10.1186/1471-2474-15-33

Xie, D., Zhang, J., Ding, W., Yang, S., Yang, D., Ma, L., & Zhang, J. (2019). Abnormal change of paravertebral muscle in adult degenerative scoliosis and its association with bony structural parameters. Eur Spine J, 28(7), 1626-1637. https://doi.org/10.1007/s00586-019-05958-7

Xu, M., Yang, J., Lieberman, I., & Haddas, R. (2017). Finite element method-based study for effect of adult degenerative scoliosis on the spinal vibration characteristics. Comput Biol Med, 84, 53-58. https://doi.org/10.1016/j.compbiomed.2017.03.018

Xu, M., Yang, J., Lieberman, I., & Haddas, R. (2019). Stress distribution in vertebral bone and pedicle screw and screw–bone load transfers among various fixation methods for lumbar spine surgical alignment: A finite element study. Med Eng Phys, 63, 26-32. https://doi.org/10.1016/j.medengphy.2018.10.003

Yagi, M. M. D. P., Hosogane, N. M. D. P., Watanabe, K. M. D. P., Asazuma, T. M. D. P., & Matsumoto, M. M. D. P. (2015). The paravertebral muscle and psoas for the maintenance of global spinal alignment in patient with degenerative lumbar scoliosis. Spine J, 16(4), 451-458. https://doi.org/10.1016/j.spinee.2015.07.001

Yagi, M. M. D. P., Ohne, H. M. D., Kaneko, S. M. D. P., Machida, M. M. D. P., Yato, Y. M. D. P., & Asazuma, T. M. D. P. (2017). Does corrective spine surgery improve the standing balance in patients with adult spinal deformity? Spine J, 18(1), 36-43. https://doi.org/10.1016/j.spinee.2017.05.023

Yagi, M., Kaneko, S., Yato, Y., & Asazuma, T. (2016). Standing Balance and Compensatory Mechanisms in Patients with Adult Spinal Deformity. Spine (Phila Pa 1976), 42(10), E584-E591. https://doi.org/10.1097/BRS.0000000000001901

Yamada, K., Nakamae, T., Shimbo, T., Kanazawa, T., Okuda, T., Takata, H., Hashimoto, T., Hiramatsu, T., Tanaka, N., Olmarker, K., & Fujimoto, Y. (2016). Targeted Therapy for Lower back pain in Elderly Degenerative Lumbar Scoliosis. Spine, 41(10), 872-879. https://doi.org/10.1097/BRS.0000000000001524

Yang, J.-M., Lee, J.-H., & Lee, D.-H. (2015). Effects of consecutive application of stretching, Schroth, and strengthening exercises on Cobb's angle and the rib hump in an adult with idiopathic scoliosis. Journal of physical therapy science, 27(8), 2667-2669. https://doi.org/10.1589/jpts.27.2667

York, P., & Kim, H. (2017). Degenerative Scoliosis. Curr Rev Musculoskelet Med, 10(4), 547-558. https://doi.org/10.1007/s12178-017-9445-0

Youssef, J. A., Orndorff, D. O., Patty, C. A., Scott, M. A., Price, H. L., Hamlin, L. F., Williams, T. L., Uribe, J. S., & Deviren, V. (2013). Current status of adult spinal deformity. Global Spine Journal, 3(1), 51. https://doi.org/10.1055/s-0032-1326950

Zacharkow, D. (1988). Posture: sitting, standing, chair design and exercise. Springfield, Ill.: Thomas.

Zaina, F., Poggio, M., Donzelli, S., & Negrini, S. (2018). Can bracing help adults with chronic back pain and scoliosis? Short-term results from a pilot study. Prosthetics and Orthotics International, 42(4), 410-414. https://doi.org/10.1177/0309364618757769

Zhang, W., Low, L.-F., Schwenk, M., Mills, N., Gwynn, Josephine D., & Clemson, L. (2019). Review of Gait, Cognition, and Fall Risks with Implications for Fall Prevention in Older Adults with Dementia. Dement Geriatr Cogn Disord, 48(1-2), 17-29. https://doi.org/10.1159/000504340

Zheng, J., Yang, Y., Lou, S., Zhang, D., & Liao, S. (2015). Construction and validation of a three-dimensional finite element model of degenerative scoliosis. (Report). Journal of Orthopaedic Surgery and Research, 10(190). https://doi.org/10.1186/s13018-015-0334-1

Zhou, J., Li, Y., Lam, J., & Cao, X. (2010). The Poisson Ratio and Modulus of Elastic Knitted Fabrics. Textile research journal, 80(18), 1965-1969. https://doi.org/10.1177/0040517510371864

Zhu, F., Bao, H., Peng, Y., Liu, S., Bao, M., Zhu, Z., Liu, Z., & Qiu, Y. (2017). Do the disc degeneration and osteophyte contribute to the curve rigidity of degenerative scoliosis? BMC Musculoskeletal Disorders, 18(1). https://doi.org/10.1186/s12891-017-1471-y

Zhu, G., Kremenakova, D., Wang, Y., & Militky, J. (2015). Air permeability of polyester nonwoven fabrics. Autex Research Journal, 15(1), 8-12. https://doi.org/10.2478/aut-2014-0019

Zhuming, B. (2017). Finite Element Analysis Applications: A Systematic and Practical Approach.

Zupin, Ž., Hladnik, A., & Dimitrovski, K. (2011). Prediction of one-layer woven fabrics air permeability using porosity parameters. Textile research journal, 82(2), 117-128. https://doi.org/10.1177/0040517511424529